Microbial Degradation of Chromium Azo Dye

CAI, Qinhong

A Thesis Submited in Partial Fulfillment

of the Requirements for the Degree of

Master of Philosophy

in

Biology

The Chinese University of Hong Kong

September 2009

Thesis Committee

Prof. P.K. Wong (Supervisor)

Prof. C.K. Wong (Internal Examiner)

Prof. L.M. Chu (Internal Examiner)

Prof. T.L. Hu (External Examiner)

Acknowledgements

I would like to express my sincere gratitude to my supervisor, Prof. P.K. Wong, for his kind supervision, support, patience and encouragement. He has guided me to be critical and creative as well as shared a great deal of innovative ideas and suggestions with me.

I also would like to express my genuine thinks to my external examiner Prof. T.L. Hu and my internal examiners Prof. L.M. Chu and Prof. C.K. Wong, for their valuable comments and suggestions on this project and attentive evaluation on this thesis.

In addition, I would like to use this opportunity to truly thank Dr. Alex K.H. Wong, who has always been so kind and supportive during these two years' research study. I'm deeply appreciative of the numerous practical suggestions and inspiring advices provided by my colleagues: Prof. Alex T.S. Chow, Dr. W. Zhao, Dr. G.T Li, Ms L.S. Zhang, Ms. Amy O.T. Woo, Ms. T.Y. Leung, Mr. Elstan W.K. Lau, Mr. T.W. Ng and Ms. Y.M. Chen.

Moreover, I would like to truly thank Ms. Jessie P.K. Lee, Mr Thomas C.O. Tang, Mr. Freddie W.K. Kwok and Mr. Y.P. Yin for their technique assistance and kindness.

At last, I also want to express my gratitude to my family, especially to my mother and grandmother for their greatest love and continuous support. Last but not the lease I am also grateful to my husband, Mr. S.L. Huang, for his love, comfort, care and support.

Abstracts

Chromium azo dyes have been produced intensively from dye manufacture industry and widely used in textile and wool dyeing industry. Large quantity of chromium azo dyes are lost during synthesis and processing, thus resulting in pollution in industrial effluents. Once these untreated effluents were discharged into open waters, objectionably aesthetic effects can be observed even at ppb level. Meanwhile, the transfer of oxygen and light could be obstructed by the presence of dye effluents affecting the living conditions of aquatic biology. Generally, chromium azo dyes are more mutagenic and toxic than their parental azo dyes, and more recalcitrant towards biodegradation. Furthermore, degradation of chromium azo dyes may generate aromatic amines, which are normally mutagenic, cytotoxic and carcinogenic, as well as release chromium which requires further treatment.

In this project, bacterial strains which are capable to degrade one model chromium azo dye: Acid Yellow 99 (AY99) at the highest efficiency, were isolated from Sample Sludge D collected from the contact aeration tank of a primary dye treatment plant in Huizhou, China. Both of the two most effective bacterial strains were identified to be *Pseudomonas fluorescens* strain d220 by molecular analysis.

The optimum conditions of decolorizing AY99 were investigated using response surface methodology (RSM). Six factors including cell dry weight (g/L), glucose (g/L), $(NH_4)_2SO_4$ (g/L), nutrient broth (g/L), pH and temperature (^oC) were screened by a 2-level factorial design: minimal-runs resolution V design (MR5). Those factors

that are vital to the response (decolorization (%)) were selected for the subsequent optimization. As a result, cell dry weight (g/L), $(NH_4)_2SO_4$ (g/L) and pH were found to be the most important factors for decolorization. Then whether the original mid-level point was close to the real optimum point was tested with the path of steepest ascend method.Results showed the original mid-level point was close to the real optimum point, thus this point was used as the center point for the center composite design (CCD). Five levels were included in a CCD, and after 20 runs, a second-order model with good fitness of experimental data was built to approximate the response surface between the factors (cell dry weight (g/L), $(NH_4)_2SO_4$ (g/L) and pH) and response (decolorization (%)). The optimum conditions for decolorizing AY99 by the selected bacterial strain were found to be: 0.48 g/L cell dry weight, 0.51 g/L $(NH_4)_2SO_4$ (g/L) and pH = 7.30. Then, three independent experiments were conducted at the optimum conditions, and the decolorization (%) are found to be 95.7 $\pm$0.37% which is quite close to the predicted value (94.0%).

On the other hand, bacterial cells were also immobilized with polyvinyl alcohol (PVA) and polyacrylamide gels for estimating their potential for practical application. The performance of theses immobilized cells and free cells were determined within 24 h. Besides that, storage stability at 4°C of the immobilized cells and free cells were also investigated. PVA immobilized cells showed good decolorization efficiency even after 20 d storage.

Furthermore, these PVA immobilized cells were employed in a laboratory scale

(1 L) bioreactor. Five hundred mL synthetic AY99 solution was treated by 201.57 g PVA gel cubes containing 320 mg of bacterial cells. Performance of this bioreactor was evaluated as decolorization (%) efficiency, total organic carbon (TOC), the Microtox® EC_{50} test and total dissolved chromium. Besides that, 5 consecutive runs were conducted to evaluate the performance stability of the treatment system.

On the other hand, a newly developed method for speciation of chromium with interferences of Cr(III)-organic complexes was used to determine Cr(VI) in the treated system. The results indicated no detectable Cr(VI) existed in the treated solution.

Chromium distribution in both free cell treated system and immobilized cell treated solution were investigated. The results indicated the formation of high Cr content suspended particles. Beside, adsorbed amount of AY99 on different portion of the treated solution were also studied.

Lastly, the suspended particles generated during degradation were subjected to Fourier transform infrared spectroscopy (FT-IR) analysis for possible functional groups. The results indicated the presence of Cr(III) complexed compounds.

摘要

铬络合偶氮染料被染料制造工业大量的生产，并且广泛的应用于纺织品和毛织品的印染工业。大量的铬络合偶氮染料在生产和处理的过程中流失，造成了工业排水中的污染。一旦这些未经处理的工业污水被排放到开放的水体中，就会造成令人不悦的感官效果。 同时，这些含有染料的污水也会阻碍氧气和光的穿透，从而影响水生生物的生活环境。通常铬络合偶氮染料甚至比他们的母体偶氮染料具有更强的致癌性和毒性，而且更难以被生物降解。此外，铬络合偶氮染料在降解的过程中可能会产生致畸，致癌并且有细胞毒性的芳香胺；并且释放出需要进一步处理的铬。

在这个项目中，具有对一种目标铬络合偶氮染料：酸性黄 99（AY99）最高降解效率的细菌被从淤泥样品 D 中分离出来。淤泥样品 D 是从一个位于中国广东省惠州市的初级印染污水集中处理厂的接触曝气迟采集而来的。在这些有效的细菌中，最有效的两种细菌被分子技术鉴定为荧光假单胞菌 d220。

响应曲面法（response surface methodology，RSM）被用来研究对 AY99 的最优脱色条件。六个影响因素包括：细胞干重 (g/L)，葡萄糖 (g/L)，硫酸铵 (g/L)，营养培养液 (g/L)，酸碱度和实验温度 (°C) 参加了两水准因子实验 (2-level factorial design) 中的最少实验数五级解析度设计 (minimal runs resolution V) 的筛选。这些影响因素中对响应 （脱色率）最重要的被选择来进行下一步的优化。结果，细胞干重 (g/L)，硫酸铵 (g/L) 和酸碱度被发现为最重要的脱色影响因素。接下来，最速前进方向法被用来检测最初的的中间水平点是否已经接近真实的最优响应点。结果是肯定的，于是这个点被用作中心组合设计的中心点。一个

中心组合设计有五个水准，而在 20 次试验后，一个与实验数据具有很高吻合度二阶模型被建立来对脱色影响因素（细胞干重 (g/L)，硫酸铵 (g/L) 和酸碱度）和脱色率（decolorization (%)）之间的响应面进行拟合。所选菌种的最优脱色条件为：0.48 g/L 细胞干重，0.51g/L 硫酸铵和酸碱度为 7.3. 接着，在最优条件下进行了三个独立实验，得到脱色率为 95.7±0.37%，这个结果与模型预测值 (94.0%) 相当接近。

而另一方面，细菌也被聚乙烯醇和聚丙烯酰胺凝胶固定来研究它们在实际应用中的可能性。固定细菌和自由细菌在 24 小时内的脱色效果被确定了，而且酸碱度和实验温度对脱色效果的影响也被进行了研究。另外，固定细菌和自由细菌储存在 4°C 下的稳定性也得到了研究。结果表明被聚乙烯醇凝胶固定的细菌在二十天的储存后依然有很高的脱色效率。

进一步的，这些被聚乙烯醇凝胶固定的细菌被应用到了一个一升的实验室规模的生物反应器中。五百毫升的配置 AY99 溶液与含有 320 mg 细菌的 201.57 g 聚乙烯醇凝胶进行了反应。这个反应器的处理效果由脱色效率，总有机碳，Microtox® 有效中浓度和总溶解铬几个参数来评估。另外，五个连续的实验被用来测试这个反应系统的稳定性。

铬在自由细菌和固定细菌处理的系统中的分布情况也得到了研究。结果显示了含有高浓度的铬的悬浮颗粒的形成。另外，AY99 在反应体系中不同部分的吸附量也得到了测定。

另一方面，一种新的在铬的络合物干扰下进行进行铬的化合物的形态分析的方法被用来测定反应体系的六价铬。结果显示没有六价铬的含量低于方法检出

限。

最后，傅里叶转化红外光谱被用来分析降解产生的悬浮颗粒中可能的官能团。结果指示了与三价铬络合的有机化合物的存在。

Table of contents

List of Figures

List of Plates

List of Tables

1. Introduction

1.1 Pollution generated from dyeing industry

It has been estimated that ca. 15% of the total production of colorants is lost during synthesis and processing, which is corresponding to a worldwide release of ca. 128 tonnes to the environment every day. In dye manufactory industry, the wastewater generation rates are of an order of 1-700 L/Kg of products (Zollinger, 2004). And once those untreated effluents from dyestuff production and dyeing mills were discharged into the open waters, objectionably aesthetic effects could be observed even at ppb level. Meanwhile, the transfer of oxygen and light could be obstructed with the presence of dye effluents affecting the living conditions of aquatic biology (Pandey et al., 2007). Among the various dyes, azo dyes which contain azo group (s) (-N=N-) as well as aromatic ring (s) constitute the largest and most versatile class of dyes, and more than half of the annually produced amount of dyes (estimated worldwide as 1 million tons) are azo dyes (Stolz, 2001). Some azo dyes can exert mutagenic effects in the dyeing effluent, such as, Disperse Blue 373, Disperse Violet 93 and Disperse Orange 37 (Umbuzeiro et al., 2005). Furthermore, aromatic amines which are normally mutagenic, cytotoxic and carcinogenic can be produced during biodegradation of azo dyes, and they are hardly degraded under anaerobic condition (Fitzgerald and Bishop, 1995).

1.2 Occurrences and pollution of chromium azo dyes

In order to enhance the technological performances of azo dyes, including fastness towards wet treatment and light, they were treated with metal ions (primarily chromium ion) to form metal-dye complexes since very early times (Bird, 1968; Christie, 2001).

Nowadays, two manufacturing processes are extensively used to achieve this purpose. The first process is "afterchrome", in which dyes are applied to fiber and treated with sodium dichromate ($Na_2Cr_2O_7$) (Zollinger, 2004) to form chromium-dye complexes on fiber, and the dyes used in this way also called mordant dyes, which to a great extent are azo dyes (Christie, 2001). This afterchrome method has played an important role in dyeing industry for many decades, especially in dyeing loose wool in different dark shards with high fastness properties (Zollinger, 2004). However, dichromate oxidizes the cystine S-S bonds to thiosulfate groups ($S_2O_3^-$), which generate certain damage to the fibers. Although replacements such as other anionic trivalent chromium compounds are possible (Lewis and Yan, 1993), the prices of these reagents are much higher than dichromate. Meanwhile, the presence of residual chromium in the effluent of dyehouse is another pitfall of applying this technique. (Christie, 2001)

Another process is manufacturing pre-metalized dyes. They are mainly synthesized from 2,2'-dihydroxy-, 2-carboxy-2'-hydroxy- and 2-amino-2'-hydroxy-substituted azo dyes and 2,2'-dihydroxy- or 2-carboxy-2'-hydroxy-azomethine dyes (Figure 1.1) with chromium compounds.

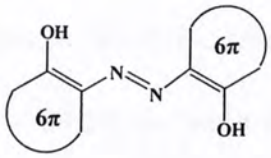

2,2'-dihydroxy azo dye

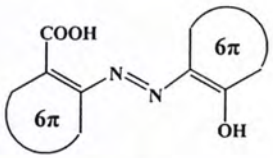

2-carboxy-2'-hydroxy-azo dye

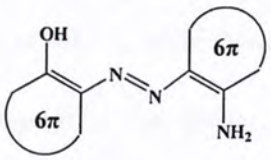

2-amino-2'-hydroxy azo dye

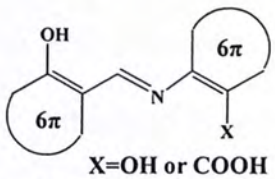

X=OH or COOH

2-carboxy-2'-hydroxy-azomethine dye

Figure 1. 1 Azo dyes commonly used for synthesis of chromium azo dyes.

For most of those ligands, a two step equilibrium has to be postulated as shown in Equations 1.1-1.2. Generally, those 1:1 complexes are stable in acidic media (pH < 4, optimum pH 1-4), whereas the corresponding 1:2 complexes are favored in weakly acidic to alkaline circumstances (pH > 5, optimum pH 5-7) (Zollinger, 2004).

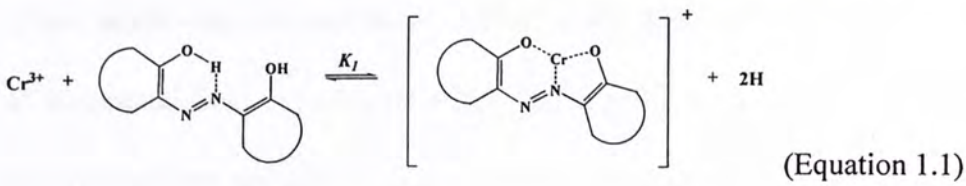

(Equation 1.1)

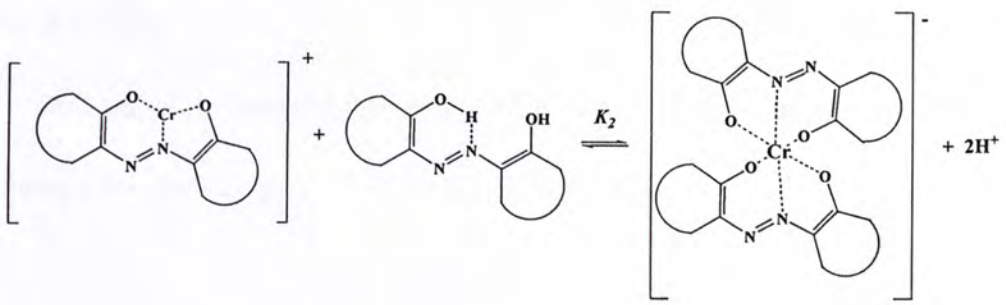

(Equation 1.2)

The pre-metalized chromium azo dyes pocess better features in terms of fastness towards light and water (Kocaokutgen and Ozkinali, 2004). There are more than 80 commonly used chromium azo dyes (Color Index International, update regularly), one of which, Acid Black 194 was ranked top five of the most often manufactured products in the 1990s (Zollinger, 2004). Over a thousand patents concerning synthesis of chromium dye with different colors and properties were registered all over the world.

Part of chromium azo dye generated from the above mentioned processes can lose to effluents during synthesis and processing (Zollinger, 2004). Besides that, it is also possible that Cr(VI) and Cr(III) in industrial effluents react with existed azo dyes following the above mentioned mechanisms to form chromium azo dye.

It was found that coexistence of dyes and chromium was common in textile industrial effluent (Lau and Ismail, 2007). Table 1.1 shows the typical characteristics of wastewater from the effluents of the dyeing and finishing processes. Coexistence of chromium and azo dyes were also typical in dye and pigment industrial (Vajpayee et al., 1999).

Besides, other heavy metals such as Cu, Cd, Zn and Fe were also used to form complexes with azo dyes (Delée et al., 1998).

Table 1.1 Typical characteristics of wastewater from a textile dyeing process (Marcucci et al., 2003).

Aspect/component	Value
pH	2-10
Temperature, °C	30-80
COD, mg/L	50-5000
BOD, mg/L	200-300
Organic nitrogen, mg/L	18-39
Total phosphorus, mg/L	0.3-1.5
Total chromium, mg/L	0.2-0.5
Color, mg/L	>300

However, these chromium azo dye complexes may generate more serious impact on the environment. On one hand, complexation of azo dyes with chromium may further increase the mutagenicity (Edwards et al., 2004) and acute toxicity (Edwards and Freeman, 2005) of the parental azo dyes. On the other hand, chromium azo dye complexes are found to be more recalcitrant towards microbial degradation as shown in Table 1.2 (Yu et al., 2001). In this case, Acid Red 183 (Figure 1.5), which is a chromium azo dye has very similar molecular structure with Acid Yellow 34 (Figure 1.6), whereas its decolorization efficiency by *Pseudomonas* sp. was much lower.

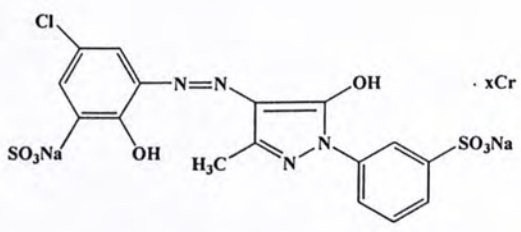

Figure 1.2 Acid Red 183

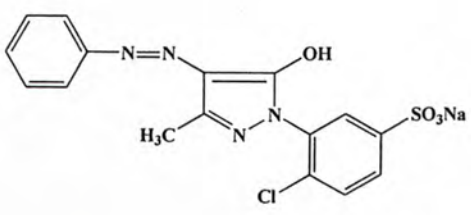

Figure 1.3 Acid Yellow 34

Table 1.2 Decolorization of dyes by *Pseudomonas* sp. (GM3, Q3 and Z1) (% Abs reduction) (Yu et al., 2001))

Dyes	Chromophore	GM3	Q3	Z1
Acid Violet 7	Monoazo	97.4	94.2	99.6
Acid Red 151	Diazo	90.3	91.4	98.9
Reactive Black 5	Diazo	91.1	87.5	94.6
Acid Yellow 34	Monoazo	91.9	90.0	89.5
Acid Red 183	Chromium complex	20.1	22.6	26.7

This might attribute to (1) the released chromium ions may inhibit the strains and/or their azoreductase (Yu et al., 2001); (2) the chromium azo dye complexes have greater steric hinder effect towards enzymatic attacks, and the transition metal will improve the delocalization of electrons, thus make it less reactive.

Another issue with chromium azo dye is the toxicity of the chromium species, which may be released or generated during treatment process. Those chromium species, no matter in hexavalent form (Cr(VI)) or trivalent forms (Cr(III)), can be toxic, thus affect aquatic life as well as human welfare when released without proper treatment (s). Meanwhile, chromium species are under stringent discharge standards in many countries as shown in Table 1.3 (Kurniawan et al., 2006).

Table 1.3 Maximum contaminant level (MCL) of chromium in surface water and their toxicities (Kurniawan et al., 2006).

Heavy metals	Toxicities	Maximum effluent discharge standards (mg/L)		
		EPA [a] (2004) USA	EPD [b] (2004) Hong Kong	PCD [c] (2004) Thailand
Cr (VI)	Headache,nausea, diarrhea, vomiting	0.05	0.05-0.10	0.25
Cr (III)		0.10		0.75

[a] Environmental Protection Agency (EPA), USA.

[b] Environmental protection Department (EPD), Hong Kong Special Administrative Region (HKSAR)

[c] Pollution Control Department (PCD), the Ministry of Natural Resources and Environment, Thailand.

1.3 Common methods for the treatment of dyeing effluents

Treatment of dyes, especially from textile wastewaters, has been a big challenge over the last few decades, a great deal of physicochemical, chemical, physical and biological treatment processes aiming at decolorizing and detoxifying the dyeing effluents have been reported. In this section, each category of treatment methods will be briefly reviewed while more details of various biological processes will be given.

1.3.1 Physicochemical methods

The coagulation/flocculation method is the most representative physicochemical method, which is widely used in textile wastewater treatment plants in many countries such as Germany and France. It can be used either as a pre-treatment, post-treatment, or even as a main treatment system (dos Santos et al., 2007).

Traditionally, coagulant agents like ferric or aluminium salts are used to form flocs with the dyes which may float to the top of the liquid, settled to the bottom or be readily filtered from the liquid. Three consecutive stages are necessary in conventional coagulation/flocculation process: (1) vigorous turbulence to achieve mixing of the coagulant and wastewater; (2) a soft mix is used to favor flocculation of the destabilized pollutants; and (3) particulate pollutants are separated by settling or dissolved air flotation (Rossini et al., 1999). The primary drawbacks of this method are the large demand of chemical input as well as production of high volumes of sludge which requires further treatment (Robinson et al., 2001). Electrochemically assisted coagulation (electrocoagulation) which consists of the *in situ* generation of coagulants by the electrodissolution of a sacrificial anode, usually of iron or aluminium has been proposed as an alternative to the conventional method (Chen, 2004). Electrocoagulation process involves reactions summarized in Equations 1.3-1.5, with the oxidation of the metallic anode (M = Fe or Al), and the reduction of water as the main reactions (Canizares et al., 2009).

Anode: $M \rightarrow M^{3+} + 3e^-$ (Equation 1.3)

$2H_2O \rightarrow O_2 + 4H^+ + 4e^-$ (Equation 1.4)

Cathode: $H_2O + e^- \rightarrow \frac{1}{2}H_2 + OH^-$ (Equation 1.5)

The simple equipment requirement and the easy automation of the process stand out among the main advantages described. This process requires no addition of

chemicals and the dosage of coagulant can be easily controlled by varying the current intensity. In this aspect, the low current requirement allows this process to be energized by green energy such as solar, wind power as well as fuel cells, and when it is cooperated with fuel cells, the hydrogen gas generated (as shown in Equation 1.5) can be used in fuel cells to further reduce energy cost (Canizares et al., 2009). Another advantage of electrocoagulation is the mild turbulence caused by gases (O_2 and H_2), which can promote the formation of flocs (Saur et al., 1996) and carry flocs to the water surface (Chen et al., 2002). Besides that, electrocoagulation produces a smaller amount of sludge due to the higher content of dry solids (Mollah et al., 2001). Canizares et al. (2009) has reported that the performance of this two processes in terms of reducing the turbidity, COD and dye concentration are similar, while the operational costs of these two methods are of the same order of magnitude.

1.3.2 Chemical methods

Oxidation is the most typical chemical process for decolorization. It has been reported that modern dyes are resistant to mild oxidation process such as biological oxidation involved in activated sludge system (Anjaneyulu et al., 2005). Thus, more powerful oxidation agents such as chlorines, ozone, UV/H_2O_2 and other oxidation techniques and combinations should be applied to accomplish decomposition of color compounds. Table 1.3 summarizes the oxidation power of different oxidants, in which hydroxyl radical (·OH) shows excellent oxidation power.

Table 1.4 Oxidation capacities of different oxidants in terms of electrochemical oxidation potential (EOP) (Metcalf and Eddy, 2003).

Oxidizing agent	EOP (V)
Fluorine (F_2)	3.06
Hydroxyl radical ($\cdot OH$)	2.80
Oxygen (atomic) (O)	2.42
Hydrogen peroxide (H_2O_2)	1.78
Hypochlorite (ClO^-)	1.49
Chlorine (Cl_2)	1.36
Chlorine dioxide (ClO_2^-)	1.27
Oxygen (molecular) (O_2)	1.23

1.3.2.1 Ozonation

Ozone is the one of the most widely used oxidants due to its high oxidation power and thus more reactive with many dyes, usually providing good colour removal efficiencies (Alaton et al., 2002). However, its high cost and inadequacy in oxidizing non-soluble disperse dyes and vat dyes limit its applications (Hassan and Hawkyard, 2002; Anjaneyulu et al., 2005). The major advantage of ozonation over other decolorization processes is the zero production of sludge and negligible increase of wastewater volume, while the short life span of ozone (typically being 20 min) requires continuous input of high expenditure (Anjaneyulu et al., 2005). It can selectively oxidize unsaturated bonds (e.g. –C=C– or –N=N–) and aromatic

structures (Adams and Gorg, 2002). The ozonation process leads to complete decolorization with a very short retention time, however effective mineralization of the dye was not observed (Peralta-Zamora et al., 1999). Typical ozonation products are dicarboxylic acids and aldehydes, which explains the little reduction of COD (0-20%) but substantial increase of BOD (biodegradability) during ozonation (Perkowski et al., 1996). Ozone can react directly with dyes or decompose at pH above 7-8 to hydroxyl radicals (·OH), which is also an effective oxidizing agent (Staehelin and Hoigne, 1982). Approximate cost analysis was made based on the electricity cost of the ozone generation and was found that 20.43 kW was needed per ton of wastewater to be treated (Hsu et al., 1998).

1.3.2.2 Fenton reaction

Compared with ozonation, Fention reaction is relatively cheap and also has high COD removal and decolorization efficiencies (dos Santos et al., 2007). The mechanism of Fention reaction is shown in Equation 1.6, in which hydrogen peroxide is added in an acid solution (pH 2-3) containing Fe^{2+}.

$$Fe^{2+} + H_2O_2 \rightarrow Fe^{3+} + \cdot OH + OH^- \qquad \text{(Equation 1.6)}$$

The result of a comparative study of the oxidation of disperse dyes by an electrochemical process, ozone, hypochlorite and Fenton's reagent indicated that the Fenton's reagent was the best among the oxidation processes studied in terms of

COD reduction and color removal (Balcioglu et al., 2001). Several full-scale Fenton reaction plants were established in South Africa to treat textile mill effluents (Gravelet Blondin et al., 1996). This technology was found to be effective in decolorizing a wide range of dyes (Namboodri and Walsh, 1995). The major drawback of applying Fenton reaction in treatment of dyeing effluent is the high sludge generation due to the flocculation of reagents and dye molecules (Robinson et al., 2001), as well as the need for decreasing the bulk pH to acidic conditions. Estimated total running cost, not including sludge disposal is around US$ 0.4/m^3, and this value is cheaper than conventional treatments such as coagulation (Lin and Peng, 1995; Vandevivere et al., 1998). The use of solar energy as assistance with Fenton reaction was proved to be clearly beneficial for the removal of color, aromatic compounds (UV_{254}) and TOC (Torrades et al., 2004). It has been reported that pre-ozonation of colored wastewaters prior to Fenton reaction not only considerably accelerated the overall color removal rates, but also decreased the sludge generation (Hassan and Hawkyard, 2002).

1.3.2.3 Sodium hypochlorite (NaOCl)

This method generates OCl^- to attack at the amino group of the dye molecule. It initiates and accelerates azo bond cleavage. Increase of chlorine concentration and decrease of pH value have reported to promote decolorization process (Robinson et al., 2001). The use of chlorine containing compounds for dye removal is becoming less frequent due to the negative effects they has when released into waterways

(Slokar and Le Marechal, 1998) and the release of aromatic amines which are carcinogenic, or otherwise toxic molecules (Banat et al., 1999).

1.3.2.4 Photocatalytic oxidation (PCO)

UV light has been used in combination of solid semiconductor catalysts such as TiO_2 for the decolorization of industrial effluents (Davis et al., 1994; Arslan et al., 2000). The results indicate that PCO is promising for potential full-scale application. Besides that, different combinations such as ozone/TiO_2, ozone/TiO_2/H_2O_2 have also been investigated, but all those processed are enormously influenced by the type of dye, dye concentration and pH (Galindo et al., 2000). TiO_2 during photocatalysis generates electron (e^-) and hole (h^+) pairs when irradiated by the light of wavelength shorter than 380 nm. The organic pollutants are thus oxidized via direct hole transfer or in most cases attacked by the ·OH formed in the irradiated TiO_2 (Xu, 2001). Many other semiconductors, like zinc oxide (ZnO) and tungsten oxide (W_2O_3) can initiate decomposition, and often the complete mineralization of organic compounds when illuminated with light having energy higher than the band gap energy of semiconductor (Anjaneyulu et al., 2005). Increased interest has been put into PCO process due to the fact that the process is carried out under ambient conditions, does not require expensive oxidants, and catalyst is inexpensive and non-toxic which can be activated by light. Recently, sunlight and other visible light sources irradiated PCO processeses which have been proposed and investigated as a betterment of traditional UV-based methods attract attentions (Wang, 2000; Villanueva and

Martinez, 2006; Pare et al., 2008). The photocatalytic process can be used as the post-treatment process for wastewaters, since it is the most effective method for treating the low concentration pollutants (Anjaneyulu et al., 2005).

1.3.3 Physical methods

The most representative and promising physical methods for treatment of dyeing industrial wastewater are adsorption and membrane filtration. Typical adsorbent is activated carbon (AC), while some other alternative low cost materials have also been investigated. For membrane filtration techniques, ultrafiltration, nanofiltration and reverse osmosis have been used for water reuse and chemical recovery in textile industry.

1.3.3.1 Adsorption

High affinity of many dyes towards adsorbent materials is the foundation of applying adsorption technique for color removal. The efficiency of this process can be influenced by many factors including dye-adsorbent interactions, adsorbent surface area, particle size, temperature, pH and contact time (dos Santos et al., 2007). The critical criteria for the selection of an adsorbent should be the characteristics such as high affinity and capacity for target compounds and the possibility of adsorbent regeneration (Karcher et al., 2001). AC is the most common adsorbent and can be very effective for many dyes (Walker and Weatherley, 1997). High removal rates are observed for cationic mordant and acid dyes, while moderate removal was

achieved for sulfur, dispersed, direct and reactive dyes (Raghavacharya, 1997). However, its efficiency is directly dependent upon the type of carbon material used and the wastewater characteristics (Robinson et al., 2001). Besides that, AC is relatively expensive and has to be regenerated by the expensive thermal desorption process off-site with about 10% loss. Waste by-products were investigated as an effective and economically cheap alternative of AC. Bagasse (pith) is an agricultural/industrial by product produced in large amount by the sugarcane mills. Removal of dyestuff from aqueous solution using bagasse was studied extensively, which was found to be an ideal adsorbent for the removal of basic dyes from aqueous solution (Khattri and Singh, 1999). Another alternative is peat which has good ability to adsorb polar compounds from dye containing effluent. Peat costs much less than AC and requires no activation, although it has found to be less effective than AC for removal of dyes from wastewater (Viraraghavan and Mihial, 1995; Bousher et al., 1997).

1.3.3.2 Membrane filtration

Membrane filtration has been successfully applied for recovering and reusing chemicals and dyes for producing reusable water. This method cannot only clarify and concentrate the dyes, but also separate the dyes from effluent in a continuous way (Xu et al., 1999). In recent years, pressure-driven membrane processes such as ultrafiltration (UF) and nanofiltration (NF) have been studied extensively in the field of textile wastewater treatment (Lopes et al., 2005; Mo et al., 2008; Sahinkaya et al.,

2008; De Souza et al., 2009; Pazdzior et al., 2009). Both UF and NF showed good efficiency for color removal (almost 100%), and membrane filtration was proven to be better performed when followed a biological treatment or coagulation/flocculation. The major drawbacks of membrane filtration method are the high investment costs, the potential membrane fouling, disposal problem of concentrated dyes generated and inefficiency in reducing dissolved contents (Anjaneyulu et al., 2005; dos Santos et al., 2007)

The advantages and disadvantages of these physicochemical, chemical and physical methods are summarized in Table 1.5.

1.3.4 Biological treatments

When compared with those non-biological methods mentioned in previous sections, biological methods are generally more cost-effective and efficient even at low concentrations with the production of negligible secondary pollution. This section will mainly focus on decolorization of azo dyes by bacteria in anaerobic, anoxic and aerobic conditions. Their mechanisms will be reviewed. In addition, studies that investigated roles of fungi and algae in decolorization process are summarized.

1.3.4.1 Decolorization of azo dyes by bacteria

Efforts to isolate bacterial cultures capable of degrading azo dyes started in the

Table 1.5 Advantages and limitations of some physicochemical, chemical and physical decolorization process applied to textile wastewaters (Robinson et al., 2001; Anjaneyulu et al., 2005; dos Santos et al., 2007).

Physical/chemical methods	Stage of treatment	Advantages	Limitations
Coagulation/flocculation	Pre/main treatment	Short detention time and low capital costs Good removal efficiencies	Dewatering and sludge handling problems
Ozonation	Main/post treatment	Effective for azo dye removal	Not suitable for dyes with low solubility Inefficient minerization
Fention's reagent	Pre/main treatment	Effective decolorization of variety of dyes	Sludge generation
NaOCl	Post treatment	Initiation and acceleration of azo-bond cleavage	Release of aromatic amines
Photocatalytic oxidation	Post treatment	Complete minerization with short times. Effective even with low concentrations of pollutions	Expensive process
Activated carbon	Pre/post treatment	Economically attractive Good removal efficiency	Cost intensive regeneration process
Membrane filtration	Main/post treatment	Recovery and reuse of chemicals and water at high efficiencies	Disposal of concentrate stream Inadequate for dissolved contents High running costs Membrane fouling problem

1970s with study of *Bacillus subtilis* (Horistsu et al., 1977). Numerous bacteria capable of decolorization have been reported during the last few decades (Banat et al., 1996). Reductive cleavage of the –N=N– bond is the initial step of the bacterial degradation of azo dyes. Decolorization of azo dyes occurs under anaerobic (methanogenic), anoxic and aerobic conditions by different trophic groups of bacteria.

1.3.4.1.1 Under anaerobic conditions

Dye decolorization under anaerobic conditions requires an organic carbon/energy source (Pandey et al., 2007). Simple substrates like glucose, starch, acetate and ethanol, more complex ones have been used for dye decolorization under anaerobic conditions (Talarposhti et al., 2001; Yoo et al., 2001; Isik and Sponza, 2005; van der Zee and Villaverde, 2005).

Extensive studies have been conducted to investigate the mechanisms of those anaerobic decolorization processes. Some studies have associated decolorization with methanogenic and acidogenic bacteria (Bras et al., 2000; Chinwekitvanich et al., 2000), whereas the use of molecular methods to characterize microbial populationin anaerobic reactors treated industrial dye waste showed that the dominant members are sulfate-reducing bacteria (SRB) (Plumb et al., 2001). The latter results was also in accordance with the results of decolorization inhibitory effects using inhibitor specific to methanogens and SRB, which indicated the importance of SRB in

anaerobic bacterial culture for decolorizing industrial effluents (Yoo et al., 2001).

Reduction under anaerobic conditions appears to be non-specific, as majority of a varied group of azo compounds are decolorized, although the rate of decolorization is dependent on the added organic carbon source, as well as the dye structure (Bromley-Challenor et al., 2000; Stolz, 2001). Anaerobic azo dye decolorization is generally regarded as non-specific extracellular reactions occurring between reduced compounds generated by anaerobic biomass (van der Zee et al., 2001), or as a process where dye might act as an acceptor of electrons supplied by carriers of the electron transport chain (Pandey et al., 2007). In most cases, first-order kinetics with respect to dye concentration has been generally reported for the course of dye decolorization, whereas zero order was also observed in few studies (van der Zee et al., 2001; Isik and Sponza, 2005). It has also been reported that quinine-like compounds formed during azo dye reduction can act as redox mediators, thus contributes to a significant extent to the overall reduction process (van der Zee et al., 2000; Mendez-Paz et al., 2005).

1.3.4.1.2 Under anoxic conditions

Anoxic decolorization of various azo dyes associated with mixed aerobic and facultative anaerobic microbial consortia in many cases (Nigam et al., 1996; Kapdan et al., 2000; Khehra et al., 2005; Moosvi et al., 2005). Although most of these cultures were able to grow in aerobic conditions, decolorization was achieved under

conditions with extremely low oxygen concentration. Pure bacterial cultures, such as *Pseudomonas luteola*, *Aeromonas hydrophila*, *Bacillus subtilis*, *Pseudomonas* sp. and *Proteus mirabilis*, decolorized azo dyes under anoxic conditions (Yu et al., 2001; Chen et al., 2003).

Azo dye decolorization generally required complex organic source and carbohydrate (Chen et al., 2003; Khehra et al., 2005). In anaerobic conditions, glucose is favored, while its suitability for anoxic decolorization by facultative anaerobes and fermenting bacteria seems to vary depending on the bacterial culture. For example, *Sphingomomas xenophaga* Strain BN6 used to decolorize Mordant Yellow 3 was greatly enhanced by glucose. However, for *Pseudomonas luteola*, *Aeromonas* sp. and few other mixed cultures, a significant decrease in azo dye decolorization in the presence of glucose was reported (Kapdan et al., 2000; Chen et al., 2003). This negative effect was attributed either to pH effect of acid formation, or to catabolic repression (Chen et al., 2003). Presence of aromatic amines as well as partially reduced products was identified from culture filtrates after the decolorization of azo dyes by *Pseudomonas luteola* (Chang et al., 2001), which is also an evidence of the two-step reduction mechanism of azo bond first proposed by (Gingell and Walker, 1971). The azo bond cleavage involves a transfer of four electrons (reducing equivalents), which proceeds through two stages at the azo linkage. In each stage two electrons are transferred to the azo dye, which acts as a final electron acceptor as shown in Equations 1.7 and 1.8.

$$R_1 - N = N - R_2 + 2e^- + 2H^+ \rightarrow R_1 - HN - NH - R_2$$
(Hydroazo intermediate) (Equation 1.7)

$$R_1 - HN - NH - R_2 + 2e^- + 2H^+ \rightarrow R_1 - NH_2 + R_2 - NH_2$$
(Reductive cleavage of the azo bond) (Equation 1.8)

1.3.4.1.3 Under aerobic conditions

In the past few years, various bacterial strains that can aerobically decolorize azo dyes by reductive mechanisms have been isolated. Many of these strains require organic carbon sources, such as glucose, as they cannot use dye as the sole growth substrate (Stolz, 2001). Zissi et al. (1997) have isolated a *Bacillus subtilis* strain which can reductively cleave *p*-aminoazobenzene to aniline during aerobic growth on glucose. Similarly, strains of *Acetobacter liquefaciens* and *Klebsiella pneumoniae* were found to be able to reductively cleave Methyl Red to its corresponding aromatic amines during aerobic growth on glucose (So et al., 1990; Wong and Yuen, 1996). Furthermore, the reductive decolorization of sulfonated azo dyes (e.g. Acid Orange 7, Acid Orange 10, Acid Red 88) by different bacterial strains (*Sphingomonas* sp. 1CX, *Bacillus* sp. OY1-2, *Xanthomonas* sp. NR25-2, *Pseudomonas* sp. PR41-1, *Pseudomonas aeruginosa*) under aerobic conditions in the presence of additional carbon sources has been reported (Coughlin et al., 1999; Sugiura et al., 1999; Nachiyar and Rajkumar, 2003). These studies are summarized in Table 1.6.

Table 1.6 Studies using bacterial culture to decolorize azo dyes under aerobic condition.

Culture	Dye(s)	Decolorization (%) /time (h)	Reference
Acetobacter liquefaciens S-1	Methyl Red	100 / 13-24	So et al., 1990
Klesiella pneumoniae RS-13	Methyl Red	100 / <50	Wong and Yuen, 1996
Bacillus subtilis	*p*-Aminoazobenzene (pAAB)	>90/ 24	Zissi et al., 1997
Sphingomonas sp. 1CX	Orange II Acid Orange 8 Acid Orange 10	97/ 62 99/ 62 99/ 62	Coughlin et al., 1999
Bacillus sp. OY1-2 *Xanthomonas* sp. NR25-2 *Pseudomonas* sp. PR41-1	Methyl Red Roccellin NS 200 Sumifix Red B Remazol Golden Yellow G Sumifix Black B	Efficient decolorization (data not show)	Sugiura et al., 1999
Pseudomonas aeruginosa	Navitan Fast Blue S5R 100 mg/L	92 / 48	Nachiyar and Rajkumar, 2003

On the other hand, few studies have found bacteria capable of using azo dyes as the sole source of carbon and energy while degrading them. These bacteria cleave –N=N– bonds reductively and use amines as the source of carbon and energy for their growth. Such organisms are specific towards their substrates. *Xenophilus azovoras* KF 46 and *Pigmentiphaga Kullae* K24 are examples of this kind of strains

(Zimmermann et al., 1982; Kulla et al., 1983). They can grow aerobically on carboxy-orange I and II, respectively. More recently, Adedyo et al. (2004) have isolated four bacterial species using Methyl Red as the sole carbon source. Two of them were identified as *Vibrio logei* and *Pseudomonas nitroreducens*.

Additionally, certain bacteria, mainly *Streptomyces* species, can produce peroxidase to decolorize azo dyes. This oxidation process involves an extracellular peroxidase that is restrictedly substrate-specific (Pasti-Grigsby et al., 1996).

1.3.4.2 Mechanisms of azo dye reduction by bacteria

The first step in the bacterial degradation of azo dyes is the reduction of –N=N– bonds, no matter in anaerobic, anoxic or aerobic conditions. This cleavage may be achieved by different mechanisms, such as enzymes, low molecular weight redox mediators and biogenic reductants like sulfide, or a combination of these (Figure 1.7). Additionally, the location of the reactions can be either intracellular or extracellular.

The direct enzymatic azo dye reduction involves enzyme-mediated transfer of reducing equivalents, generated from oxidation of the substrate/coenzyme to azo dyes (Pandey et al., 2007). These enzymes can be specific, catalyzing only azo reduction, or non-specfic. Reduced flavins can act as an electron shuttle from nicotinamide adenine dinucleotide phosphate (NADPH)-dependent flavoproteins to azo dye as electron acceptor (Gingell and Walker, 1971). Intracellular azo dye reduction cannot be responsible for the conversion of all types of azo dyes, especially

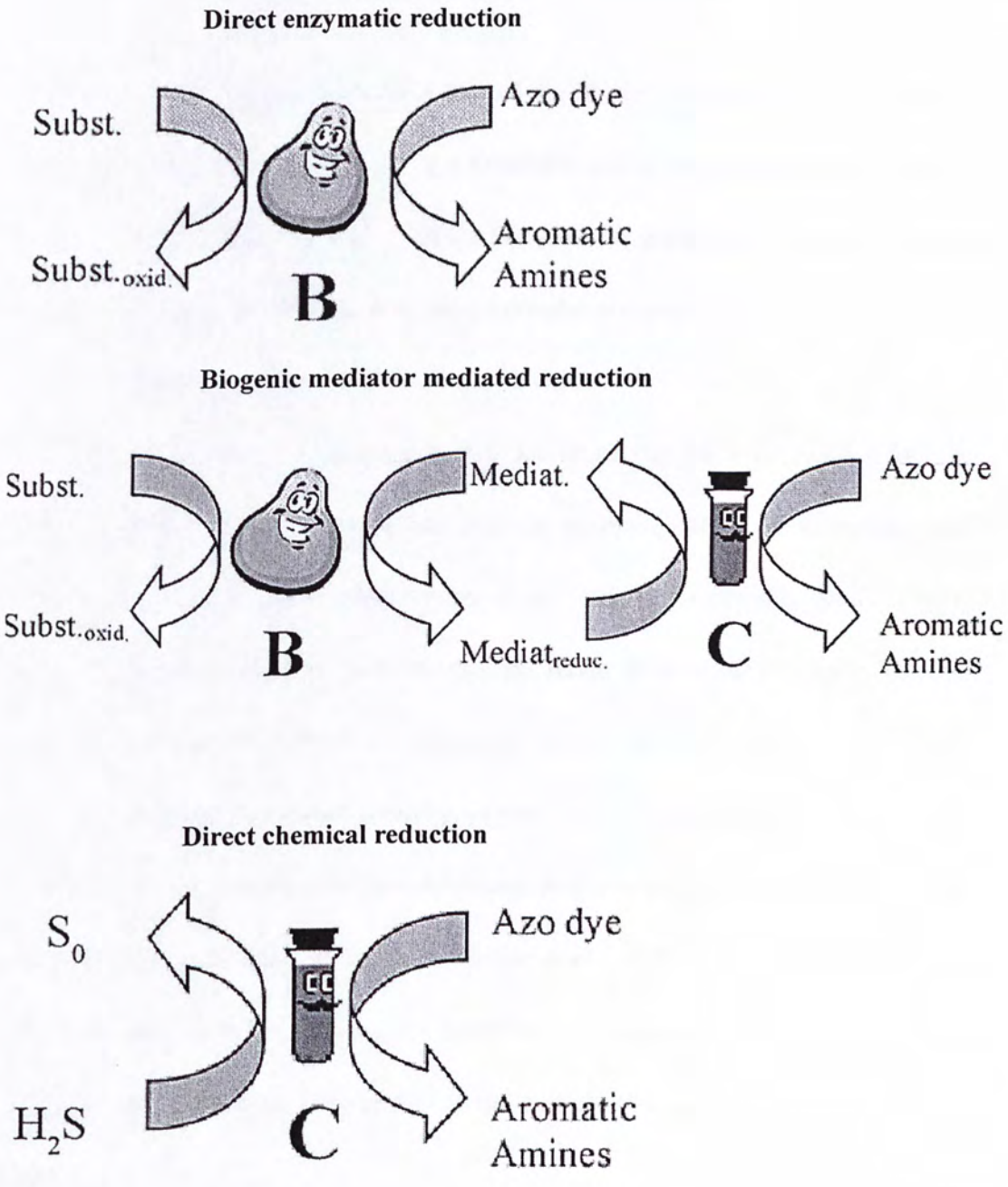

Figure 1.4 Schematic for different mechanisms of azo dye reduction. B and C are biological and chemical steps, respectively. Subst. stands for substrates, while mediat. stands for mediator (dos Santos et al., 2007).

for sulfonated azo dyes, which have limited membrane permeability (Stolz, 2001). The current hypothesis is that azo dye reduction mostly occurs by extracellular or membrane-bond enzymes (Stolz, 2001). Reduced cytoplasmatic cofactors such as reduced flavins do not contribute to the chemical dye reduction due to their inability to cross living cell membranes (Russ et al., 2000).

Redox mediators are compounds that accelerate the electron transfer from a primary electron donor to a terminal electron acceptor, which may increase the reaction rates dramatically (dos Santos et al., 2007). Extensively studies have reported that flavin-based compounds like flavin adenine dinucleotide (FAD), flavin mononucleotide (FMN) and riboflavin, as well as quinone-based compounds like anthraquinone-2-sulfonate (AQS), anthraquinone-2,6-disulfonate (AQDS) and 2-hydroxy-1,4-naphthoquinone (lawsone) have play a role of redox mediators during azo dye reduction (Field and Brady, 2001; Rau et al., 2002; dos Santos et al., 2004). The two steps shown in Figure 1.7 involves a non-specific enzymatic mediator reduction and a chemical re-oxidation of the mediator by the azo dyes (Keck et al., 1997).

Redox potential E_0' values for different azo dyes are generally between -0.430 and -0.180 V (Dubin and Wright, 1975) and the nicotinamide adenine dinucleotide (phosphate) NAD(P)H cofactor has the lowest E_0' value of -0.320 V. Therefore, only

those redox mediators have E_0' value between -0.320 V to -0.180 V can be used effectively. The reason for this is that mediators with a more negative E_0' value will not be reduced by the cell enzymes, while mediators with E_0' value greater than -0.180 V cannot effectively reduce the azo bonds. Figure 1.8 shows the E_0' value for both quinine-based and non quinine-based redox mediators.

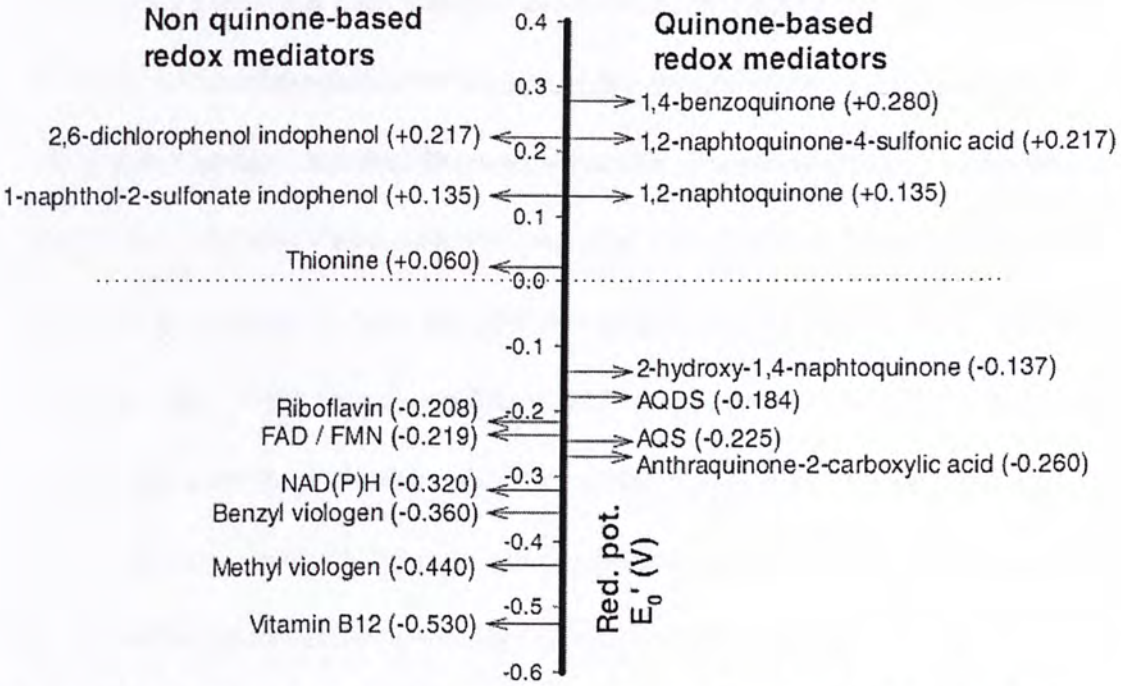

Figure 1.5 E_0' value for both quinine-based and non quinine-based redox mediators (dos Santos et al., 2007).

Besides the above mentioned two mechanisms, biogenic reductants like sulfide, cysteine, ascorbate or ferrous ions also contribute to the reductive decolorization of azo dyes (Yoo, 2002; van der Zee et al., 2003). However, oxygen is more competitive

than azo dyes as electron acceptor, thus these mechanisms seldom occurr in aerobic conditions (dos Santos et al., 2007).

1.3.4.3 Decolorization of azo dyes by fungi and algae

Certain fungi are able to decolorize azo dyes as they can syntheses lignin degrading exoenzymes such as lignin and manganese peroxidases or laccases. The mechanism of the decolorization process starts with the enzyme oxidation by H_2O_2 to an oxidized state during their catalytic cycle. Then, in a mechanism involving two successive electron transfers, azo dyes reduce the enzyme to its original form (Stolz, 2001). Fungi species including *Trametes versicolor*, *Phanerochaete chrysosporium, Geotrichum candidum, Pycnoporus cinnabarinus, Penicillium spp.* (mainly white rot fungi), were reported to have azo dye decolorizing ability (Zheng et al., 1999) (Rodriguez et al., 1999; Swamy and Ramsay, 1999; Schliephake et al., 2000).

Limited amount of work is available on the use of algae for decolorization purpose. Several species of *Chlorella and Oscillatoria* were capable of degrading azo dyes to their aromatic amines and further mineralize them (Jinqi and Houtian, 1992). Some were even capable of utilizing a few azo dyes as their sole source of carbon and nitrogen. Use of such algae in stabilization ponds was proposed by Banat et al. (1996) as they play an important role in aromatic amine removal.

1.4 Chromium species and their impacts on environment

Chromium is widely used in various industries such as metallurgical (steel, ferro-

and nonferrous- alloys), refractories (chrome and chrome magnesite), and chemical (pigments, electroplating, tanning and others). Due to these industrial processes, large quantities of chromium compounds are discharged in liquid, solid, and gaseous wastes into the environment and can ultimately have significant adverse biological and ecological effects. This section will review the toxicity effects of different oxidation state of chromium as well as their speciation. In this context, speciation was defined as an analytical process that consists of identification and quantification of various forms of a given element present in analyzed samples (Kotaś and Stasicka, 2006). Treatment methods of chromium in industrial effluents will be briefly reviewed.

1.4.1 Chromium toxicology and speciation techniques

The importance of chromium speciation lies on the extremely different properties and effects of Cr(VI) and Cr(III). Cr (VI) is highly water soluble, bioavailable while fairly toxic and carcinogenic, while Cr(III) is considered as an essential element with relatively poor water solubility and bioavailability (Shanker et al., 2005; Gómez and Callao, 2006; Kotaś and Stasicka, 2006)

Few techniques including electroanalytical methods such as potentiometry (Gholivand and Raheedayat, 2004; Svancara et al., 2004) and amperometry (Domínguez Renedo et al., 2004), which require selective sensors and/or special electrodes, can determine Cr(III) and/or Cr(VI) directly and selectively with

marginally satisfactory accuracy. Other prevailing instrumental techniques for determining chromium species such as flame/graphite atomic absorption spectrometry (F/GF-AAS), inductively coupled plasma-optical emission spectrometry (ICP-OES) and inductively coupled plasma-mass spectrometry (ICP-MS). These analyses should either (1) directly coupled with a separation system (i.e. on-line methods) such as flow-injection analysis (FIA) (Luo et al., 1997; Prokisch et al., 1997) and high performance liquid chromatography (HPLC) including ion chromatography (IC) (Barnowski et al., 1997), ion-pair chromatography (IPC) (Padarauskas and Kazlauskiene, 1993) and reversed-phase chromatography (RP) (Andrle et al., 1997), or (2) incorporated with a separation-preconcentration pretreatment (i.e. off-line methods) such as cloud-point extraction (Nan and Yan, 2005), solvent extraction (Tsogas et al., 2004), co-precipitation (Ueda et al., 1997) and solid phase extraction (SPE) (Tunçeli and Türker, 2002; Bulut et al., 2007).

However, most of the chromium speciation studies have not taken interferences of Cr(III)-organic complexes into account, although several studies have already demonstrated that organic ligation was critical in the speciation of chromium: Menden et al. (1990) found that methyl isobutyl-ketone (MIBK) extracted considerable amounts of unidentified Cr(III)-organic complexes which were counted as Cr(VI). Milacic et al. (1992) working on leachate from wet blue shavings, found IC and IP-RP-HPLC

suffering from positive interference from organic Cr(III) complexes for Cr(VI) determination. Colorimetric method with addition of 1,5-diphenylcarbazide (DPC) also encountered the positive interferences due to colored organic material. Walsh and O'halloran (1996) investigated DPC spectrophotometry, MIBK extraction, and co-precipitation with iron and bismuth salts and concluded that chromium speciation in the presence of organic chromium complexes can lead to erroneous results. There are possible errors of applying other methods to determine chromium speciation in environmental samples since organic chromium complexes are significant fraction of total chromium in river, soil (Pankow et al., 1977; Bartlett and James, 1979) and especially in tannery and textile dyeing effluent with high organic content (Walsh and O'halloran, 1996). However, in recent studies analyzing tanning water, attentions on organic chromium complexes are negligible, except Bobrowski et al. (2004) who used catalytic adsorptive stripping voltammetry (CAdSV) has proved Cr(III) complexes with organic ligands are almost voltammetrically inactive in their speciation conditions.

This project includes a newly developed method which speciate and determine chromium species with interferences of chromium organic complexes. This method is based on the work of Tunçeli and Türker (2002), which applied Amberlite XAD-16 resin to pre-concentrate the purple complex (Cr(III)-diphenylcarbazone (Cr-DPC)) formed with a specific two step reaction

between Cr(VI) and 1,5-diphenylcarbazide (DPC) (Willems et al., 1977), and subsequently, Cr(VI) was determined by flame atomic absorption spectrophotometry (FAAS).

1.4.2 Common treatment methods for chromium

Several treatment technologies have been developed to remove chromium from water and wastewater, among which, hemical precipitation has traditionally been the most extensively used method (Mohan and Pittman, 2006). Chemical precipitation usually employs the following four major steps. The Cr^{6+} is first reduced to less toxic and less soluble Cr^{3+}, the Cr^{3+} is then precipitated as $Cr(OH)_3$ at high pH, the insoluble metal hydroxides is settled afterwards. Finally the sludge has to be dewatered and disposed of properly (Kongsricharoern and Polprasert, 1993). Because the particle size of sludge produced in the process is relatively small and difficult to settle completely, a filtration process is necessary after sedimentation. Alternative technique like foam flotation has been used in which surfactant is added to increase the contact between the flocs and the bubbles (Kongsricharoern and Polprasert, 1996). More recently, an electrochemical method using iron electrode has attracted significant attention due to its simple operation (Chen et al., 2000; Chen et al., 2002). In the electrocoagulation (EC) cell, iron anodes produce Fe^{2+}. This newly produced Fe^{2+} directly reduce Cr^{6+} to Cr^{3+} resulting in co-precipitation of $Cr(OH)_3$ and $Fe(OH)_3$. Major reactions taking place in the EC cell is shown in Equation 1.9 to

Equation 1.14 (Chen et al., 2000; Chen et al., 2002):

Anode (oxidation): $Fe \rightarrow Fe^{2+} + 2e^{-}$ (Equation 1.9)

Cr^{6+} reduction: $Cr^{6+} + 3Fe^{2+} \rightarrow Cr^{3+} + Fe^{3+}$ (Equation 1.10)

Cathode (reduction): $2H_2O + 2e^{-} \rightarrow H_2 + 2OH^{-}$ (Equation 1.11)

Co-precipitation: $Cr^{3+} + 3OH^{-} \rightarrow Cr(OH)_3$ (Equation 1.12)

$Fe^{3+} + 3OH \rightarrow Fe(OH)_3$ (Equation 1.13)

$Fe^{2+} + 2OH^{-} \rightarrow Fe(OH)_2$ (Equation 1.14)

In this kind of system, iron anode is favored as it is not only a very good reductant for Cr^{6+}, but also an effective coagulant which can greatly increase the settling rate of $Cr(OH)_3$ (Gao et al., 2005). The treated water should be subjected to sedimentation/filtration or flotation process to separate the sludge from the treated water (Gao et al., 2005).

Besides chemical precipitation, chromium removal using adsorption is quite widely used too. Adsorbents including activated carbon (Khezami and Capart, 2005), agricultural by-products (Yu et al., 2003; Unnithan et al., 2004; Sumathi et al., 2005), zeolites (Kesraouiouki et al., 1994), clay minerals and oxides (Erdem et al., 2005; Potgieter et al., 2005) and biosorbents (Brierley, 1990) have been investigated for chromium removal. The major disadvantages of the adsorption method are recovery of the adsorption column as well as further treatment of the backwash water (Gao et

al., 2005). When the concentration of chromium is low, ion exchange is usually adopted. However, the high cost of resins limit its application (Kurniawan et al., 2006).

1.5 Studies concerning treatment of chromium azo dyes

Very limited amount of work have been conducted to treat chromium azo dyes. Arlan-Allaton et al. (2006) used Fenton reaction as a pretreatment of an acid dyebath effluent containing chromium complex azo dyestuff. The pretreated effluent can be degraded appreciably faster (in terms of COD remval) than the untreated solution by long-term activated sludge treatment. Arslan-Alaton and Tureli (2008) used Fenton and Photo-Fenton processes to decolorize a Cr(III)-complex azo dye - Acid Red 183. After 40 min treatment of Fenton's reagent, 98% color and 56% COD were removed. UV-A assisted Fenton treatment Fenton reaction process significantly faster. Ozonation was also used to oxidize chromium azo dyes – Acid Red 180 and HFANS-Cr. With comparison of the their parental compounds without chromium complex, ozone consumption for chromium azo dyes was found to be higher (Yildiz and Boztepe, 2003). However, these three studies only focused on the organic portion of chromium azo dyes while leaving chromium out of consideration. No toxicity tests have been conducted, although it was highly possible that Cr(III) was converted to Cr(VI) under such advanced oxidation processes (AOPs).

Zhao et al. (2005) used heating and acidification as pretreatment to dissociate

chromium azo complex, followed by neutralization-flocculation method to precipitate Cr^{3+} in terms of $Cr(OH)_3$. The residual chromium in the wastewater was dropped below 1.0 mg/L after the treatment. This study did not take the organic portion of chromium azo dyes into account.

Microbial decolorization of a chromium azomthine dye was also investigated using an aerobically grown mixed bacterial culture (Matanic et al., 1996). The decolorization was around 27-50%, while Cr(III) concentration was found to be higher at the end of the treatment due to chromium release by partial degradation of the dye, followed by partial adsorption by bacterial cells and subsequent release by bacterial cell decay.

1.6 Response surface methodology (RSM)

The development of RSM began with the publication of a landmark article by Box and Wilson (1951). It is a collection of statistical and mathematical techniques useful for developing, improving, and optimizing processes. It also has important applications in design, development, and formulation of new products, as well as in the improvement of existing product designs (Myers et al., 2008). As an example, Figure 1.9 shows graphically the relationship between the response variable yield (y: decolorization) in a microbial degradation process and two process variables (or factors), pH (x_1) and cell dry weight of the added bacterial cells (x_2). It should be noticed that for each value of x_1 and x_2, there is a corresponding value of response

value (y), and these values of response can be viewed as a surface lying above the x_1 -

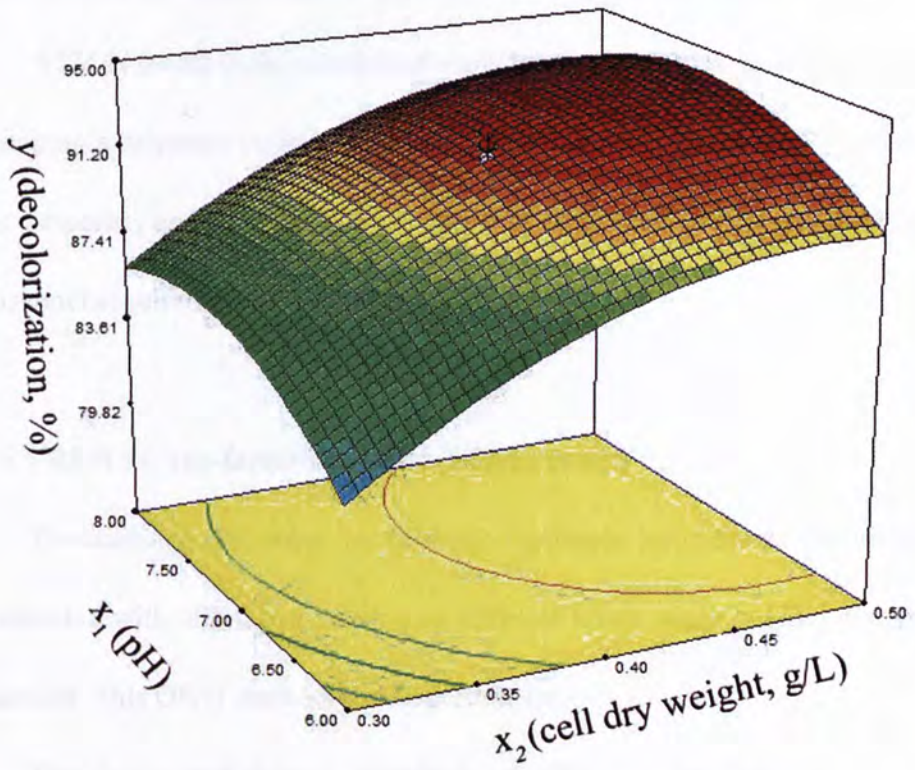

x_2 plane, as in Figure 1.9. It is the graphical perspective of RSM.

Figure1.6 A response surface showing the relationship between decolorization (%) of the microbial degradation process and the two process variables pH (x_1) and cell dry weight of the added bacterial cells (x_2).

Clearly, if the graphical display in Figure 1.9 can be constructed, it is very straightforward to find the optimum conditions as well as the optimum response. The field of response surface methodology consists of the experimental strategy for exploring the space of the process or independent variables, empirical statistical modeling to develop an appropriate approximating relationship between responses and variables, and optimization methods for finding the values of the variables that

can produce desirable values of the responses (Myers et al., 2008).

RSM is useful in the solution of many types of industrial problems, including (1) mapping a response surface over a particular region of interests; (2) optimization of the response, and (3) selection of operating conditions to achieve specifications or customer requirements.

1.6.1 RSM vs. one-factor-at-a-time (OFAT) design

Traditionally, in order to find the optimum conditions, experiments were conducted with one factor varying to different levels while holding everything else constant. This OFAT method is inferior to RSM.

The most predominant drawback of OFAT is its inability to detect the interactions of factors, which in many cases are surprisingly vital. To illustrate this point, an example will be excerpted from the work of Anderson and Whitcomb (2007). Take the most common response surface, which is the rising ridge as shown in Fig. 1.10, as an example.

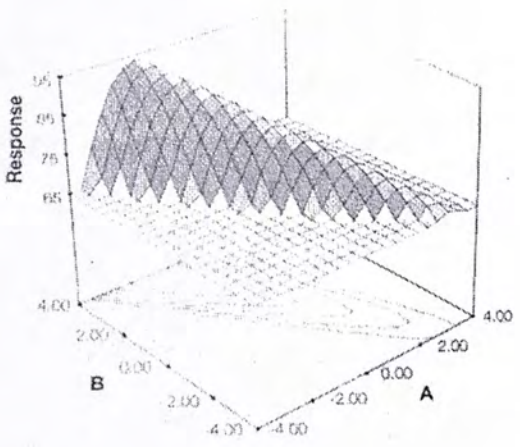

Figure 1.7 A rising ridge surface response lying upon the plane of factors A and B.

The corresponding predictive model for this surface can be described as Equation 1.15:

$$\hat{y} = 77.57 + 8.80A + 8.19B - 6.95A^2 - 2.07B^2 - 7.59AB \qquad \text{(Equation 1.15)}$$

Assuming the OFAT experiment starts with factor A and varying it systematically over 9 levels from -2 to 2 while holding factor B at mid-level (0), the resulting response curve can be seen on Figure 1.8.

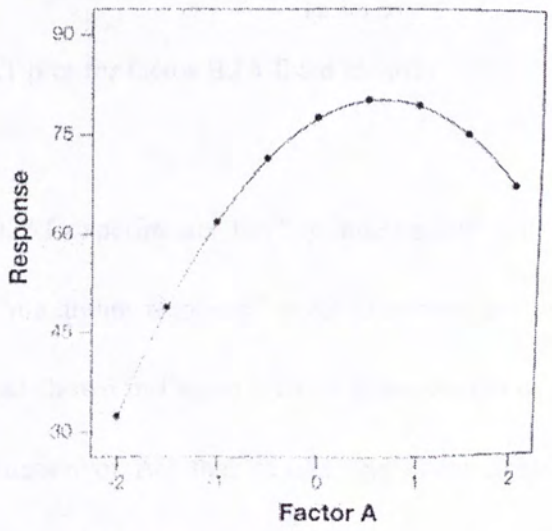

Figure 1.8 OFAT plot after experimenting on factor A.

Observing from this curve, the maximum point can be found at 0.63. Then fix factor A at 0.63 while varying B over 9 levels from -2 to 2. The results of the second OFAT experiment is shown in Figure 1.12

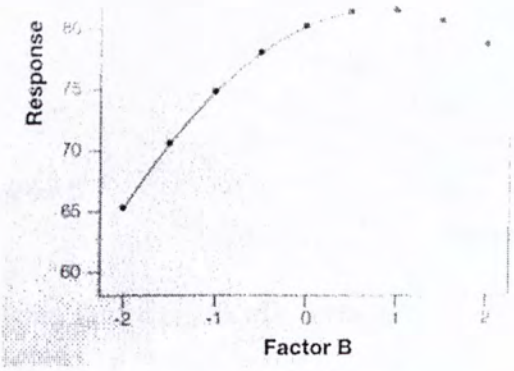

Figure 1.9 OFAT plot for factor B (A fixed at 0.63).

After the OFAT experiments, the "optimum point" will be found at A = 0.63 and B = 0.82 with "maximum response" at 82. However, the real optimum is far higher than this value as shown in Figure 1.13. A better design of experiments is needed to detect the interaction of AB that causes this unanticipated increase. RSM which simultaneously vary both A and B and analyze the results with statistical and mathematic tools is an effective alternative.

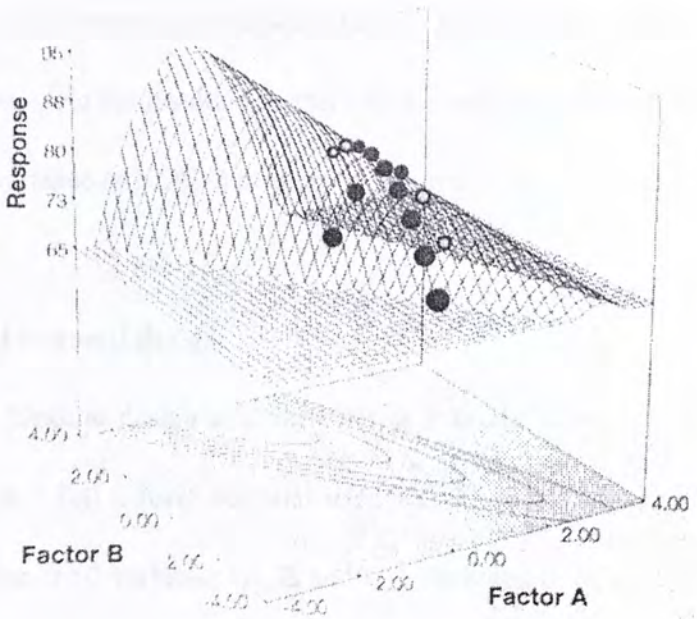

Figure 1.10 OFAT point shown on the true surface.

1.6.2 Phases of RSM

RSM generally involves 3 phases: the first one, which is referred as phase zero, is a screening experiment. The objective of the screening experiment is to reduce the list of candidate variables to a relative few that are more important, so that subsequent experiments will be more efficient and require fewer runs or tests. The screening experiment is often conducted with a 2-level factorial design. Once the important variables (factors) are identified, RSM can formally started with phase one, which is to determine if the current levels of variables resulted in a value of response that is near the optimum. Path of steepest method is useful to achieve this goal. When the process is near the optimum, phase two of a response surface study begins. At

this point a second-order model will be obtained with the help of a sophisticated higher level design (central composite design (CCD) in most cases) to predict the response surface. And the resulting model may be analyzed with statistical tests such as analysis of variance (ANOVA) to exam its fitness.

1.6.3 Two-level factorial design

Two-level factorial design sets variables at 2 levels: high (+) and low (-), and runs required in a full 2-level factorial design is 2^n, in which n is the number of variables. If there are 3 variables (A, B and C) included in a full 2^3 design, 3 main effects (A, B and C), 3 2-factor interaction effects (AB, BC and AC) and 1 3-factor interaction (ABC) can be estimated. The experimental design of 2^3 design in order to estimate effects of factors and interactions can be expressed in Table 1.7.

Table 1.7 Test matrix in standard order with coded levels (+ and -).

Standard runs	Main effects			Interaction effects				Response
	A	B	C	AB	AC	BC	ABC	Y
1	-	-	-	+	+	+	-	y_1
2	+	-	-	-	-	+	+	y_2
3	-	+	-	-	+	-	+	y_3
4	+	+	-	+	-	-	-	y_4
5	-	-	+	+	-	-	-	y_5
6	+	-	+	-	+	-	-	y_6
7	-	+	+	-	-	+	+	y_7
8	+	+	+	+	+	+	+	y_8
Coefficient	β_a	β_b	β_c	β_{ab}	β_{ac}	β_{bc}	β_{abc}	β_0

It can be observed that for main effects, the first factor change sign every other row, the second factor every second row, the third factor every fourth row, and so on, based on power of 2. While for interactions, the signs are determined by multiplying the parent terms, e.g. for row 1, sign of interaction ABC is calculated from -A × -B × -C which is a "-". To calculate coefficients, which quantify the effects of factors, the following equation will be used (Equation 1.16):

$$\beta_i = \frac{\sum y_+}{n_+} - \frac{\sum y_-}{n_-} \qquad \text{(Equation 1.16)}$$

For example, $\beta_a = \frac{y_2 + y_4 + y_6 + y_8}{4} - \frac{y_1 + y_3 + y_5 + y_7}{4}$, the intercept is calculated from the mean of response, $\beta_0 = \frac{\sum_{i=1}^{n} y_i}{n}$. After calculation, a first-order model with 3 variables A, B, C and their interaction can be expressed in the following equation

$$\hat{y} = \beta_0 + \beta_a A + \beta_b B + \beta_c C + \beta_{ab} AB + \beta_{ac} AC + \beta_{bc} BC + \beta_{abc} ABC \qquad \text{(Equation 1.17)}$$

On the other hand, β_i and β_0 in this first-order model can be calculated by the method of least squares which will be introduced later.

However, when the number of factors increases, the number of runs will dramatically increase in a full 2-level factorial design (e.g. 128 experiments are needed when 7 factors are included for the 2^7 design). And some of those runs are

used to estimate 3-factor interactions or higher interactions which were proven to be of negligible significance towards the response (Anderson and Whitcomb, 2007). In this case, fractional factorial designs or mimimal-run designs which can cut down the run numbers may be applied.

Both fractional factorial designs and mimimal-run designs eliminate certain runs in the matrix of the full factorial design, resulted in aliases, which refer to identical calculation equation for effects of different terms. For example, if we cut off the runs in which ABC are "-" in Table 1.6, in the resulting 4 rows, some columns will have exactly the same designs (e.g. A = BC, B = AC, C = AB). Thus these effects can not be differentiated. In order to minimize the effects of aliases, main effects and 2 factor interaction effects should not aliase with other main effects and 2 factor interaction effects. Because they are more vital towards the response (their coefficients are relatively bigger).

In 2002, a new design called minimal run resolution V (MR5) design was proposed by Oehlert and Whitcomb (2002). This design prevents aliasing of main effects and 2 factor interactions with the lowest run number. Both main effects and 2 factor interaction effects are only aliased with 3 factor interactions and higher interactions. For 6 factors, only 26 runs are required with 4 replicates of center points (vs. 64+4 runs in a 2^6 factorial design)

The ability to estimate curvature is a feature of 2-level factorial design. If replicates of center points are added into a 2-level factorial design, curvature can be

estimated by comparison between the real response of the mid-level variables and the response generated with the first-order model at mid-level. If the curvature term is significant, the response surface is better to be approximated with a second-order model from designs like CCDs.

1.6.4 Path of steepest ascent (PSA)

Box and Wilson (1951) proposed the path of steepest ascent method to move the mid-level point to the region near to the real optimum. Starting from the original mid-level point, a few steps (with same distance from each other) are taken along a line that is perpendicular to the contour lines (Figure 1.14).

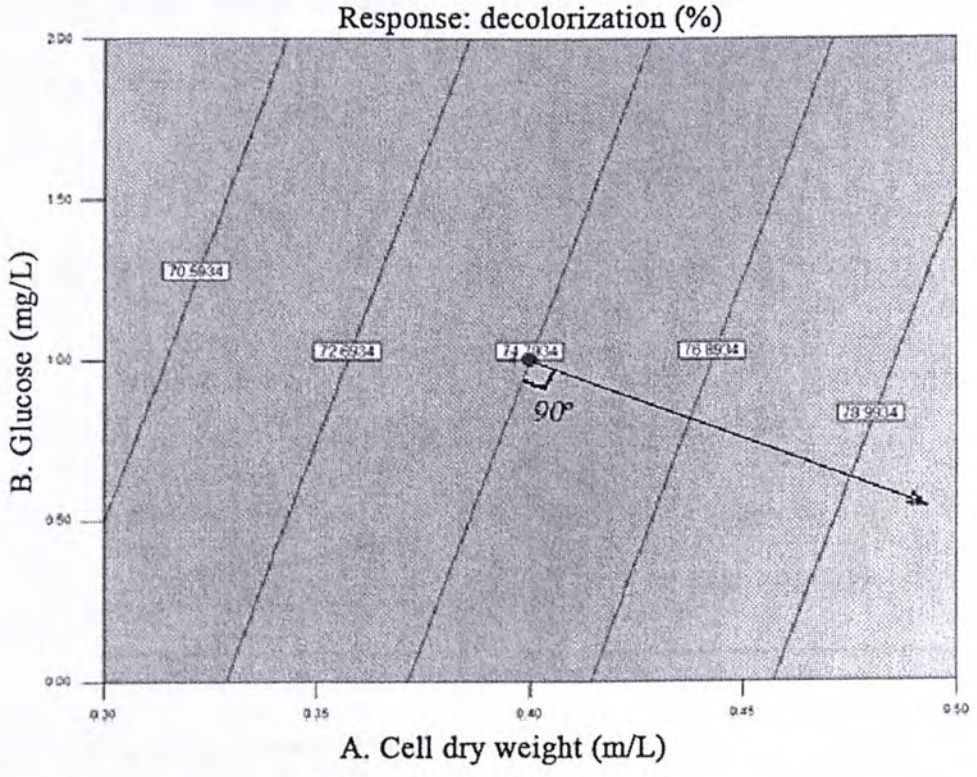

Fig. 1.11 Direction of PSA showing on a contour graph.

The corresponding responses are tested for those points. The point with the highest response is regarded as the point most close to the real optimum point, which will be used as the new center point for the subsequent CCD design.

1.6.5 Central composite design (CCD)

The CCD involves a full 2^n factorial design, 2n axial points (also expressed as α) and center points. Figure 1.15 shows the three factor CCDs. It can provide solid foundation for generating a response surface map. CCD contains five levels: -α (axial), -1 (factorial), 0 (center), +1 (factorial), +α (axial). With this many levels, it generate enough information to fit a second-order polynomial also called a "quadratic" model, which is capable of characterize curvatures (Anderson and Whitcomb, 2005).

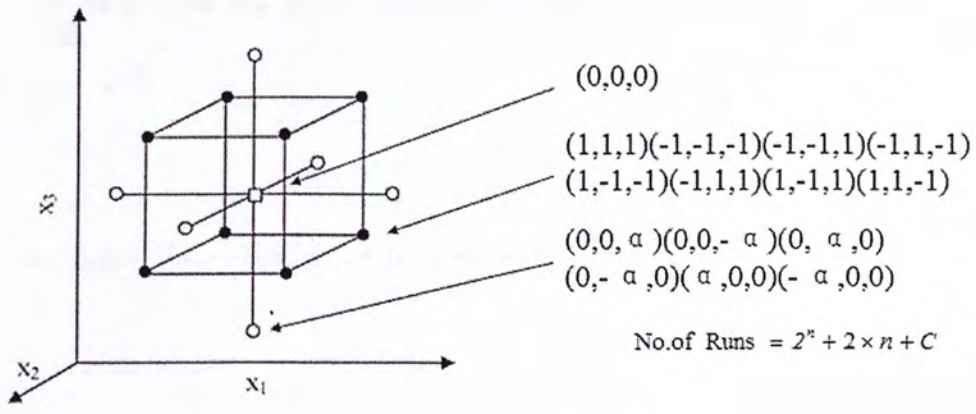

Figure 1.12 Experiment layout of three factor CCDs.

1.6.6 Estimation of the parameters in linear regression models

The method of least squares is typically needed to estimate the regression coefficients in a multiple linear regression models. This method is very useful in estimate coefficients in CCD generated models.

Suppose there are n observations on the response and corresponding variables, and totally k variables are available as shown in Table 1.7.

Table 1.7 Data for multiple linear regression.

y	x_1	x_2	...	x_k
y_1	x_{11}	x_{12}	...	x_{1k}
y_2	x_{21}	x_{22}	...	x_{2k}
...	...	...		...
y_n	x_{n1}	x_{n2}	...	x_{nk}

We may write the model equation in terms of observations in Table 1.7 as Equation 1.18:

$$y_i = \beta_0 + \beta_1 x_{i1} + \beta_2 x_{i2} + ... + \beta_k x_{ik} + \varepsilon_i = \beta_0 + \sum_{j=1}^{n} \beta_j x_{ij} + \varepsilon_i , \qquad i=1,2,...,n$$

(Equation 1.18)

where β_0 is the intercept, β_i are coefficients of variables x_i, and ε_i is the random errors.

Equation 1.16 may be expressed in matrix notation as Equation 1.19

$$\mathbf{y} = \mathbf{X}\boldsymbol{\beta} + \boldsymbol{\varepsilon} \qquad \text{(Equation 1.19)}$$

Where

$$\mathbf{y} = \begin{bmatrix} y_1 \\ y_2 \\ \cdots \\ y_n \end{bmatrix}, \quad \mathbf{X} = \begin{bmatrix} 1 & x_{11} & x_{12} & \cdots x_{1k} \\ 1 & x_{21} & x_{22} & \cdots x_{2k} \\ \cdots & \cdots & \cdots & \cdots \\ 1 & x_{n1} & x_{n2} & \cdots x_{nk} \end{bmatrix}, \quad \boldsymbol{\beta} = \begin{bmatrix} \beta_0 \\ \beta_1 \\ \cdots \\ \beta_n \end{bmatrix}, \text{ and } \quad \boldsymbol{\varepsilon} = \begin{bmatrix} \varepsilon_1 \\ \varepsilon_2 \\ \cdots \\ \varepsilon_n \end{bmatrix}$$

In general, $\mathbf{y}$ is an $n \times 1$ vector of the observations, $\mathbf{X}$ is an $n \times p$ model matrix consisting of the levels of the independent variables expanded to model form plus an additional column of 1s to account for the intercept term in the model, $\boldsymbol{\beta}$ is a $p \times 1$ vector of the regression coefficients, and $\boldsymbol{\varepsilon}$ is an $n \times 1$ vector of random errors.

We wish to find the vector of the least squares estimators, $\mathbf{b}$, that minimizes

$$\begin{aligned} L &= \sum_{i=1}^{n} \varepsilon_i^2 = \boldsymbol{\varepsilon}'\boldsymbol{\varepsilon} = (\mathbf{y} - \mathbf{X}\boldsymbol{\beta})'(\mathbf{y} - \mathbf{X}\boldsymbol{\beta}) \\ &= \mathbf{y}'\mathbf{y} - \boldsymbol{\beta}'\mathbf{X}'\mathbf{y} - \mathbf{y}'\mathbf{X}\boldsymbol{\beta} + \boldsymbol{\beta}'\mathbf{X}'\mathbf{X}\boldsymbol{\beta} \end{aligned} \qquad \text{(Equation 1.20)}$$

The least squares estimators must satisfy:

$$\left.\frac{\partial L}{\partial \boldsymbol{\beta}}\right|_{\mathbf{b}} = -2\mathbf{X}'\mathbf{y} + 2\mathbf{X}'\mathbf{X}\mathbf{b} = \mathbf{0}$$

which simplifies to

$$\mathbf{X}'\mathbf{X}\mathbf{b} = \mathbf{X}'\mathbf{y} \qquad \text{(Equation 1.21)}$$

Thus the least squares estimator of $\boldsymbol{\beta}$ is

$$\mathbf{b} = (\mathbf{X}'\mathbf{X})^{-1}\mathbf{X}'\mathbf{y} \qquad \text{(Equation 1.22)}$$

The fitted regression model is

$$\hat{\mathbf{y}} = \mathbf{Xb} \qquad \text{(Equation 1.23)}$$

In scalar notation, the fitted model is

$$\hat{y}_i = b_0 + \sum_{j=1}^{k} b_j x_{ij}, \qquad i=1,2,\ldots,n \qquad \text{(Equation 1.24)}$$

The difference between the observation y_i and the fitted value $\hat{y}_i$ is a residual, which is $e_i = y_i - \hat{y}_i$ (Myers et al., 2008).

1.6.7 Test of fitness

In order to test the fitness of a generated second-order model, a few parameters including correlation coefficient (R^2), adjusted correlation coefficient (R^2_{adj}), predicted residual sum squares (PRESS), predicted correlation coefficient (R^2_{pred}) and F or P value of lack-of-fit test (LOF).

R^2 measures the proportion of variation explained by the model relative to the mean (overall average of the response). It is calculated from Equation 1.25:

$$R^2 = 1 - \frac{SS_{residual}}{SS_{model} + SS_{residual}} \qquad \text{(Equation 1.25)}$$

where sum of square (SS) is the sum of the squared differences between the average values for the blocks and the overall mean, SS_{model} is the total sum of squares for the

terms in the model and $SS_{residual}$ equals the sum of squares for all the terms not included in the model (those terms fall on the half normal plot, which is not significant).

R^2_{adj} normalize R^2 with degree of freedom, as shown in Equation 1.26.

$$R_{adj}^{2} = 1 - \frac{SS_{residual}}{df_{residual}} \times \frac{(df_{residual} + df_{model})}{(SS_{residual} + SS_{model})} \qquad \text{(Equation 1.26)}$$

The PRESS for the model is a measure of how well a particular model fits each point in the design. The coefficients for the model are calculated without the first point. This new model is then used to estimate the first point and calculate the residual for point one. This is done for each data point and the squared residuals are summed. PRESS value should be minimized.

The R^2_{pred} is the R^2-like statistic converted from PRESS (Equation 1.27).

$$R^2_{pred} = 1 - \frac{PRESS}{SS_{model} + SS_{residual}} \qquad \text{(Equation 1.27)}$$

The lack-of-fit test compares the error from excess design points (beyond what's needed for the model, which also called residual without pure error) with the pure error from the replicates (center points). It tests whether the model adequately describes the actual response surface. Insignificant lack-of-fit test is desired.

2. Objectives and significance of the project

The objectives of this project are:

(1) To screen and isolate effective bacteria for aerobic degradation of a target chromium azo dye - AY99.

(2) To immobilize bacterial cells for application in laboratory scale reactor.

(3) To use RSM for studying the effects of experimental factors and find the optimum conditions.

(4) To investigate the degradation mechanism (s).

This project is original in the following aspects:

(1) Pure bacterial strains with clear identification were isolated for degrading a chromium azo dye.

(2) Bacterial cells were immobilized for more practical applications, and their performances in a laboratory scale reactor were monitored.

(3) Response surface methodology was employed for microbial degradation process. Besides, the newly developed MR5 designs were used to screen important variables.

(4) The degradation mechanisms concerning both organic portion and heavy metal portion of chromium azo dye were investigated.

(5) A method for separately determination of Cr(VI) and Cr(III) with interferences of Cr(III)-organic complexes was developed.

3. Material and methods

3.1 Chemicals

3.1.1 Chemicals for preparation of bacterial culture media

Acid Yellow 99 (AY99, Sigma, St. Louis, USA) was chosen as the model chromium azo dye for this study. Except from AY99, the nutrient media used to provide extra carbon sources and nitrogen sources, trace elements and growth factors for the bacteria were prepared by D-glucose (> 99.9%, Riedel-de Haën, Seelze, Germany), ammonium sulfate (99.0%, Univar USA, Redmond, USA), nutrient broth (3 g beef extract + 5 g peptomeat, Biolife, Milano, Italy). Bacterial media were buffered with 50 mM phosphate buffer of different ratio of potassium phosphate dibasic and potassium phosphate monobasic (both from Riedel-de Haën, Seelze, Germany) in ultra pure water (Milli-Q, Billerica, USA). Agar plates were prepared by adding 15 g/L Bacto agar (Becton, Dickinson and Company, Sparks, USA) to the liquid media. Cryoprotectant – glycerol solution was prepared by dissolving 20 g glycerol (99.5%, Univar USA, Redmond, USA) in 20 mL water. The resulting 50% stock solution was autoclaved before use.

3.1.2 Chemicals for identification of bacteria

For the Sherlock® microbial identification system (MIDI Inc., Newark, Delaware, USA), 4 standard reagents were required. Reagent 1 was prepared by dissolving 6 g NaOH (Riedel-de Haën, Seelze, Germany) in 20 mL ultra pure water (Milli-Q, Billerica, USA) and 20 mL methanol (99.9%, TEDIA Fairfield, USA). Reagent 2 was prepared by mixing 26 mL 6N HCl (Mallinckrodt, Hazelwood, USA) and 22 mL methanol (99.9%, TEDIA Fairfield, USA). Reagent 3 was a mixture of 25 mL

tert-butyl methyl ether (MTBE) (99%, (Riedel-de Haën, Seelze, Germany) and 25 mL Hexane (95%, TEDIA Fairfield, USA. Reagent 4 was prepared by dissolving 0.54 g NaOH in 45 mL ultra pure water.

For Biolog® microstation system, all chemicals are purchased from Biolog Inc. (Hayward, USA) and prepared from its standard protocol.

3.1.3 Chemicals for chromium speciation

In order to study the speciation of Cr (VI), ionic Cr(III) and AY99, as well as determine Cr(VI) from the reaction system, 1,5-Diphenylcarbazide (DPC) was used to form purple complex with Cr(VI) which can be quantitatively retained in the Amberlite XAD-4 column. 1,5-Diphenylcarbazide (DPC) solution (50 mM) was prepared freshly by dissolving appropriate amount of DPC (≧98%, Sigma, St. Louis, USA) in 5 mL of acetone (99.8% Labscan, Gliwice, Poland) and diluting to 10 mL with ultrapure water. The solution was kept in a 50 mL Duran bottle wrapped with aluminum foil.

Amberlite XAD-4 resin (Rohm and Haas Bellefonte, USA; 800 m^2/g surface area; wet mesh size 20–60) was used after washing with methanol (99.9%, TEDIA Fairfield, USA), 1 M HCl solution (prepared by 37–38% HCl from Merck, Darmstadt, Germany) and ultra pure water (Milli-Q, Billerica, USA), respectively, and dried for 2 h at 60°C. Methanol (99.9%, TEDIA Fairfield, USA) with 1 M H_2SO_4 (98%, Labscan, Gliwice, Poland) was used for eluting organic compounds and regeneration of XAD-4, while 1 M NaOH (99%, Sigma, St. Louis, USA) solution was used to regenerate XAD-4 from proteins or peptides.

Stock solutions of Cr(VI), Cr(III), AY99 (1,000 g/L) were prepared from $K_2Cr_2O_7$ (Merk, Darmstadt, Germany), $CrCl_3 \cdot 6H_2O$ and Acid Yellow 99 (Sigma, St. Louis, USA). Casein, albumin, glumatic acid and glycine (>99%) were purchased from Sigma (St. Louis, USA), and ammonia oxalate (99.8%) was from Peking Chemical Industrial Factory (Beijing, China). Sodium citrate and sodium acetate (both ≧ 99%) were purchased from Merck (Darmstadt, Germany) and used to synthesize Cr complexes. Fifty mM phosphate buffers (pH ≈ 7, 40 mM potassium phosphate dibasic and 10 mM potassium phosphate monobasic, both from Riedel-de Haën, Seelze, Germany) was used.

3.1.4 Chemicals for immobilization of bacterial cells

Polyvinyl alcohol (PVA)-124 (degree of polymerization of 2400-2500, Xilong Chemical Factory, Shantou, China) was used to prepare PVA gels for cell entrapment. On the other hand, 20% acrylamide stock solution was prepared by dissolving 18.2 g acrylamide (>99.9% Bio-Rad, Hercules, USA) and 1.8 g N,N'-methylene-bis-acrylamide (Sigma, St. Louis, USA) in 50 mL ultra pure water, and diluted to 100 mL with ultra pure water in v-flask. The resulting solution was transferred to a 100 mL duran bottle which was then wrapped with aluminum foil and stored at 4°C in dark before use. Ten percent ammonium persulfate was freshly prepared by dissolving 1 g ammonium persulfate (Sigma, St. Louis, USA) in 5 mL ultra pure water in a test tube. Besides that N,N,N',N'-Tetramethylethylenediamine (TEMED) (Sigma, St. Louis, USA) was purchased from Sigma, St. Louis, USA.

3.2 Sludge samples

Four sludge samples were collected for isolating of effective bacterial strains in this project. Sludge sample A was collected from the contact aeration tank of Shatin Sewage Treatment Works, Shatin, Hong Kong. Shatin Sewage Treatment Works is the largest wastewater treatment plan in Hong Kong. It serves Shatin New Town, Ma On Shan New Town and the surrounding villages with a flow capacity of 150,000 m^3/d (Water Technology, update regularly). Municipal wastewaters from various places are centralized and treated by activated sludge in its contact aeration tank. Therefore, microorganisms capable of aerobically degrading organic compounds present in sludge sample A with large variety and quantity. Sludge sample B was collected from the downstream of Fu River in Chengdu, Sichuan, China. Sludge sample C was collected from a wastewater duct of a small plastic manufactory in Chengdu. Both sites B and C were considerately contaminated as they were quite smelly and they showed blue-green colour. Sludge sample D was collected at the contact aeration tank of a primary dye treatment plant in Huizhou, China. These sludge samples were shown in Plate 3.1. Sludge from the last three sites were chosen for isolation as they were contaminated by organic effluent with colour.

.

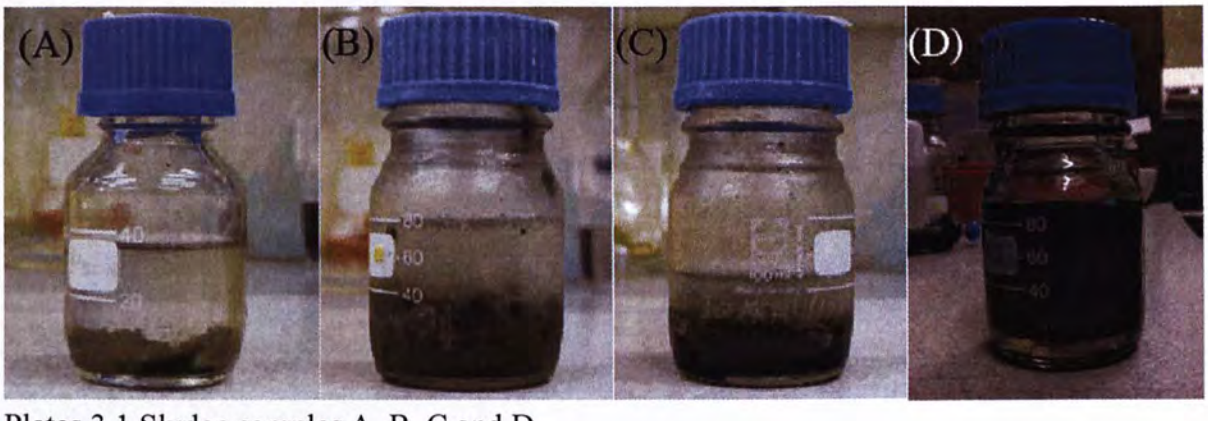

Plates 3.1 Sludge samples A, B, C and D

3.3 Characterization of Acid Yellow 99

AY99 (C.I. 13900) which is a chromium monoazo dye was selected in this study. AY99 is one of the 80 commonly used chromium azo dyes (Color Index International, update regularly), and it is easily purchased from various big suppliers such as Sigma (St. Louis, USA) and Acros Organics (Geel, Belgium). The molecular structure of AY99 was shown in Figure 3.1. The absorption peaks (from 400-700 nm) of AY99 was determined by spectrophotometric scanning using a Helis Gamma UV-vis spectrophotometer (Thermo Fisher Scientific, Waltham, USA, shown in Plate 3.2). Unique absorption peaks of these dyes without overlapping with those of Cr (III) (green), Cr (VI) (yellow) and colored complex of Cr (VI) and 1, 5-diphenylcarbazide (pink) was selected to build the relationship between the absorbance and concentration of AY 99. The total Cr (mg/L) of AY99 was determined according to the standard method (APHA, 2005). The relationship of total Cr (mg/L) and concentration of AY 99 (mg/L) was plotted.

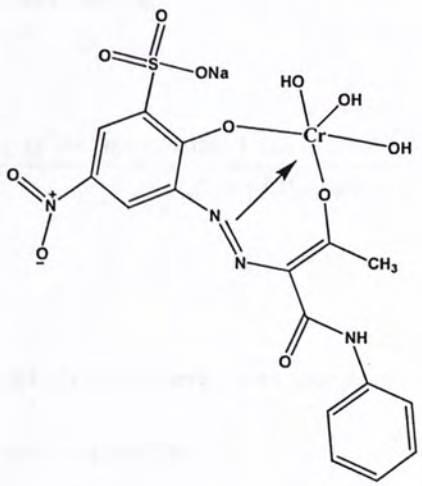

Figure 3.1 Molecular structure of AY99.

Plate 3.2 Helis Gamma UV-vis spectrophotometer (Thermo Fisher Scientific, Waltham, USA).

3.4 Monitoring of azo dye decolorization

One mL of reacted culture medium were centrifuged by a MicroCentaur micro-centrifuge (MSE, London, UK) at 13,400 xg for 10 min, and the supernatant was transferred to a cuvette and tested at the wavelength of 451 nm by the spectrophotometer, and uninoculated controls were used as the standards to monitor the color loss during the experiment (Equation 3.1).

Decolorization (%) was defined as:

$$\text{Decolorization (\%)} \equiv \frac{\text{Abs of the uninoculated azo dye - Abs of the azo dye during cultivation}}{\text{Abs of the uninoculated azo dye}} \times 100$$

(Equation 3.1)

3.5 Isolation of bacterial strains which can degrade Acid Yellow 99

One mL sludge was suspended in 5 mL 0.85% NaCl solution, and mix throughout by vortex for 5 min. The solid-liquid mixture was filtered by Grade No. 1 Qualitative filter papers (Whatman, Dawsonville, USA, Particle Retention: 11 μm), the filtrate was subjected to enrichment with 20% nutrient broth solution containing

100 mg/L of AY99. After incubation of 3-5 d, one mL of the supernatant from the enrichment medium was serial diluted with 0.85% NaCl solution and spread on screening medium (SM) agar plates. The SM agar plates had the following composition: ammonium sulfate, 1 g; nutrient broth, 0.8 g; AY99 99, 0.1 g; Bacto agar, 15 g, 1 L water was added and pH of the medium was adjusted to 7.0. Glucose was autoclaved separately and added to the medium solution to make the concentration of 5 g/L. After 5 to 7 d of incubation at 30°C, those SM agar plates was examined and morphologically different colonies was selected (Plate 3.4) and streaked to new SM agar plates.

Plate 3.4 Morphologically different colonies on a SM agar plate.

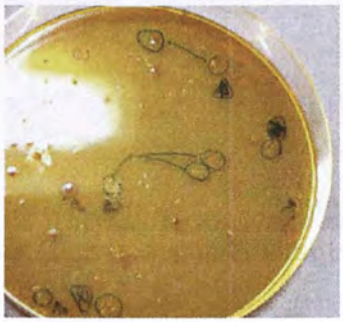

After 5 to 7 d incubation at 30°C, the bacterial strains which made the color of the SM agar plates lighter were selected (Plate 3.5).

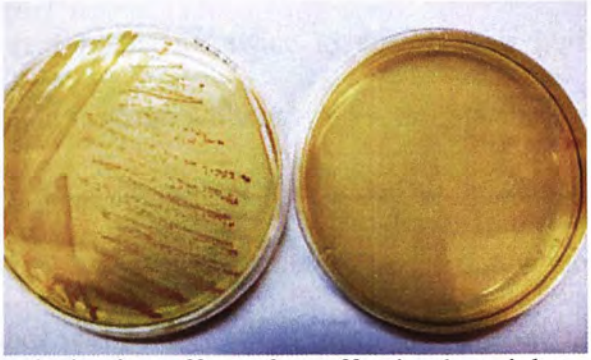

Plate 3.5 Visual decolorization effect of an effective baterial strain on SM plates. Left: SM plate streaked with an effective baterial strain. Right: a control SM plate.

The selected bacterial strains were inoculated to a 125 mL flask containing 50 mL liquid medium with the following composition: $(NH_4)_2SO_4$, 1 g; nutrient broth, 0.8 g; AY 99, 0.1 g, 1 L water and 50 mM K_2HPO_4-KH_2PO_4 buffer was added and pH of the medium was adjusted to 7.0. Glucose was autoclaved separately and added to the medium solution to make the concentration of 5 g/L. Those flasks were incubating at 30°C in a compact rotary shaker (Edmund Bühler GmbH, Hechingen, Germany, shown in Plate 3.6) at 200 rpm for 7 to 10 d.

Plate 3.6 Compact rotary shaker (Edmund Bühler GmbH, Hechingen, Germany).

After incubation, decolorization (%) of each culture was determined according to the method described in the above session. The culture with more than 70% decolorization was selected. A loopful of each best performance culture was streaking on SM agar plates for twice to ensure their purity. Each isolate was inoculated to the liquid medium without AY 99, and incubate at 30 °C for 1-3 d. Five mL of the resulting bacterial culture was added to an autoclaved Eppendrof tubes with 5 mL autoclaved 50% glycerol solution. After throughout mixing with vortex, those eppendrof tubes was store at -80 °C ultra low freezer (So Low Environmental Equipment, Cincinnat, USA) for permanent storage.

3.6 Identification of selected bacterial strains

3.6.1 Gram stain

A loopful of bacterial colonies were picked up and streaked on a microscope slide (Sail Brand, Jiangsu, China) followed by dampening with 1 droplet of ultrapure water. The resulting slides were placed in 65°C oven to dry for 5-10 min. After that, one drop of crystal violet solution was dropped on the fixed bacterial streak. After 30-60 s, the crystal violet was washed away by ultra pure water. Then, a droplet of iodine solution was added and waited for 1 min before washed away with 99.9% methanol. Lastly, one droplet of Safranin Red was added and waited for 30 s before washed away with ultra pure water. After that, the prepared microscope slides were dried in 65°C oven for 5-10 min again. The microscopic images of each stained bacterial strain were recorded.

3.6.2 Sherlock® microbial identification system

The Sherlock® microbial identification system (MIDI Inc., Newark, Delaware, USA) identifies bacteria by comparison of the whole cell fatty acid profiles between the samples and the system's database, using gas chromatography (Plate 3.8)

Plate 3.7 The Sherlock® microbial identification system (MIDI Inc., Newark, Delaware, USA).

All the operations were conducted exactly followed the user guide provided from the manufacturer.

3.6.3 Biolog® microstation system

Biolog microstation system (Biolog Inc., Hayward, USA) test the ability of microorganisms to utilize a preselected panel (containing 96 wells with one control) of different carbon sources to generate a metabolic fingerprint which can be matched with its library.

All reagents and accessories were purchased from the Biolog Inc. and used according to the instructions of the manufacturer.

3.6.4 Selection of the most effective bacterial strains

Those effective bacterial strains were used to decolorize 3 different mono azo dyes AY99, Procion Red MX-5B (MX-5B) and Acid Orange 7 (AO7) under the same conditions: a single colony was inoculated in a nutrient medium consists of 10% nutrient broth, 1 g/L $(NH_4)_2SO_4$ and 5 g/L glucose and incubated at 30°C, 200 rpm for 1 d. After that 1 mL of the resulting sub-culture was inoculated to the treatment system which had pH = 7 and buffered with 50 mM K_2HPO_4-KH_2PO_4. Five g/L glucose, 1 g/L $(NH_4)_2SO_4$ and 100 mg/L selected dye were also added to the treatment conical flasks which were incubated at 30°C, 200 rpm for 4 d. The bacterial strains with the highest decolorization efficiency were selected.

3.6.5 16S ribosomal RNA sequencing

Molecular technique was also applied to identify the most effective 2 bacterial strains (conducted by Hong Kong University of Science and Technology), and a partial 16S ribosomal RNA of the selected bacterial strains was sequenced.

3.7 Chromium speciation with interferences of chromium organic complexes

3.7.1 Instrumentation

The measurements were performed with a Hitachi atomic absorption spectrophotometer equipped with a Hitachi Z-2300 flame AAS main unit and single element cathode lamp (Hitach Inc., Chiyoda-ku, Japan) using an air-acetylene flame (Plate 3.8). The wavelengths for monitoring concentration of Cr species were 357.9/359.3 nm.

The pH value of the solutions was adjusted by a Thermo Orion A420 bench-top pH meter (Thermo Fisher Scientific Inc., Waltham, USA). A New Brunswick Scientific C24 incubation shaker was used for mixing. Twenty five mL syringes (Terumo, Tokyo, Japan) attached with a filter holder and a 0.45 μm filter (Millipore, Billerica, USA) were used for filtration.

Plate 3.8 Hitachi atomic absorption spectrophotometer equipped with a Hitachi Z-2300 flame AAS main unit and single element cathode lamp (Hitach Inc., Chiyoda-ku, Japan) using an air-acetylene flame.

3.7.2 Column preparation

Two glass columns (250 mm in length and 15 mm i.d.; Interflon, Cleveland, UK) with glass wool plug on stopcock containing 3 g of XAD-4 (~ 50 mm bed height) were used for performing speciation. A plug of cotton was placed on top of the resin to avoid the distribution of resin during sample passage (Plate 3.9).

Sulfuric acid (0.1 M) and ultrapure water were passed through the column in order to condition and clean it. After each run, the columns were washed with 10 mL methanol with 1 M H_2SO_4 to regenerate XAD-4 from organic compounds and preconditioned with 20 mL ultrapure water. When proteins and peptides were used, 20 mL 1 M NaOH was used to regenerate the resin.

Plate 3.9 Setup of separation columns containing XAD-4 resin.

3.7.3 Determination of percentage retained and recovery

In order to investigate the conditions for separation of different chromium species, it is important to understand how XAD-4 would interact with each singe component of chromium compounds. Retention efficiency (%) in the column (Equation 3.1) and recovery efficiency (%) from the column (Equation 3.2) were determined. Each analyte was filtered with a 0.45 μm filter. Five mL analyte was passed through the column, and 13 mL ultrapure water was used to rinse the column. The resulting solution was collected as an effluent. Afterwards, 5 mL 99.9% methanol with 0.1 M of H_2SO_4 was added to wash out water in the column into a waste bottle, and 18 mL methanol with 0.1 M of H_2SO_4 was added to elute content retained on XAD-4. The flow rate for all procedures was 2 mL/min. Analyte, effluent and eluent were acidified to pH < 2 with 65% HNO_3, quantified in a volumetric flask and added with 1% resulting volume of 30% (v/v) H_2O_2 for total dissolved chromium determination according to the Standard Method (American Public Health Association, 2005). Total dissolved

chromium concentrations of the analyte, effluent and eluent were determined by FAAS, and corrections were made for dilution effect of added reagents.

$$\text{Retention efficiency (\%)} = \frac{\text{Total Cr amount of analyte(μg) - Total Cr amount of effluent (μg)}}{\text{Total Cr amount of analyte (μg)}} \times 100\%$$

(Equation 3.2)

$$\text{Recovery efficiency (\%)} = \frac{\text{Total Cr amount of analyte(μg) - Total Cr amount of eluent (μg)}}{\text{Total Cr amount of analyte (μg)}} \times 100\%$$

(Equation 3.3)

3.7.4 Speciation of Cr(VI), ionic Cr(III) and chromium azo dye

Figure 3.2 illustrates the principle and key procedures of separation of the three chromium species from a mixture. A spiked mixture consisting of 1 mg/L of Cr(VI), 1 mg/L of ionic Cr(III) and 50 mg/L AY99 (with 1.3 mg/L chromium species) was prepared with 50 mM phosphate buffer and filtered with a 0.45 μm filter before adjusted to pH 5 with 1M HCl or NaOH. Eight mL of the spiked solution was passed through a column (Column A), and rinsed with 8 mL ultrapure water twice at a flow rate of 1.5 mL min^{-1}. The resulting solution was added with 1 mL of 50 mM DPC and adjusted to pH = 1. The solution was passed through another XAD-4 packed column (Column B) at a flow rate of 1.5 mL/min. This final effluent (Solution 1) was corresponding to the ionic Cr(III) in the spiked solution. Five mL 99.9% methanol with 0.1 M of H_2SO_4 was added to remove water in both columns, and then 18 mL methanol with 0.1 M of H_2SO_4 was added to elute the content retained on XAD-4. The eluents from Column A (Solution 2) and Column B (Solution 3) were corresponding to AY9

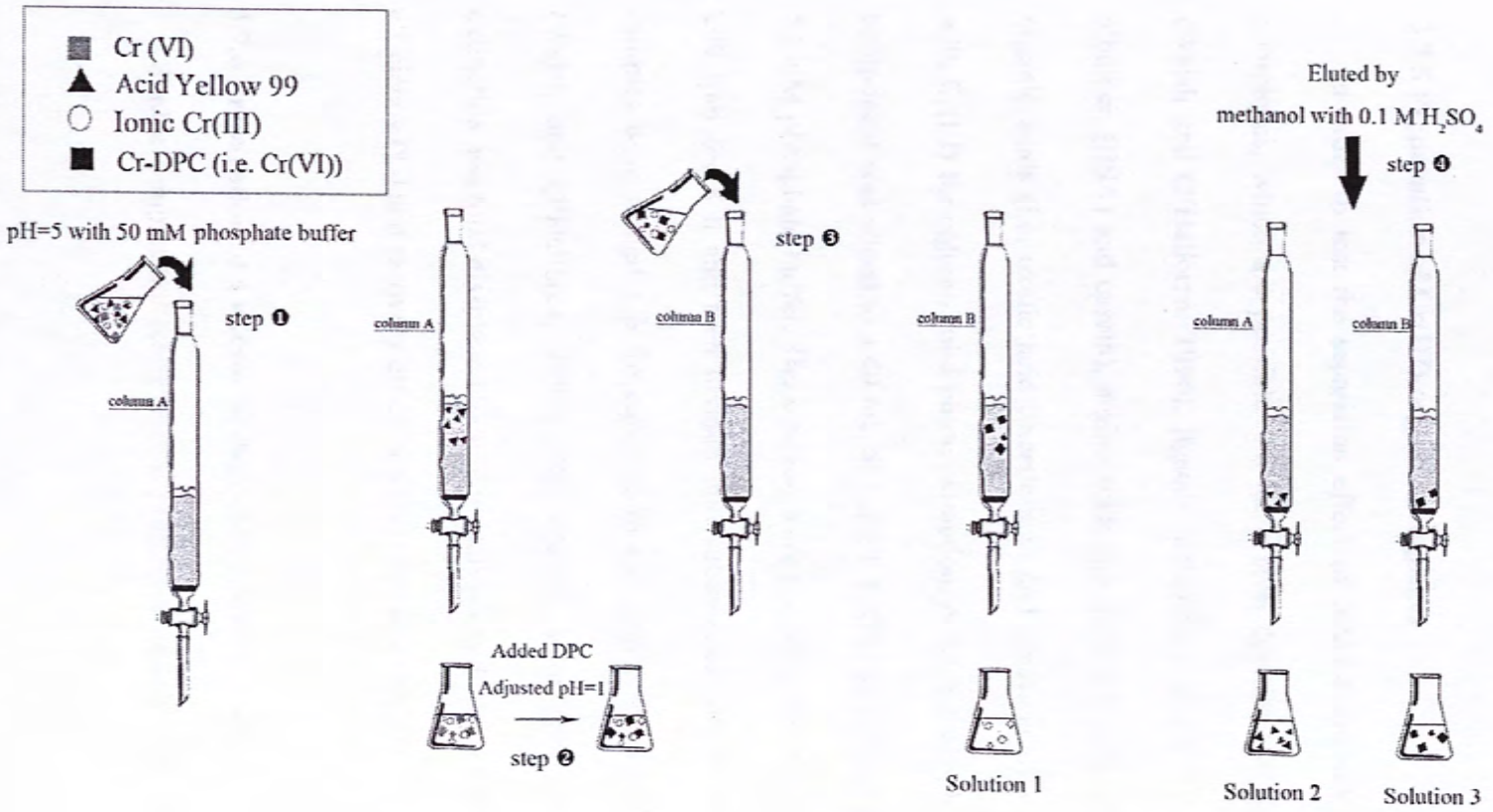

Figure 3.2. Schematic diagram of the principle and procedures of the determination of various chromium species in a mixture.

and Cr-DPC (i.e. Cr(VI)), respectively. The single component controls and Solutions 1, 2 and 3 were subjected to total dissolved chromium determination by FAAS. Corrections were made for dilution factors.

3.7.5 Preparation of Cr(III)-organic complexes

In order to test the separation effect of XAD-4 towards Cr(III)-organic complexes, which are possible and have been described in the environment (Walsh and O'Halloran, 1996), ligands including proteins (i.e. bovine serum albumen (BSA) and casein), amino acids (i.e. glutamic acid and glycine) and organic acids (i.e. oxalic acid , acetic acid and citrate acid) were complexed with Cr(III) for column solid phase extraction. A 2.5 mg sample of the organic component was added to a 40 mL of 1 mg/L Cr(III) solution at pH of 4.5 with 50 mM phosphate buffer. The solution were mixed in the incubation shaker at 200 rpm for 8 h and then divided into subsamples for pH adjustment. The samples were settled 1 h for equilibrium and passed through 0.45 μm filters (Walsh and O'Halloran, 1996). The filtrates were gone through XAD-4 extraction and total dissolved chromium analyses as described above. Retention efficiency (%) and recovery efficiency (%) were determined.

3.7.6 Preparation of a microbial degraded chromium azo dye sample

Sludge samples collected from a primary treatment tank of a centralized

dye industry zone in Huizhou, Guangdong, China, were used for screening and isolating bacteria which can degrade a chromium azo dye, AY99. One of the most effective AY99-degrading bacterium, *Pseudomonas* sp. 10MO, was selected. The treatment conditions were 0.5 g/L cell dry weight, pH = 7 with 40 mM K_2HPO_4-10 m M KH_2PO_4, 30℃, shaking at 200 rpm for 6 d. The culture medium was 5 g/L glucose, 1 g/L $(NH_4)_2SO_4$, 0.08 g/L nutrient broth and 100 mg/L AY99. The resulted solution was centrifuged at 24,000 x g for 5 min. The supernatant which has 94.5% of decolorization was adjusted to a required pH value and filtered with a 0.45 μm millipore filter. Afterwards, 20 mL samples were subjected to speciation study. Five and 10 mg additional Cr(VI) were spiked with microbial degraded AY99 samples to test the feasibility of this method under these conditions, and controls with ultra pure water were used to determine the exact total Cr amount added.

3.8 Chromium distribution in a free cells treated solution

Chromium distribution in the microbial degraded sample described in the above session was investigated. Forty mL of treated solution was centrifuged by a Hermle Z323 universal centrifuge (HERMLE Labortechnik, Wehingen, Germany, shown in Plate 3.10) at 24,000 xg for 10 min,

Plate 3.10 Hermle Z323 universal centrifuge (Hermle Labortechnik, Wehingen, Germany).

then the supernatant was transfer to a conical flask A. After that, pellet was washed with 50 mM phosphate buffer, pH = 7 for two times, and the washing solution was transfer to conical flask A and finally quantified in a 100 mL v-flask. This supernatant solution (A) represented released chromium during degradation. The remaining pellet was added with 30 mL 1 M HCl and sonicated in a Branson 2510 ultrasonicator (Branson Com., Branson, USA) for 1 hour, and this process was repeated for 3 times.

The resulting acid washed solution was quantified in a 100 mL v-flask. This Acid washed solution (B) represented the portion of chromium adsorbed on bacterial cells with ionic bonding. Lastly, the remaining pellet was resuspended in 5 mL 65% HNO_3 and transferred to digestion tubes and fluxed at 150°C for 4 h. The acid digested sample was transferred and quantified in 20

mL v-flask. This acid digested solution (C) represented the chromium contents inactivated (e.g. binding with proteins) inside bacterial cells. Solutions A, B and C were subjected to total dissolved chromium analyses.

3.9 Distribution of AY99 in a free cells treated solution

AY 99 standard were prepared by dissolving certain amount of AY99 in 99.9% methanol as a stock. Then different volumes of stock solution were added to several v-flasks and diluted with 99.9% methanol to the mark. The analyzing samples including the original treatment solution with no addition of bacteria (total), supernatant and water washed solution of the treated sample (supernatant). And lastly an extraction sample (extraction) was prepared by adding 1:1 1M HCl and 99.9% methanol to the cell pellets followed by one hour sonication. This process was repeated for several times, until the color of cell pellets return to light yellow. These 3 samples were subjected to freeze dry by a Labconco Freeze Dry System (Labconco Corporation, Kansas, USA, shown in Plate 3.11) for 2 d.

The freeze dried samples were redissolved in 99.9% methanol and subject to high performance liquid chromatography (HPLC) analysis using a Waters HPLC system (Waters 2695 seperation system equipped with 2996 Photodiode Array Detector (PAD), Waters, Milford, USA, shown in Plate 3.12) with those AY 99 standards. The mobile phases were consist of 79% methanol, 19%

ultrapure water and 2% acetic acid, and were degassed by sonication for 30 min before analysis. For PAD detector the wavelength was set at 451 nm.

Plate 3.11 Labconco Freeze Dry System (Labconco Corporation, Kansas, USA).

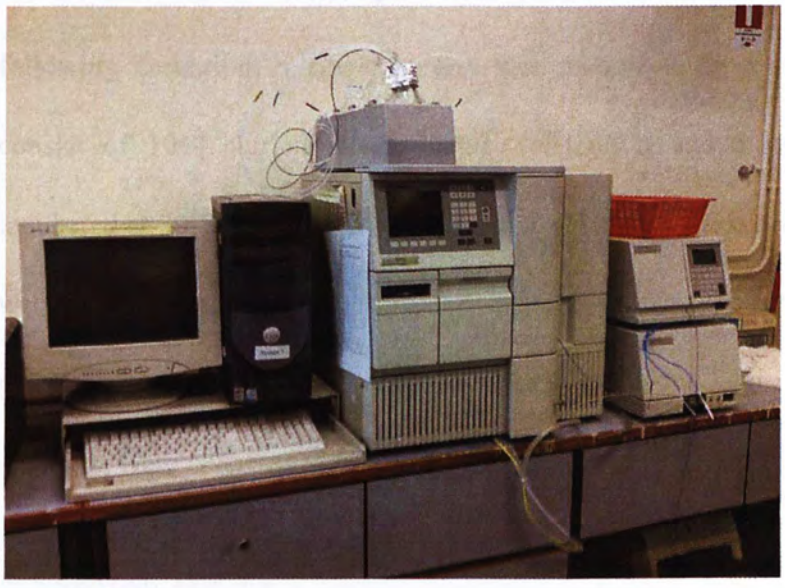

Plate 3.12 Waters HPLC system (Waters 2695 seperation system equipped with 2996 Photodiode Array Detector (PAD), Waters, Milford, USA).

3.10 Optimization of decolorization process with response surface methodology (RSM).

3.10.1 Correlation of cell mass and cell density of selected bacteria

Correlation of the cell mass (cell dry weight, g/L) and cell density (spectrophotometric absorbance at 520 nm (A_{520}) were studied. Linear relationships between cell mass and cell density of these bacterial cultures grown in 10% nutrient broth with 1g/L $(NH_4)_2SO_4$ and 5g/L glucose were established by determining the dry weights of 10 mL aliquots of bacterial cultures with different cell density.

3.10.2 Preliminary investigation of the optimum conditions.

After a few trials, the optimum decolorization was achieved under the following condition: a single colony was inoculated in a nutrient medium consist of 10% nutrient broth, 1 g/L $(NH_4)_2SO_4$ and 5 g/L glucose and incubated at 30°C, 200 rpm for 1 d. After that 1 mL of the resulting sub-culture were inoculated again to different conical flasks containing the above mentioned nutrient medium and incubated again for 2 d. Those medium solutions were centrifuged at 9,820 xg by Avanti® J-E Centrifuge system with a JA-14 Rotor (Beckman Coulter, Inc., Fullerton, USA, shown in Plate 3.13).

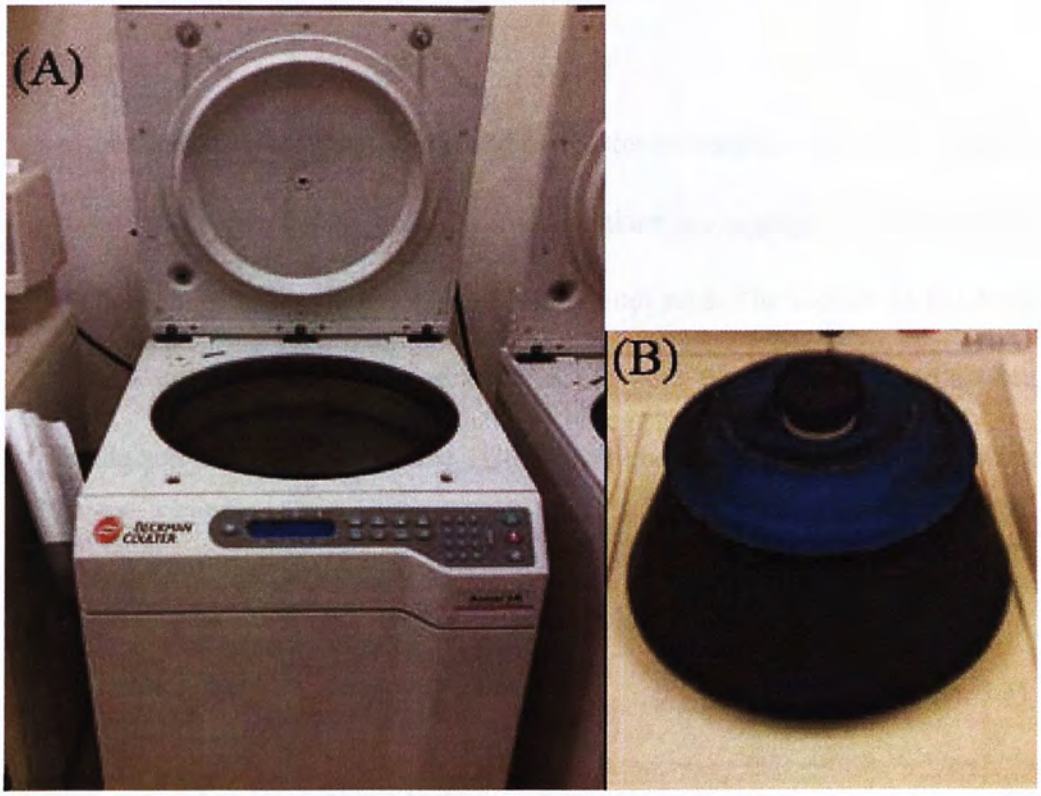

Plate 3.13 Avanti® J-E Centrifuge system (A) with a JA-14 Rotor (B) (Beckman Coulter, Inc., Fullerton, USA).

Cell mass of each selected bacterial culture were harvested and transferred to the treatment system which had pH=7 and buffered with 50 mM K_2HPO_4-KH_2PO_4. Five g/L glucose, 1 g/L $(NH_4)_2SO_4$ and 100 mg/L AY99 were also added to the treatment conical flasks which were incubated at 30°C, 200 rpm for 1 d. These conditions were set as the mid-level points for the subsequent minimal-run resolution V (MR5) design

3.10.3 Minimal-run resolution V (MR5) design

The influences of six factors on decolorization were investigated using a MR5 design. The MR5 designs are very powerful designs, allowing the unique

estimation of all the main effects and two factor interactions. Since the effects if three factor interactions and higher interactions are negligible, MR5 designs work well with the vital factors with minimum runs. The layouts of the MR5 design were shown in Tables 3.1 and 3.2. And the real experiments were conducted in random order. The factors were coded according to the following equation:

$$x_i = \frac{(X_i - X_0)}{\Delta X}, \qquad i = 1, 2, \ldots, k \qquad \text{(Equation 3.5)}$$

where x_i was the coded independent factor, X_i was the real independent factor, X_0 was the value of X_i at the center point and ΔX was the step change value.

Table 3.1 Levels of the factors tested in the experimental design.

factors	**Level of factors**		
	-1	0	+1
Cell dry weight (X_1, g/L)	0.3	0.4	0.5
Glucose (X_2, g/L)	0	2	4
$(NH_4)_2SO_4$ (X_3, g/L)	0	0.5	1
Nutrient broth (X_4, g/L)	0	0.04	0.08
Temperature (X_5, °C)	25	30	35
pH (X_6)	5	7	9

Table 3.2 Experimental design of the MR5 design.

Standard runs	x_1	x_2	x_3	x_4	x_5	x_6
1	-1	-1	1	1	-1	1
2	1	1	-1	-1	-1	-1
3	-1	-1	-1	-1	1	-1
4	1	1	1	1	-1	-1
5	-1	1	-1	1	-1	1
6	1	1	1	-1	-1	1
7	1	-1	-1	1	-1	1
8	-1	1	-1	1	1	-1
9	1	-1	1	-1	-1	-1
10	1	-1	1	1	1	1
11	1	-1	-1	1	1	-1
12	1	1	-1	1	1	1
13	-1	1	-1	-1	1	1
14	1	1	1	-1	-1	-1
15	-1	-1	1	1	1	-1
16	1	-1	-1	-1	1	1
17	-1	1	1	-1	-1	-1
18	-1	-1	-1	-1	-1	1
19	-1	-1	-1	1	-1	-1
20	-1	1	1	1	1	1
21	1	1	1	-1	1	-1
22	-1	-1	1	-1	1	1
23	0	0	0	0	0	0
24	0	0	0	0	0	0
25	0	0	0	0	0	0
26	0	0	0	0	0	0

The factors, which were significant at 95% of confidence level ($P < 0.05$) from the regression analysis were considered to have greater effects on decolorization and were further optimized by a central composite design. The first-order model used tofit the results of fractional factorial design was represented as:

$$Y = \sum \beta_i X_i + \beta_0 \qquad \text{(Equation 3.4)}$$

where Y was the predicted response; β_0 was the intercept; β_i was the linear coefficient and X_i was the coded independent factor.

3.10.4 Path of steepest ascent (PSA)

The direction of steepest ascent was the direction in which Y increased most rapidly. The direction of steepest ascent was parallel to the normal of contour line of response curve of the model generated from the MR5 design and passed through the center point of MR5 design. The steps along the path were proportional to the regression coefficients β_i. Experiments were performed along the steepest ascent path until the response did not increase any more. This point would be near the optimal point and could be used as center point to optimize (Chen et al., 2009).

3.10.5 Central composite design (CCD) and RSM

The three most significant factors for enhancing decolorization screened by fractional factorial design were used in this design. The three independent factors were studied at five different levels ($-\alpha$, -1, 0, +1 and $+\alpha$) and a set of 20 experiments were carried out. The factor α is depend on amount of variables included in the CCD as $\alpha = (2^n)^{\frac{1}{4}}$, in which n is the number of variables. In a CCD of 3 variables, α=1.68.

The factors were coded according to the following equation:

$$x_i = \frac{(X_i - X_0)}{\Delta X}, \qquad i = 1, 2, \ldots, k \qquad \text{(Equation 3.5)}$$

where x_i was the coded independent factor, X_i was the real independent factor, X_0 was the value of X_i at the center point and ΔX was the step change value.

The layout of experimental design was shown in Table 3.3. And the real experiments were conducted in random order.

The behavior of the system was explained by the following second-order polynomial equation:

$$Y = \beta_0 + \sum \beta_i x_i + \sum \beta_{ii} x_i^2 + \sum \beta_{ij} x_i x_j, \qquad i = 1, 2, \ldots, k \qquad \text{(Equation 3.6)}$$

where Y was the predicted response, β_0 was the intercept, x_i and x_j were the coded independent factors, β_i was the linear coefficient, β_{ii} was the quadratic coefficient and β_{ij} was the interaction coefficient.

Table 3.3 Experimental layout of the CCD design.

Standard runs	x_1	x_2	x_3
1	-1	-1	-1
2	1	-1	-1
3	-1	1	-1
4	1	1	-1
5	-1	-1	1
6	1	-1	1
7	-1	1	1
8	1	1	1
9	-1.68	0	0
10	1.68	0	0
11	0	-1.68	0
12	0	1.68	0
13	0	0	-1.68
14	0	0	1.68
15	0	0	0
16	0	0	0
17	0	0	0
18	0	0	0
19	0	0	0
20	0	0	0

3.10.6 Statistical analysis

Design expert, version 7.0 (STATEASE Inc., Minneapolis, USA) was used for the experimental designs and regression analysis of the experimental data. Statistical analysis of the model was performed to evaluate the analysis of variance (ANOVA).

The quality of the polynomial model equation was judged statistically by the R^2, R^2_{adj}, R^2_{pred}, PRESS and lack of fit (LOF)

3.9.6 Experimental validation of the optimized conditions

In order to validate the optimization of medium composition, three tests were carried out using the optimized condition, to confirm the results from the analysis of the response surface.

3.11 Immobilization of bacterial cells

3.11.1 Immobilization by polyvinyl alcohol (PVA) gels

PVA solid powder was heated to dissolve in KH_2PO_4–K_2HPO_4 buffer (50 mM, pH 7.2), and kept overnight at room temperature. The bacterial cells were collected by centrifugation at 9,820 xg for 5 min, then washed with KH_2PO_4–K_2HPO_4 buffer once. The concentrated cells were related to cell dry weight and added to the mixture which containing 14% PVA and 5% glycerol (the final concentration of bacteria was set as 0.8 g/L cell dry weight, which is determined according to preliminary optimization results), and stirred to be uniform. The mixture was frozen in a refrigerator at−20 °C for 24 h and then thawed at 4°C. The freezing and thawing process was repeated for two additional cycles to increase the mechanical strength of immobilized cells (Ariga et al., 1987). Finally, PVA gel was cut into 5 mm×5 mm×2 mm cubes (EI-Naas et al., 2009) (Plate 3.14), then washed thoroughly with

KH_2PO_4–K_2HPO_4 buffer and kept at 4°C (Liu et al., 2009).

Plate 3.14 PVA gel cubes inflated after adsorbing 50 mM phosphate buffer solution.

And control PVA gels without bacterial cells were also prepared in the same way, expect concentrated cells were replaced by same volume of phosphate buffer solution.

3.11.2 Immobilization by polyacrylamide gels

Concentrated cells were prepared as described in the above session. Mixed 5 mL of 20% acrylamide solution with 5 mL concentrated cells in a disposable petri dish, followed by addition of 0.1 mL of 10% ammonium persulfate and mix well. Started the polymerization by adding 0.01 mL TEMED, and let the polymerization continue for 30 min at 25°C (Petrov et al., 2007). The bacterial cell concentration in polyacrylamide was quantified and set as the same as PVA

gels. Cut the polymerized polyacrylamide gel into 5 mm×5 mm×2 mm cubes (Plate 3.15). Controls are prepared with phosphate buffer instead of concentrated cells. Prepared gels were stored at 4°C.

Plate 3.15 Polyacrylamide gel cubes.

3.11.3 Performances of immobilized cells and free cells

PVA and polyacrylamide immobilized gels containing 8 mg bacterial cells as well as 8 mg free cells were added to different 125 mL conical flasks with 20 mL synthetic AY99 solution containing 2 g/L glucose, 0.5 g/L $(NH_4)_2SO_4$, 0.04 g/L nutrient broth, 100 mg/L AY99 and 50 mM phosphate buffer (pH=7), and incubate at 30°C with 200 rpm shaking. At 0, 6, 12, 18 and 24 h, the treated solutions were sampled and decolorizations (%) were determined. Controls without cells are also treated in the same way. The results are from duplication tests.

3.11.4 Storage stabilities of immobilized cells and free cells

PVA immobilized cell, polyacrylamide immobilized cell and free cell are stored at 4°C. Their decolorization efficiencies were determined and recorded at 0, 5^{th}, 10^{th}, 15^{th} and 20^{th} d. Storage stabilities were then represented by the decolorization efficiencies varying along with storage time. Results were duplicated.

3.12 Performance of a laboratory scale bioreactor

In a 1 L beaker, 201.57 g PVA gel cubes containing 320 mg of bacterial cells reacted with 500 mL synthetic AY 99 solution at pH=7.2-7.4. Nutrient medium and pH were set at optimum value determined by RSM. The amount of bacterial cells added (0.64 g/L) was higher than the optimum amount (0.48 g/L) as consecutive runs were conducted. Temperature were set at room temperature (25°C) as temperature effect was not obvious in the range of 25-35°C according to results of 2-level factorial design. An air diffuser collected with an air pump was set at the bottom of the beaker. The provided air gas was used for both oxidative respiration of bacteria and mixing. After 2, 4, 6, 12, 18 and 24 h, samples were taken for analysis of decolorization (%), total organic carbon (TOC) (Plate 3.16), the Microtox® EC_{50} test (Plate 3.17) and total dissolved chromium.

Plate 3.16 Shimadzu® total organic carbon (TOC) V-CSH analyzer (Kyoto, Japan).

Plate 3.17 Microtox® toxicity analyzer (Model 500, Strategic Diagnostics Inc., Newark, USA).

After one run, the synthetic AY 99 solution will be removed from the beaker, while fresh synthetic AY 99 solution will be supplied. The above mentioned parameters were measured again for duplication. This process was repeated for another 3 consecutive runs to evaluate the stability of the system. Data were

presented as mean ± S.D. Statistical analyses were performed by statistical program SIGMASTAT version 3.0 (Jandel Scientific Software, San Jose, USA) and the differences were considered to be significant at p-value < 0.05 by one-way analysis of variance (ANOVA) and Turkey Multiple Comparison Test.

3.12.1 Chromium distribution in the bioreactor

After 5 runs, 20 mL solution was collected for centrifugation, and supernatant was subjected for determination of total Cr, while the remaining pellet (suspended particles) was resuspended in 5 mL 65% HNO_3 and transferred to digestion tubes and fluxed at 150°C for 4 h. The acid digested sample was quantified in a 50 mL v-flask. In addition, 8.1 g reacted PVA gel cubes were weighted and acid digested too, and quantified in a 50 mL v-flask. Supernatant, the acid digested pellet solution (suspended particles) and the acid digested PVA gel cubes were all subjected to determination of total dissolved Cr.

3.12.2 Distribution of AY99 in the bioreactor

After 5 runs, 8.1 g PVA gel cubes as well as centrifuged pellet (suspended particles) from 20 mL treated solution were dried in 60°C oven for 3 h. After that, the resulting dried PVA gel cubes and suspended particles were extracted with 10 mL 99.9% methanol in sonicator for 1 h 3 times. The extracted solution was quantified in a 50 mL v-flask and subjected to HPLC analysis. The mobile phases were consist of

79% methanol, 19% ultrapure water and 2% acetic acid, and were degassed by sonication for 30 min before analysis. For PAD detector the wavelength was set at 451 nm. Three replicates were conducted with three times of sampling.

3.12.3 Fourier transform-infrared spectroscopy (FT-IR) analysis of suspended particles in the treated solution

It was observed that suspended particles were generated during the biodegradation of AY99 in the laboratory scale bioreactor system. These particles were mixed with biomass presented in the treated solution. Thus, they were subjected to saponification and heating to separate biomass from those non-dissolved compounds generated from degradation of AY99 synthetic solution. Reagent 1 of Sherlock® microbial identification system which was prepared by dissolving 6 g NaOH into 20 mL 99.9% methanol and 20 mL ultra pure water was used to saponificate and thus lyses those bacterial cells. Suspended particles were collected by centrifuge, and the pellets were transferred to a screwed test tube. One mL reagent 1 was added to the test tube, after mixing, the test tube was heated at 100°C in a water bath for 30 min. After that, bacterial cells were throughout lysed and dissolved in the solution, while non-dissolved compounds were still suspended in the solution. These suspended particles were collected by centrifuge, and washed by ultra pure water for 3 times. After that, the suspended particles were dried at 60°C oven for 3 h.

Subsequently, those suspended particles were used to prepare KBr disk and subjected to analysis by the Nicolet® Fouier-transformation infra-red spectroscopic system (Plate 3.18). The resulting spectrum was matched with vibration features of different functional groups (Nakamoto, 1978; Pavia et al., 2001; Silverstein et al., 2005; Zhao et al., 2005). Thus the functional groups contained in the suspended particles can be determined.

Plate 3.18 Nicolet® Fouier-transformation infra-red spectroscopic system.

4. Results

4.1 Characterization of AY99

AY99 has an absorbance peak at 451 nm. The relationship between concentration of AY99 and its absorbance at 451 nm was shown in Figure 4.1.

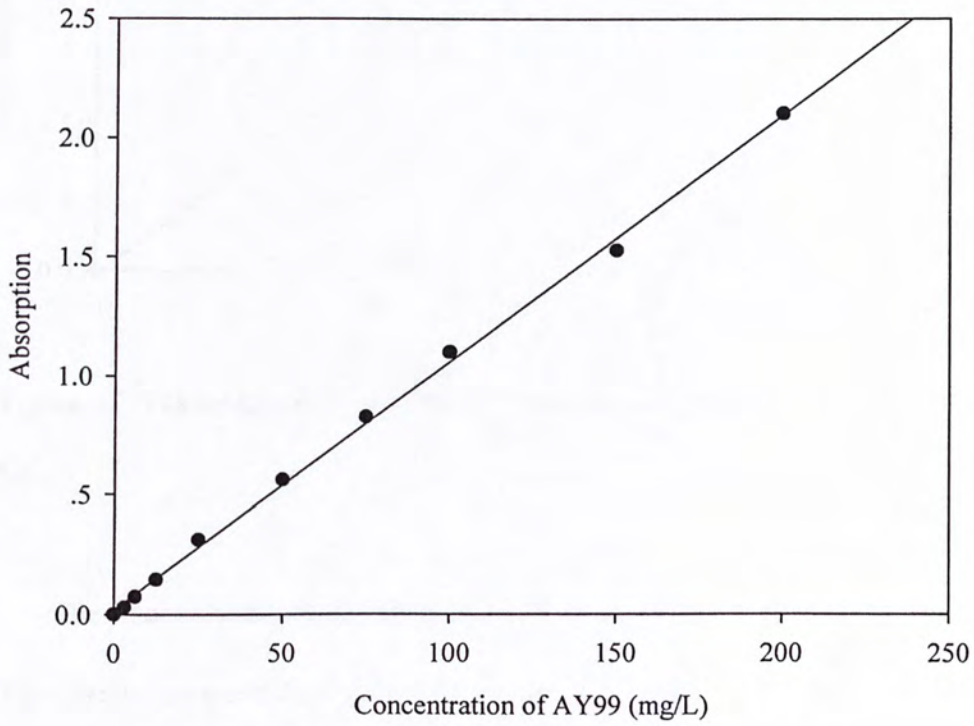

Figure 4.1 The relationship between concentrations of AY99 and its absorbance at 451 nm.

The linear regression equation was calculated as: $y = 0.0105x$ (Equation 4.1). The correlation coefficient of this equation: $R^2 = 0.9979$.

On the other hand, the relationship between concentration of AY99 and its corresponding total dissolved Cr was shown in Figure 4.2.

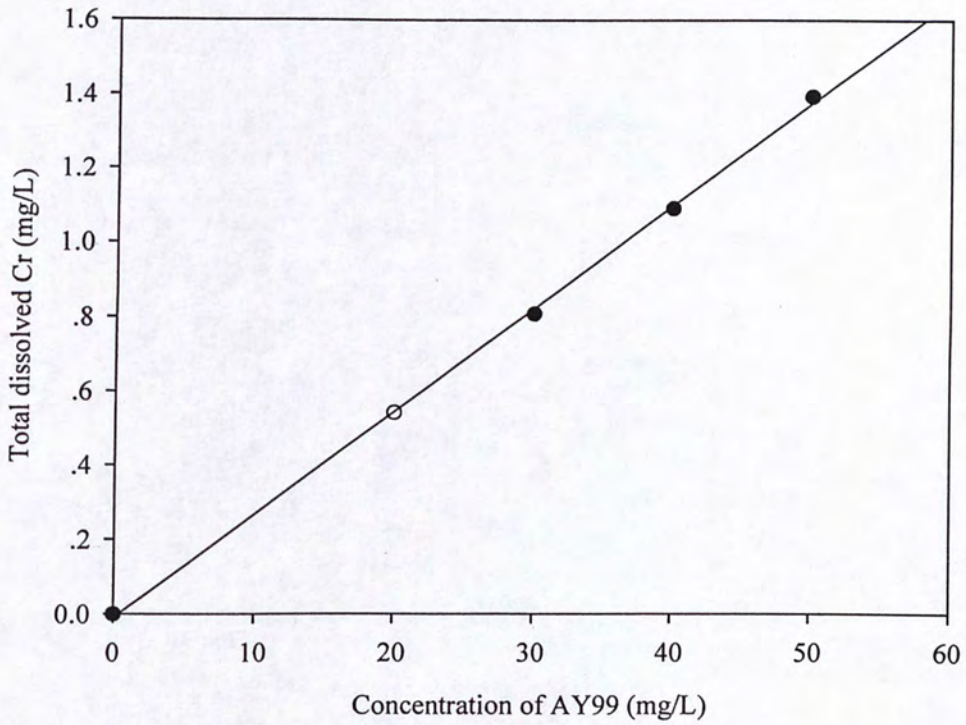

Figure 4.2 The relationship between concentrations of AY99 and its total dissolved Cr.

The linear regression equation was calculated as: $y = 0.0275x$ (Equation 4.2). The correlation coefficient of this equation: $R^2 = 0.9993$. Thus, it can be estimated that 100 mg/L AY99 contains 2.75 mg/L Cr.

4.2 Identification of isolated bacterial strains

Fourteen effective bacterial strains were selected, and they were all isolated from the Sludge Sample D. Twelve of them were Gram negative, while only two of them were Gram positive. Their microscopically images were shown in Figure 4.3.

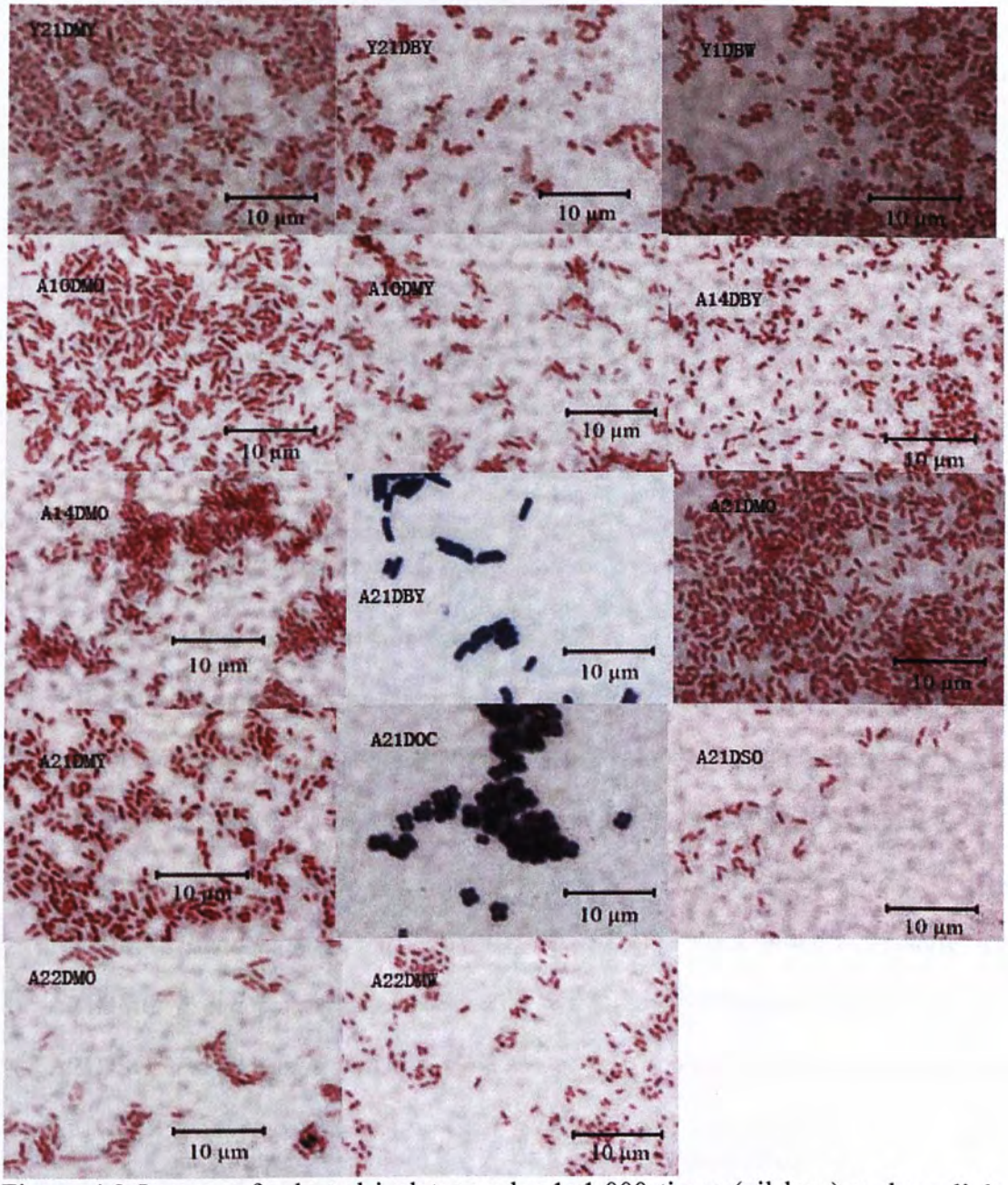

Figure 4.3 Images of selected isolates under 1×1,000 times (oil lens) under a light microscopy.

The identifications of these bacterial strains were conducted with the Sherlock® microbial identification system (MIDI Inc., Newark, Delaware, USA) and the Biolog® microstation system (Biolog Inc., Hayward, USA). Their results were shown in Table 4.1.

Table 4.1 Identification results of Sherlock® microbial identification system (MIDI) and Biolog microstation system (BIOLOG).

Name	MIDI[a]		BIOLOG[b]	
	Species name	SIM[c]	species name	SIM
Y1DBW	*Klebsiella pneumoniae* pneumoniae GC subgroup B	0.871	*Klebsiella pneumoniae*	0.657
Y21DBY	*Brevundimonas vesicularis (Pseudomonas vesicularis)*	0.466	*Sphingomonas sanguinis*	0.538
Y21DMY	*Brevundimonas vesicularis (Pseudomonas vesicularis)*	0.403	*Sphingomonas sanguinis*	0.848
A10DMY	*Pseudomonas putida* biotype B	0.853	*Pseudomonas fluorescens*	0.263
A10DMO	*Pseudomonas putida* biotype A	0.935	*Pseudomonas fluorescens*	0.639
A14DBY	*Pseudomonas putida* biotype B	0.521	*Pseudomonas marginalis*	0.721
A14DMO	*Pseudomonas putida* biotype B	0.614	*Pseudomonas marginalis*	0.766
A21DBY	*Bacillus cereus* GC subgroup A	0.715	*Bacillus cereus*	0.342
A21DMY	*Pseudomonas putida* biotype B	0.519	*Pseudomonas marginalis*	0.610
A21DMO	*Pseudomonas vancouverensis*	0.824	*Burkholderia glumae*	0.843
A21DSO	*Pseudomonas putida* biotype A	0.889	*Pseudomonas fluorescens*	0.529
A21DOC	*Staphylococcus arlettae* GC subgroup B	0.531	*Staphylococcus haemolyticus*	0.588
A22DMW	*Pseudomonas putida* biotype B	0.500	*Pseudomonas marginalis*	0.518
A22DMO	*Pseudomonas vancouverensis*	0.871	*Pseudomonas marginalis*	0.531

[a] MIDI has been conducted for 3 times.

[b] BIOLOG has been conducted for 3 times.

[c] The highest similarity index (SIM) and the corresponding species name were listed in this table. For MIDI, the acceptable SIM should be higher than 0.5, and for 16-24 h BIOLOG, the acceptable SIM should be higher than 0.5.

4.3 Selection of the most effective bacterial strains

Reduction activity towards MX-5B and AO7 were used to indicate the presence of azoreductase in selected bacterial isolates. However, since the treatment conditions were preliminary optimized with AY99, the best performer was only chosen according to its efficiency with AY99.

Only 3 selected bacterial strains showed decolorization capability for AY99, MX-5B and AO7. They are A21DSO, A10DMO and A21DMO, as shown in Figure s 4.4 - 4.6. The best two of them, A10DMO and A21DSO were subjected to molecular analysis, and a partial 16S ribosomal RNA of the selected bacterial strains was sequenced. As a result, 255 bp was obtained. After matching with the database in best alignment search tool (BLAST), both bacterial strains were identified as *Pseudomonas fluorescens* strain d220.

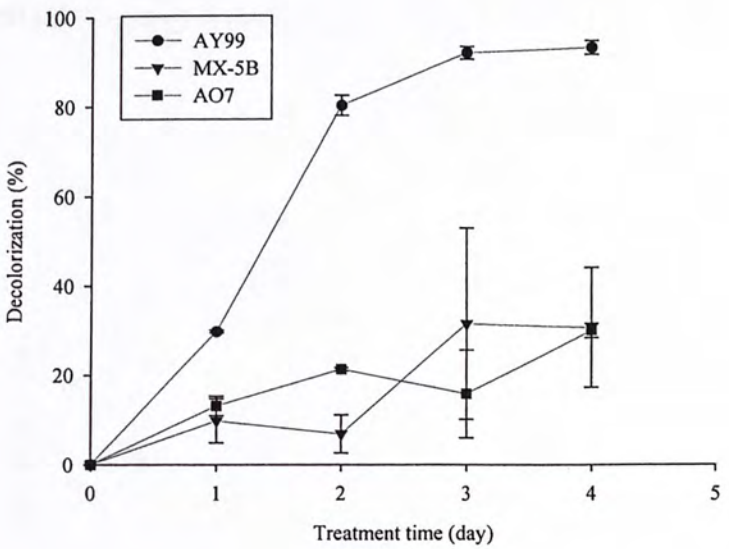

Figure 4.4 Decolorization efficiencies of A21DSO for AY99, MX-5B and AO7 after

4 d treatment (N = 3, error bars indicate S.D. of replicates).

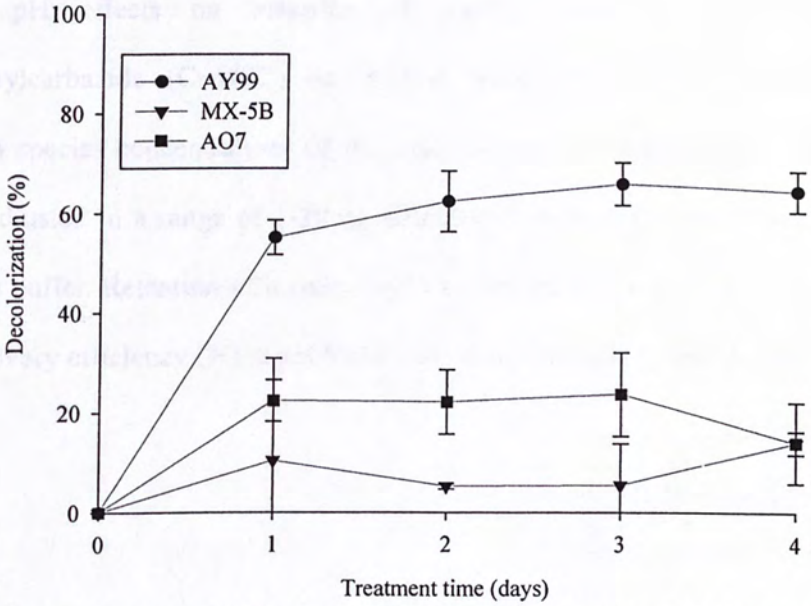

Figure 4.5 Decolorization efficiencies of A21DMO for AY99, MX-5B and AO7 after 4 d treatment (N = 3, error bars indicate S.D. of replicates).

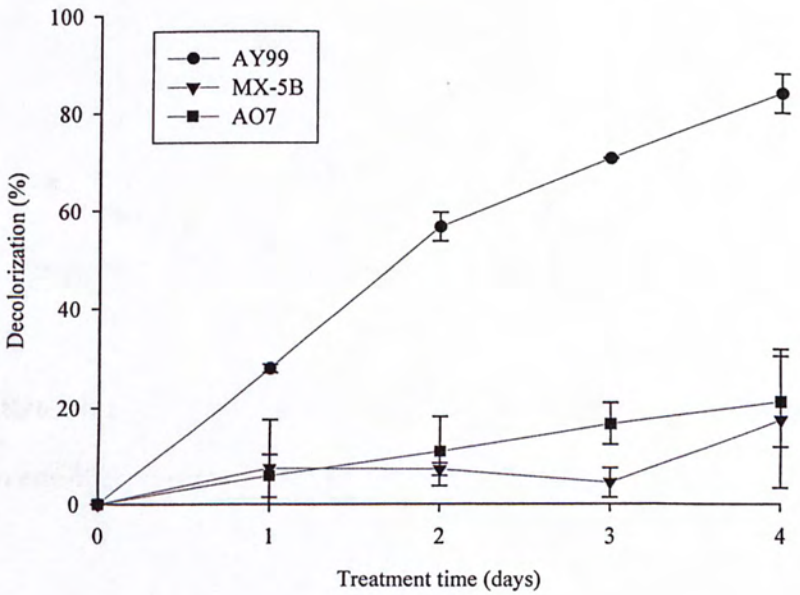

Figure 4.6 Decolorization efficiencies of A10DMO for AY99, MX-5B and AO7 after 4 d treatment (N = 3, error bars indicate S.D. of replicates).

4.4 Chromium speciation with interferences of chromium organic complexes

4.4.1 Effect of pH

The pH effects on retention of Cr(VI), ionic Cr(III), AY99 and Cr-diphenylcarbazide (Cr-DPC) on XAD-4 were investigated separately. The chromium species concentrations of the analytes were approximately 1 mg/L. The pH was adjusted in a range of 1-10 by diluted 1M HCl or 1M NaOH with 50mM phosphate buffer. Retention efficiency (%) was determined as shown in Figure 4.7, while recovery efficiency (%) at pH 5 and 1 were investigated (Table 4.2).

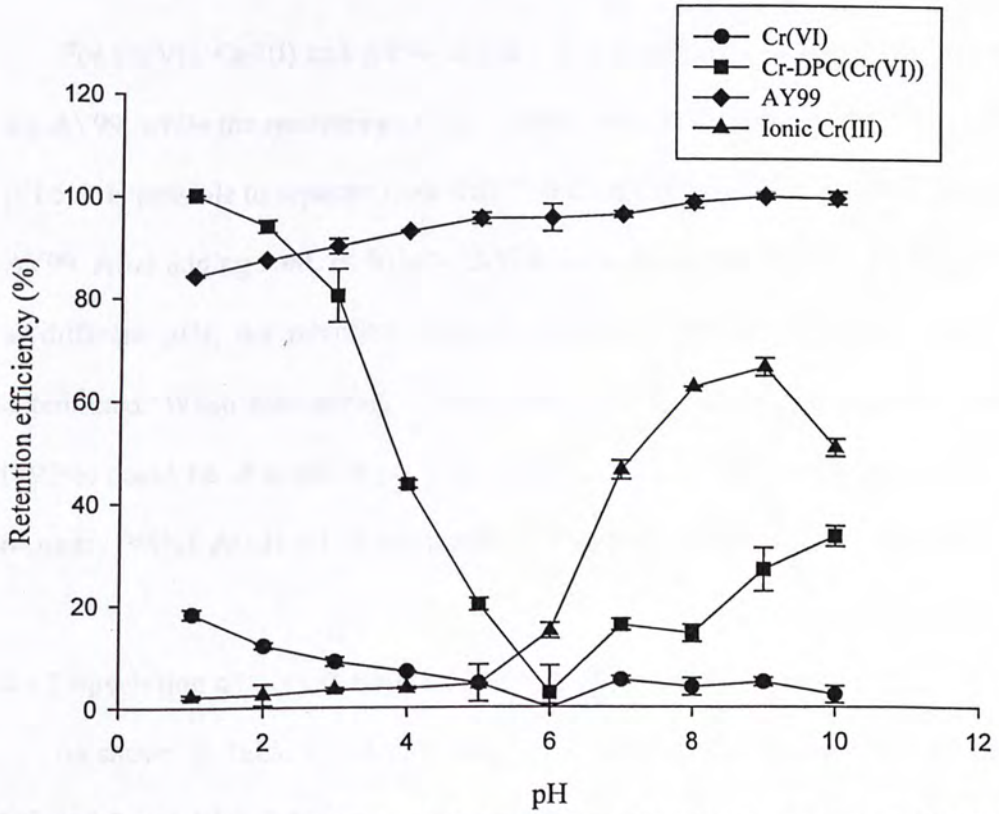

Figure 4.7 Retention efficiency (%) of different chromium species on Amberlite XAD-4 resin at different pH (N = 3, error bars indicate S.D. of replicates).

	Ionic Cr(III)		Cr(VI)		AY99		Cr-DPC (Cr(VI))	
pH	Retention efficiency (%)	Recovery efficiency (%)	Retention efficiency (%)	Recovery efficiency (%)	Retention efficiency (%)	Recovery efficiency (%)	Retention efficiency (%)	Recovery efficiency (%)
5	4.73±0.32	4.52±0.78	4.45±0.93	4.61±0.27	95.7±0.7	94.5±0.5	-	-
1	2.33±0.22	1.96±0.75	-	-	-	-	99.2±1.2	102±0.8

Table 4.2 Retention efficiency (%) and recovery efficiency (%) of various species of chromium at pH 5 and 1 (N = 3, expressed as mean±S.D.).

- not detectable

For Cr(VI), Cr(III) and AY99, at pH = 5, a quantitative recovery was achieved for AY99, while the recoveries of ionic Cr(III) and Cr(VI) were < 5%. Therefore, at pH 5, it is possible to separate ionic Cr(III) and Cr(VI) from the chromium species of AY99. After adding 1 mL of 50 mM DPC to convert approximately 1 mg/L of Cr(VI) at different pHs, the retention efficiency (%) and recovery efficiency (%) were determined. When considering Cr-DPC and ionic Cr(III), a quantitative recovery (>95%) could be obtained at pH 1 for Cr-DPC, while Cr(III) had a extremely low recovery (<5%). At pH = 1, it was possible to separate ionic Cr(III) from Cr(VI).

4.4.2 Speciation of Cr(VI), ionic Cr(III) and chromium azo dye

As shown in Table 4.3, AY99, ionc Cr(III), Cr(VI) had recoveries of 94.7±1.7, 103.0±2.5 and 96.7±3.6%, respectively. The results indicate the proposed method could effective determine Cr(VI), ionic Cr(III) and chromium azo dye (i.e. AY99) in a mixture.

Table 4.3 Spiked results of different species of chromium (N = 4, expressed as mean±S.D.).

	Ionic Cr(III)	AY99	Cr(VI)
Spiked amount (μg)	8.89	9.97	8.87
Detected amount (μg)	9.06±0.22	9.24±0.17	8.58±0.32
Recovery (%)	103.0±2.5	94.7±1.7	96.7±3.6

4.4.3 Effect of other Cr(III)-organic complexes

At pH = 1 and 5, retention efficiency (%) and recovery efficiency (%) were determined for the seven selected Cr(III)-organic complexes.

Table 4.4 Retention efficiency (%) and recovery efficiency (%) of various Cr(III)-organic complexes at pH 1 and 5 (N = 3, expressed as mean±S.D.).

		pH = 1		pH = 5	
		Retention efficiency (%)	Recovery efficiency (%)	Retention efficiency (%)	Recovery efficiency (%)
Proteins	Cr-casein	N.D[a]	N.D	N.D	N.D
	Cr-albumen	N.D	N.D	8.61±0.21	8.53±0.35
Amino acids	Cr-glutamate	N.D	N.D	5.26±0.19	5.02±0.28
	Cr-glycine	2.11±0.26	1.87±0.32	14.53±0.37	12.98±0.41
Organic acids	Cr-oxalate	N.D	N.D	6.84±0.23	6.86±0.22
	Cr-citrate	N.D	N.D	21.18±0.67	19.78±0.83
	Cr-acetate	N.D	N.D	2.89±0.12	2.55±0.37

[a] not detected

From Table 4.4, at pH = 1, all of the eight complexes would not be quantitatively retained by the XAD-4, while at pH = 5, the results were more complex and varying with species. Therefore, after AY99 was separated from

the mixture at pH = 5, Cr-DPC (Cr(VI)) could be separated quantitatively from other chromium species at pH = 1.

4.4.4 Limit of detection

The limit of detection (LOD) of the newly developed method was calculated under optimized conditions after application of the preconcentration procedure to blank solutions. The LOD of Cr(VI) based on three times the standard deviations of the blank (k =3, N= 20) was 1.37 μg/L.

4.4.5 Capacity of Amberlite XAD-4 resin

In order to investigate the adsorptive capacity of XAD-4, batch mode analysis was used. A hundred mg XAD-4 was added to 20 mL of solution containing 1.5 mg/L of Cr(VI) chelated with DPC at pH 1. After shaking for 8 h, the mixture was filtered. Then total dissolved chromium species was determined by FAAS. The capacity of sorbent (N=3) was 281.6±2.8 μg/L Cr-DPC (Cr(VI)).

Ten cycles of adsorption and regeneration process were performed to study the regeneration effect of XAD-4. Two hundred mg XAD-4 was packed in a 10 mL syringe. Ten mL 1.5 mg/L of Cr-DPC at pH 1 was passed through the column, and subsequently eluted with 10 mL 99.9% methanol with 0.1 M H_2SO_4. Ten mL ultrapure water was used to wash the column before the next cycle. After ten cycles, syringe containing XAD-4 was dried for 10 h at 37°C. A hundred mg of dried resin was weight and placed in a Polyethylene bottle, and 1 mL 99.9% methanol was added. After 30 min evaporation in room temperature (ca. 25°C), the weighted resin was added to 20 mL of solution containing 1.5

mg/L of Cr-DPC at pH 1 to perform another batch mode analysis. The adsorption capacity of regenerated XAD-4 was 278.6±3.5 μg/L (N = 3), which is not significantly different from the original capacity according to a t-test.

4.4.6 Determination of Cr(VI) in a microbial degraded chromium azo dye solution

The microbial treatment system is more complicated than a three chromium species system, and possible existence of Cr(III)-organic complexes (other than chromium azo dyes) makes it difficult to determine Cr(III) and chromium azo dye. As a result, Cr(VI) will be the only target species to be determined. In that case, pH value of the prepared solution could be higher than 5 to allow AY99 to be retained and Cr(VI) passed through the column (Figure 4.7). In this experiment, the sample has a pH value of 7, thus no further adjustment was conducted. From Table 4.5, Cr(VI) was undetectable in the treatment system, and the detected amount of Cr(VI) matched well with the added amount.

Table 4.5 Cr(VI) detected in *Pseudomonas* sp. 10MO degraded Acid Yellow 99 samples (N = 3, expressed as mean±S.D.).

	Added amount (μg)	Detected amount	Recovery (%)
Pseudomonas sp. 10MO degraded AY99	0	N.D.[a]	N.D.
	11.3	11.0±0.1	97.3±0.9
	23.2	22.9±0.4	98.7±1.7

[a] not detected

4.5 Chromium distribution in a free cells treated solution

One single colony of bacterial strains A10DMO and A21DSO were inoculated

in a nutrient medium containing 10% NB and 5g/L glucose. The inoculated solutions were incubated at 30°C and 200 rpm for 24 h. After that 1 mL of the resulting sub-culture were inoculated again to different conical flasks containing the above mentioned nutrient medium and incubated again for 2 d. Those medium solutions were centrifuged at 9820 xg by Avanti® J-E Centrifuge system with a JA-14 Rotor.

Cell mass of these two bacterial culture were harvested and transferred to the treatment system which had pH = 7 and buffered with 50 mM K_2HPO_4-KH_2PO_4. Five g/L glucose, 1 g/L $(NH_4)_2SO_4$ and 100 mg/L AY99 were also added to the treatment conical flasks which were incubated at 30°C, 200 rpm for 5 d. Mean decolorization (%) of duplication for A10MO and A21DSO were 95.7±2.3 and 94.1±1.7%, respectively. These solutions were subjected to chromium distribution test. The results were summarized in Table 4.6.

Table 4.6 Percentage distribution of chromium in different portion of well treated solutions (N = 2, expressed as mean±S.D.).

Sample	Percentage distribution (%)		
	A	B	C
A10DMO	64.0±2.7	14.0±1.2	21.0±1.6
A21DSO	61.0±4.2	18.0±1.0	19.0±0.9

4.6 Distribution of AY99 in a free cells treated solution

For the AY99 standards, their retention times were around 3.13 min as shown in Figure 4.8.

The standard curve of AY99 was shown in Figure 4.9. The linear regression equation was calculated as: $y = 8438.6x$ (Equation 4.3). The correlation coefficient

of this equation: $R^2 = 0.9949$.

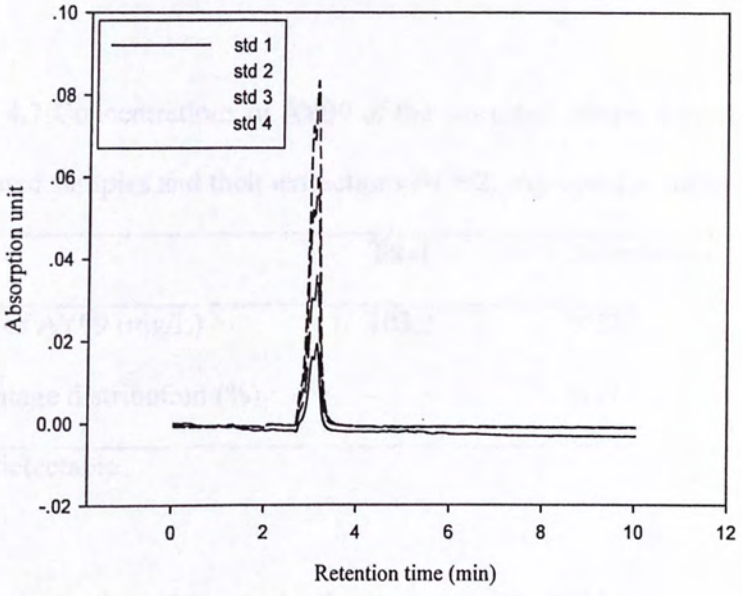

Figure 4.8 HPLC chromatograph AY99. AY99 was dissolved in 99.9% Methanol, the composition of mobile phase is: 19% water, 78% methanol and 2% acetic acid.

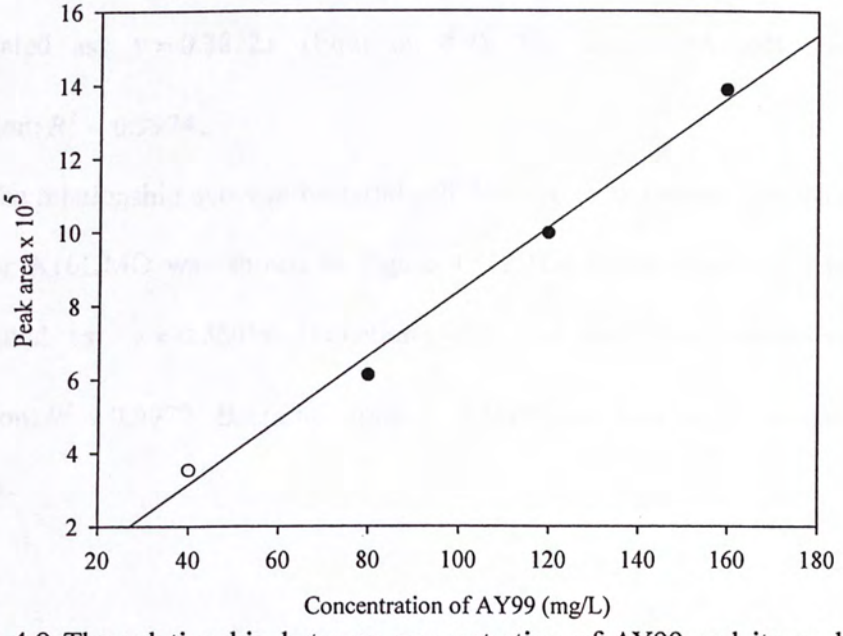

Figure 4.9 The relationship between concentration of AY99 and its peak areas on HPLC chromatograph.

The concentrations of AY99 of the untreated samples (controls), the supernatant of treated samples and their extractions were shown in Table 4.7

Table 4.7 Concentrations of AY99 of the untreated sample (control), the supernatant of treated samples and their extractions (N = 2, expressed as mean±S.D.).

	Total	Supernatant	Extraction
Conc. of AY99 (mg/L)	103.2	N.D.[a]	13.8±0.7
Percentage distribution (%)	-	N.D.	13.4±0.7

[a] Not detectable

4.7 Optimization of decolorization process with RSM

4.7.1 Correlation of cell mass and cell density of selected bacteria

The relationship between bacterial cell dry weight and optical absorbance at 520 nm for A21DSO was shown in Figure 4.10. The linear regression equation was calculated as: $y = 0.3822x$ (Equation 4.4). The correlation coefficient of this equation: $R^2 = 0.9974$.

The relationship between bacterial cell dry weight and optical absorbance at 520 nm for A10DMO was shown in Figure 4.11. The linear regression equation was calculated as: $y = 0.3501x$ (Equation 4.4). The correlation coefficient of this equation: $R^2 = 0.9979$. Bacterial strain A10DMO was selected for the optimization process.

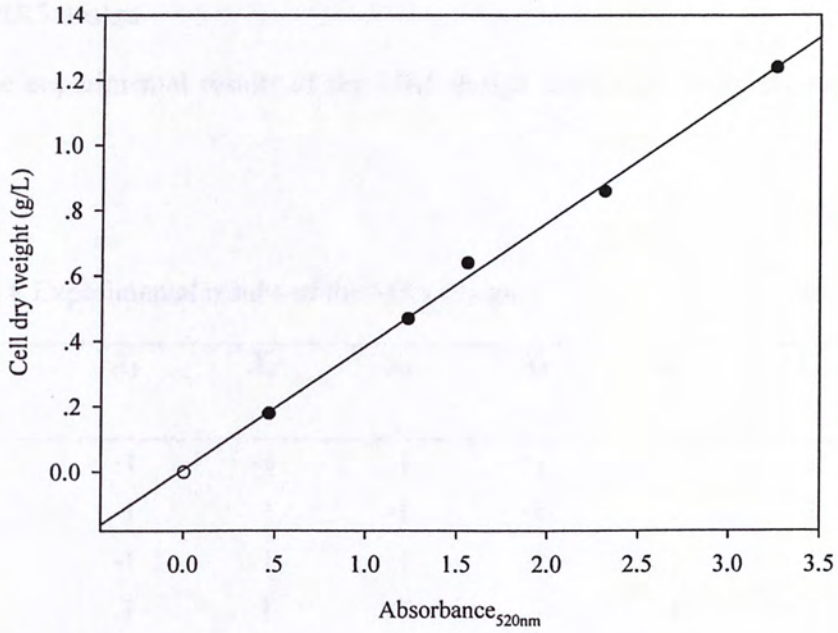

Figure 4.10 The relationship between bacterial cell dry weight and optical absorbance at 520 nm for bacterial strain A21DSO.

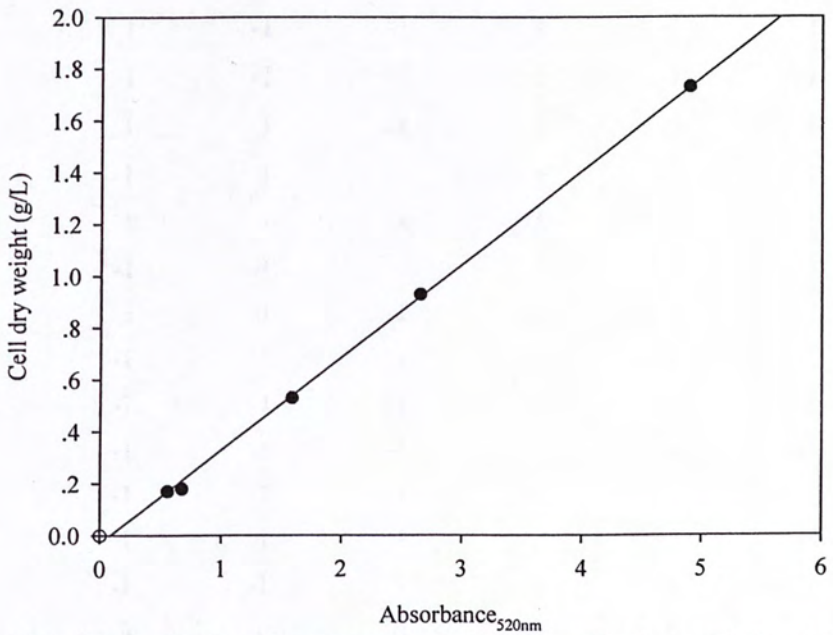

Figure 4.11 The relationship between bacterial cell dry weight and optical absorbance at 520 nm for bacterial strain A10DMO.

4.7.2 MR5 design

The experimental results of the MR5 design experiment were shown in Table 4.8.

Table 4.8 Experimental results of the MR5 design.

Std no.	X_1	X_2	X_3	X_4	X_5	X_6	Decolorization (%)
1	-1	-1	1	1	-1	1	84.36
2	1	1	-1	-1	-1	-1	84.64
3	-1	-1	-1	-1	1	-1	81.18
4	1	1	1	1	-1	-1	86.45
5	-1	1	-1	1	-1	1	62.00
6	1	1	1	-1	-1	1	80.36
7	1	-1	-1	1	-1	1	71.54
8	-1	1	-1	1	1	-1	67.00
9	1	-1	1	-1	-1	-1	85.09
10	1	-1	1	1	1	1	72.09
11	1	-1	-1	1	1	-1	88.00
12	1	1	-1	1	1	1	72.27
13	-1	1	-1	-1	1	1	62.64
14	1	1	1	-1	-1	-1	87.45
15	-1	-1	1	1	1	-1	80.36
16	1	-1	-1	-1	1	1	74.82
17	-1	1	1	-1	-1	-1	76.18
18	-1	-1	-1	-1	-1	1	59.54
19	-1	-1	-1	1	-1	-1	62.36
20	-1	1	1	1	1	1	60.73
21	1	1	1	-1	1	-1	80.54
22	-1	-1	1	-1	1	1	65.83
23	0	0	0	0	0	0	90.18
24	0	0	0	0	0	0	92.18
25	0	0	0	0	0	0	89.64
26	0	0	0	0	0	0	92.64

The results of ANOVA test of the fitted model of the MR5 design were summarized in Table 4.9.

Table 4.9 Results of ANOVA test of the fitted model of the MR5 design.

Source	Sum of Squares	df	Mean Square	F value	Prob > F	Coefficients
Model	1872.571	12	156.0476	16.21541	< 0.0001*	74.84(intercept)
x_1: Cell dry weight	385.3075	1	385.3075	40.03856	< 0.0001*	4.58
x_2: Glucose	20.33192	1	20.33192	2.112756	0.1717	-1.05
x_3: $(NH_4)_2SO_4$	124.7885	1	124.7885	12.96719	0.0036*	2.52
x_4: NB	2.315621	1	2.315621	0.240624	0.6326	-0.35
x_5: Temperature	22.86813	1	22.86813	2.376302	0.1491	-1.08
x_6: pH	350.8107	1	350.8107	36.45389	< 0.0001*	-4.29
$x_1 x_3$	70.55773	1	70.55773	7.331885	0.0190*	-1.99
$x_2 x_5$	32.89667	1	32.89667	3.418401	0.0892	-1.36
$x_3 x_4$	66.158	1	66.158	6.874694	0.0223*	1.89
$x_3 x_5$	231.0347	1	231.0347	24.00757	0.0004*	-3.49
$x_4 x_6$	27.92864	1	27.92864	2.902156	0.1142	1.25
$x_5 x_6$	135.4568	1	135.4568	14.07576	0.0028*	-2.71
Curvature	889.8861	1	889.8861	92.47097	< 0.0001*	
Residual	115.4809	12	9.62341			
Lack of Fit	108.9789	9	12.10876	5.586888	0.0920	
Pure Error	6.502061	3	2.167354			
Cor Total	2877.938	25				

* Significant at 95% confidence level

$R^2 = 0.941913$

$R^2_{adj} = 0.883825$

$R^2_{pred} = 0.618986$

The fitted first-order model with interactions in terms of coded factors was shown in Equation 4.5.

$$y = 74.84 + 4.84x_1 - 1.05x_2 + 2.52x_3 - 0.35x_4 - 1.08x_5 - 4.29x_6 - 1.99x_1x_3 - 1.36x_2x_5 + 1.89x_3x_4 - 3.49x_3x_5 + 1.25x_4x_6 - 2.71x_5x_6$$

(Equation 4.5)

As shown in Table 4.9, x_1: cell dry weight, x_3: $(NH_4)_2SO_4$ and x_6: pH are the most important factors.

4.7.3 Path of steepest ascend (PSA)

The experimental design of PSA and its corresponding results were shown in Table 4.10.

Table 4.10 Experimental design of PSA and its corresponding results.

factors	1	2	3	4	5	6
X_1: cell dry weight (g/L)	0.4	0.453	0.506	0.559	0.612	0.665
X_3: $(NH_4)_2SO_4$ (g/L)	0.5	0.65	0.8	0.95	1.1	1.25
X_6: pH	7	6	5	5	5	5
Decolorization (%)	90.91	85.36	83.18	84.36	82.64	82.27

It can be seen from Table 4.10 that the first point which is the mid-level point in MR5 design showed the highest decolorization efficiency. Therefore, this point will be used as the center point for CCD design.

4.7.4 Central composite design (CCD) and RSM

The factors and levels of CCD design were shown in Table 4.11.

Table 4.11 Factors and levels of CCD design.

Factors	Level of factors				
	-alpha	-1	0	1	+alpha
X_1: Cell dry weight (g/L)	0.23	0.3	0.4	0.5	0.57
X_3: $(NH_4)_2SO_4$ (g/L)	0.16	0.3	0.5	0.7	0.84
X_6: pH	5.32	6	7	8	8.68

The experimental results of CCD design were shown in Table 4.12.

Table 4.12 Experimental results of CCD design.

Standard runs	x_1	x_3	x_6	Decolorization (%)
1	-1	-1	-1	79.82
2	1	-1	-1	87.91
3	-1	1	-1	80.82
4	1	1	-1	89.27
5	-1	-1	1	82.02
6	1	-1	1	87.25
7	-1	1	1	85.05
8	1	1	1	89.03
9	-1.68179	0	0	79.98
10	1.681793	0	0	93.56
11	0	-1.68179	0	83.31
12	0	1.681793	0	90.07
13	0	0	-1.68179	83.56
14	0	0	1.681793	87.06
15	0	0	0	92.18
16	0	0	0	92.64
17	0	0	0	92.69
18	0	0	0	93.25
19	0	0	0	91.36
20	0	0	0	91.94

The results of ANOVA test of the fitted model of the CCD design were summarized in Table 4.13.

Table 4.13 Results of ANOVA test of the fitted model of the CCD design.

Source	SS	df	MS	F value	Prob > F
Model	390.025	9	43.33611	59.10309	< 0.0001*
x_1: Cell dry weight	144.3198	1	144.3198	196.8277	< 0.0001*
x_6: pH	25.18081	1	25.18081	34.34235	0.0002*
x_3: $(NH_4)_2SO_4$	9.545884	1	9.545884	13.01896	0.0048*
$x_1 x_6$	0.100413	1	0.100413	0.136947	0.7191
$x_1 x_3$	6.721179	1	6.721179	9.166547	0.0127*
$x_6 x_3$	0.745343	1	0.745343	1.016522	0.3371
x_1^2	88.26998	1	88.26998	120.3853	< 0.0001*
x_6^2	61.26754	1	61.26754	83.55852	< 0.0001*
x_3^2	93.61312	1	93.61312	127.6724	< 0.0001*
Residual	7.332291	10	0.733229		
Lack of Fit	5.160136	5	1.032027	2.375583	0.1821
Pure Error	2.172156	5	0.434431		

* Significant at 95% confidence level

$R^2 = 0.96494$

$R^2_{adj} = 0.892213$

$R^2_{pred} = 0.892213$

The fitted second-order model in terms of coded factors can be expressed in Equation 4.6.

$$y = 92.35 + 3.25x_1 + 1.36x_6 + 0.84x_3 - 0.11x_1x_6 - 0.92x_1x_3 + 0.30x_3x_6 - 2.47x_1^2 - 2.06x_6^2 - 2.555x_3^2$$

(Equation 4.6)

The response surface generated with the second-order model was illustrated in Figures 4.12 – 4.14.

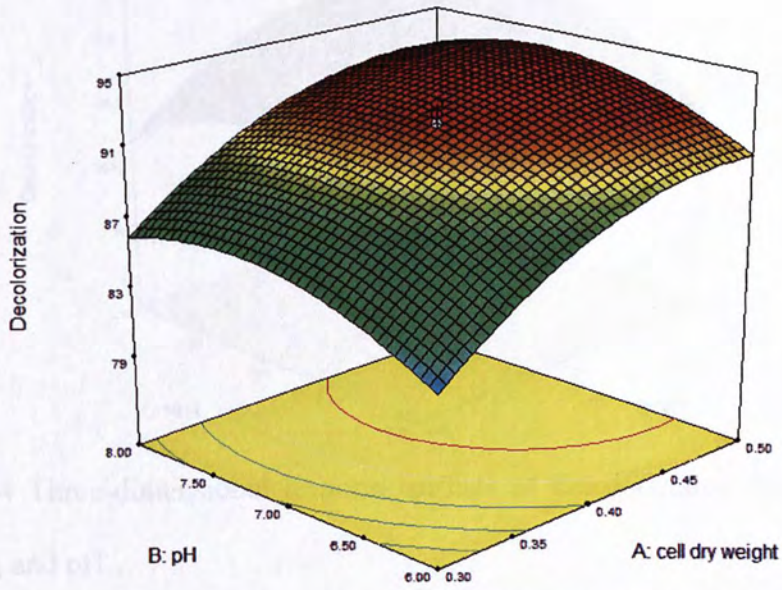

Figure 4.12 Three-dimensional response surface of decolorization (%) in terms of pH and cell dry weight.

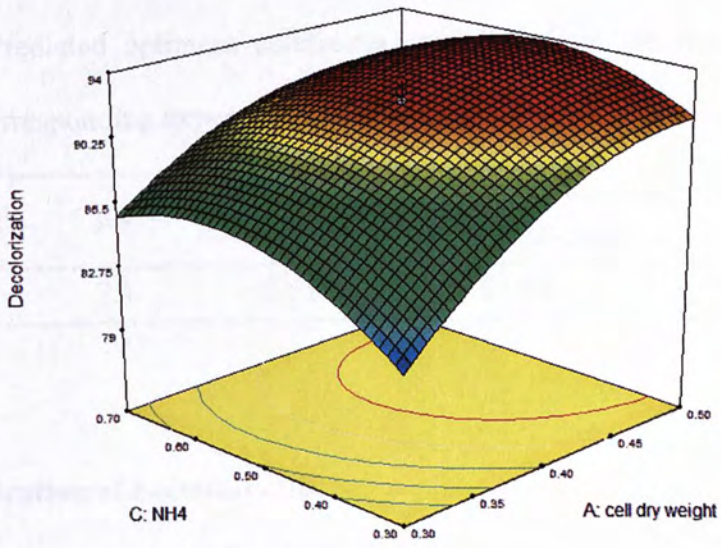

Figure 4.13 Three-dimensional response surface of decolorization (%) in terms of $(NH_4)_2SO_4$ and cell dry weight.

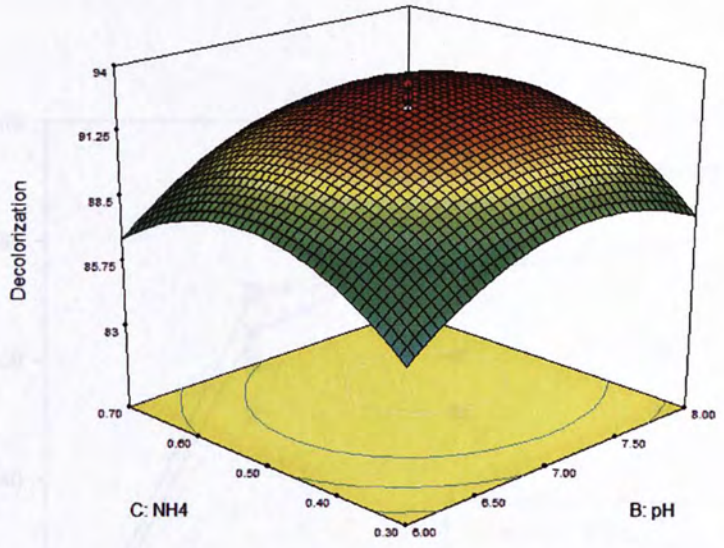

Figure 4.14 Three-dimensional response surface of decolorization (%) in terms of $(NH_4)_2SO_4$ and pH.

The predicted optimum conditions generated from the fitted second-order model and corresponding experimental results were shown in Table 4.14.

Table 4.14 Predicted optimum conditions generated from the fitted second-order model and corresponding experimental results.

Cell dry weight	pH	$(NH_4)_2SO_4$	Decolorization (Predicted)	Decolorization (Tested)
0.48	7.3	0.51	94.04	95.70±0.37

4.8 Immobilization of bacterial cells

4.8.1 Performance of immobilized cells and free cells

Within 24 h of treatment, the decolorization (%) efficiency of immobilized cells and free cells was shown in Figure 4.15.

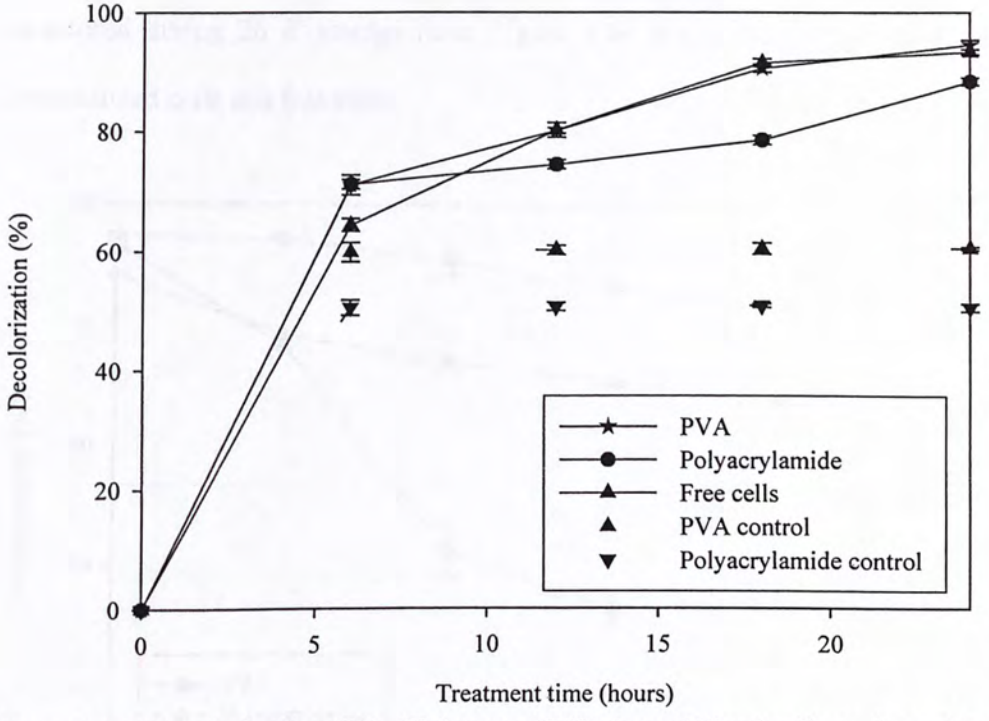

Figure 4.15 Decolorization (%) efficiency of PVA immobilized cells, polyacrylamide immobilized cells and free cells within 24 h treatment time. Dash lines shows the decolorization (%) can be achieved by adsorption on control gels without bacterial cells (N=2, error bar indicates S.D. of replicates).

It shows that PVA immobilized cells and free cells had similar decolorization (%) efficiency within 24 h, while polyacrylamide immobilized cells were slightly less effective. In addition, decolorization occurred with higher rate in the first 6 h, and gradually reached plateau after that. Besides that, control PVA gels could adsorb 60% AY99, while control polyacrylamide gels could adsorb 50% AY99.

4.8.2 Storage stabilities of immobilized cells and free cells

Decolorization (%) efficiency of immobilized cells and free cells were monitored during 20 d' storage time. Figure 4.16 shows the storage stabilities of immobilized cells and free cells.

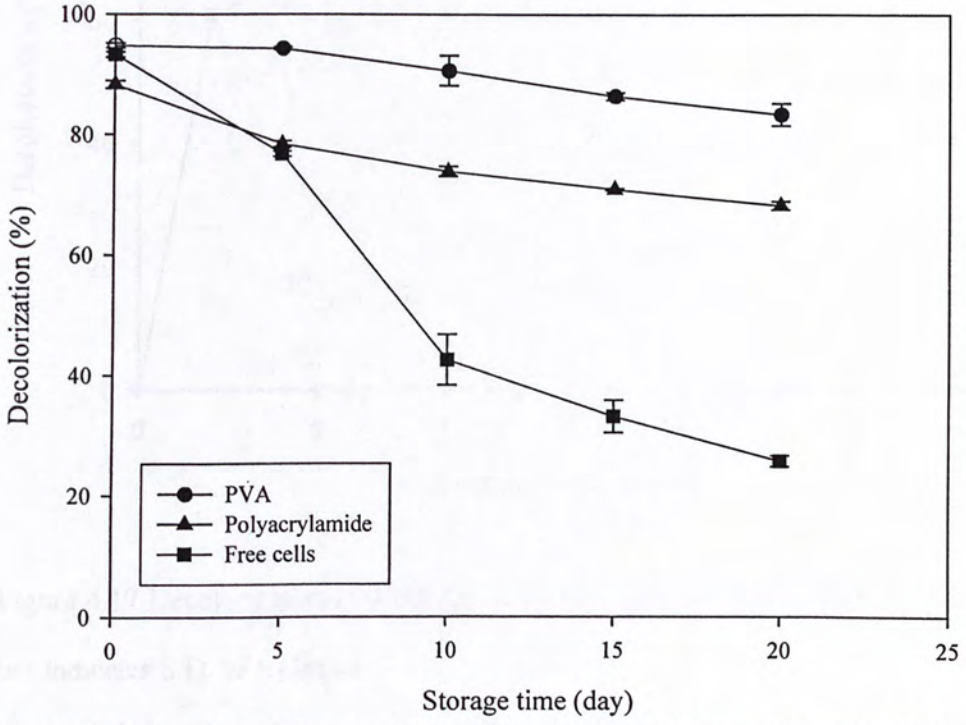

Figure 4.16 Storage stabilities of immobilized cells and free cells within 20 d (N=2, error bar indicates S.D. of replicates).

4.9 Performance of the laboratory scale bioreactor

4.9.1 Treatment efficiencies of the bioreactor

Decolorization (%) efficiency of the bioreactor within 24 h was shown in Figure 4.17.

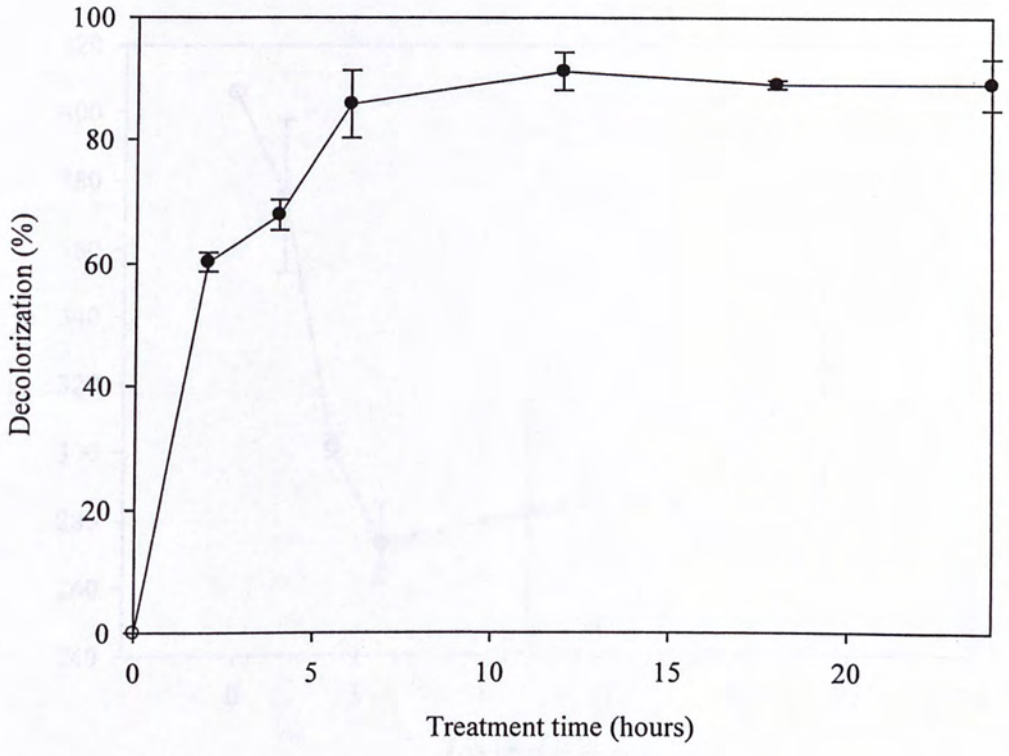

Figure 4.17 Decolorization (%) efficiency of the bioreactor within 24 h (N = 2, error bar indicates S.D. of replicates).

It can be observed that the decolorization (%) rate was higher in the first 6 h, and reach the plateau after that. The decolorization (%) efficiency of the bioreactor is around 90% within the 24 h treatment time.

The varying of total organic carbon (TOC) in the solution within 24 h was illustrated in figure 4.18.

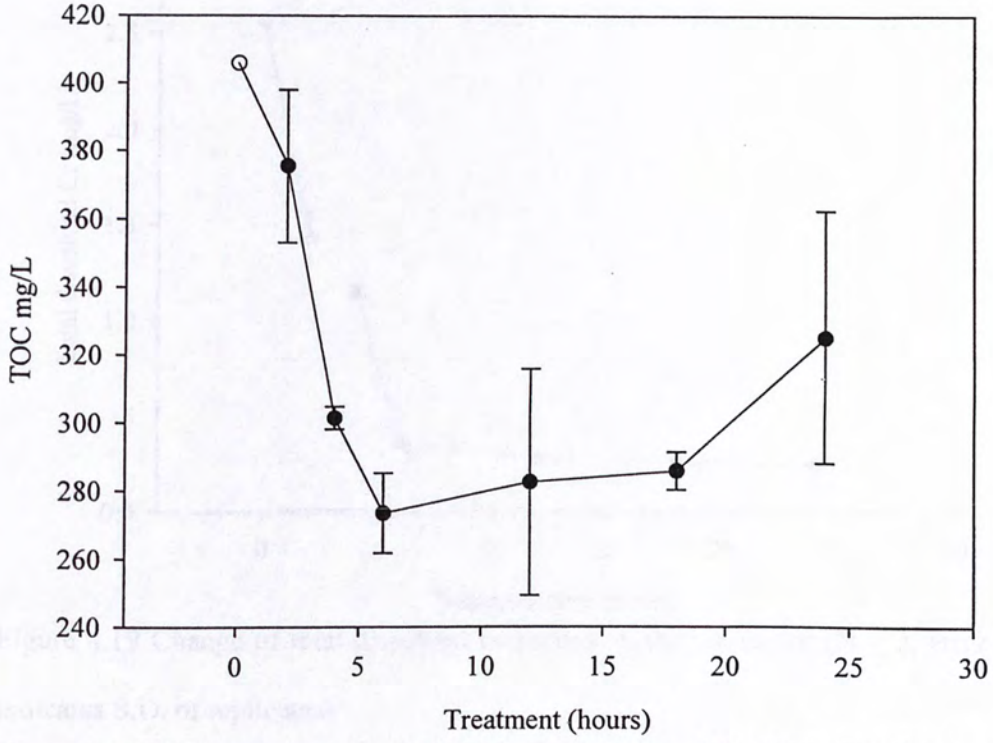

Figure 4.18 Total organic carbon (TOC) in the solution within 24 h (N = 2, error bar indicates S.D. of replicates).

The change of TOC is quite fluctuating, with large standard deviation between two consecutive runs. However, the decrease trend of TOC within the first 6 h can also be observed.

The change of total dissolved chromium in the bioreactor was shown in Figure 4.19. The total dissolved chromium in the solution of bioreactor declined very fast in the first few hours and dropped below 0.5 within 6 h. After that, the concentration of total dissolved Cr gradually decreased.

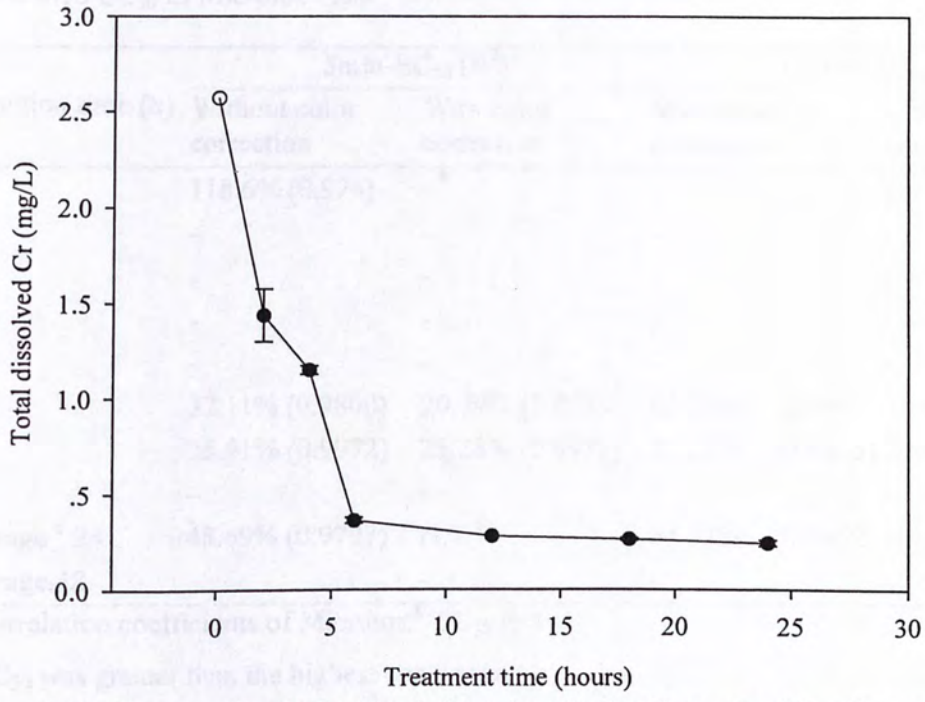

Figure 4.19 Change of total dissolved chromium in the bioreactor (N = 2, error bar indicates S.D. of replicates)

The median effective concentration (EC_{50}) generated from Microtox® test at different treatment time interval were summarized in Table 4.15.

4.9.2 Performance stability of the bioreactor in 5 consecutive runs

Decolorization (%) efficiencies of the bioreactor after treatment of 24 h in 5 consecutive runs were shown in Figure 4.21. One-way ANOVA and Turkey Mutiple Comparison Test were used to assess the significances of difference. Data are presented as means ± S.D. ($n = 3$ for each group). Significant difference ($p < 0.05$) between groups is illustrated in each figure by different letters. It can be seen from Figure 4.20 that decolorization (%) efficiencies of 5 consecutive runs were not significant different.

Table 4.15 EC_{50} of Microtox® test.

Reaction time (h)	5min-EC_{50} (R^2)[a]		15 min-EC_{50} (R^2)	
	Without color correction	With color correction	Without color correction	with color correction
0	118.6% (0.974)	-[b]	-	-
2	-	-	-	-
4	-	-	-	-
6	-	-	-	-
12	-	-	-	-
18	32.11% (0.9800)	20.79% (0.9785)	42.25% (0.9492)	25.96% (0.9584)
24	28.91% (0.9972)	25.28% (0.9978)	36.22% (0.9875)	31.69% (0.9909)
36	-	-	-	-
Storage[c] 24	48.69% (0.9797)	N.V.[d]	54.37% (0.9452)	N.V.
Storage 48	-	-	-	-

[a] Correlation coefficients of Microtox® EC_{50} test

[b] EC_{50} was greater than the highest concentration

[c] After 24 h of treatment, solution was transferred to another container, and store in 25°C

[d] Color was not visible at EC_{50}

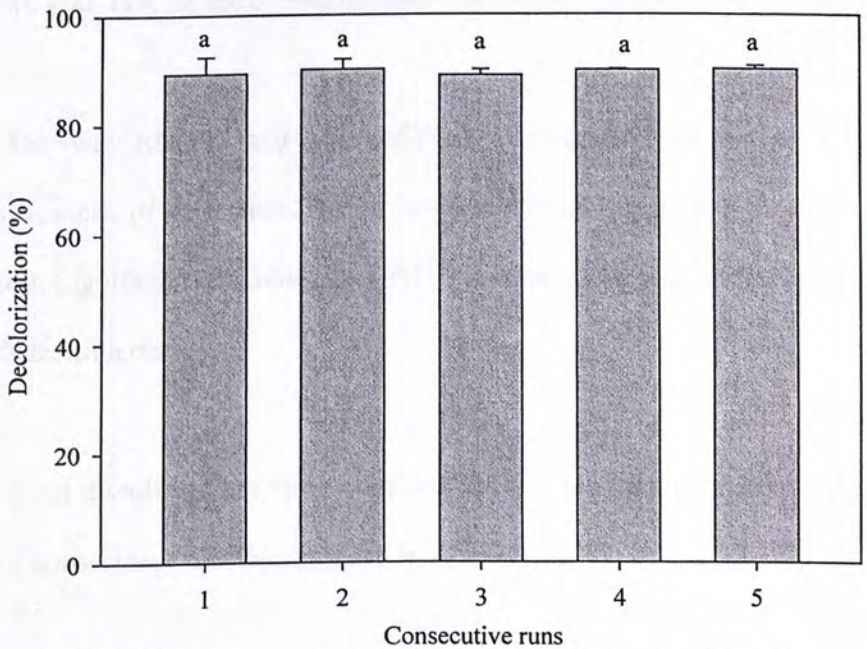

Figure 4.20 Decolorization (%) efficiencies of the bioreactor after treatment of 24 h in 5 consecutive runs.

TOC in the bioreactor after treatment of 24 h in 5 consecutive runs were shown in Figure 4.21.

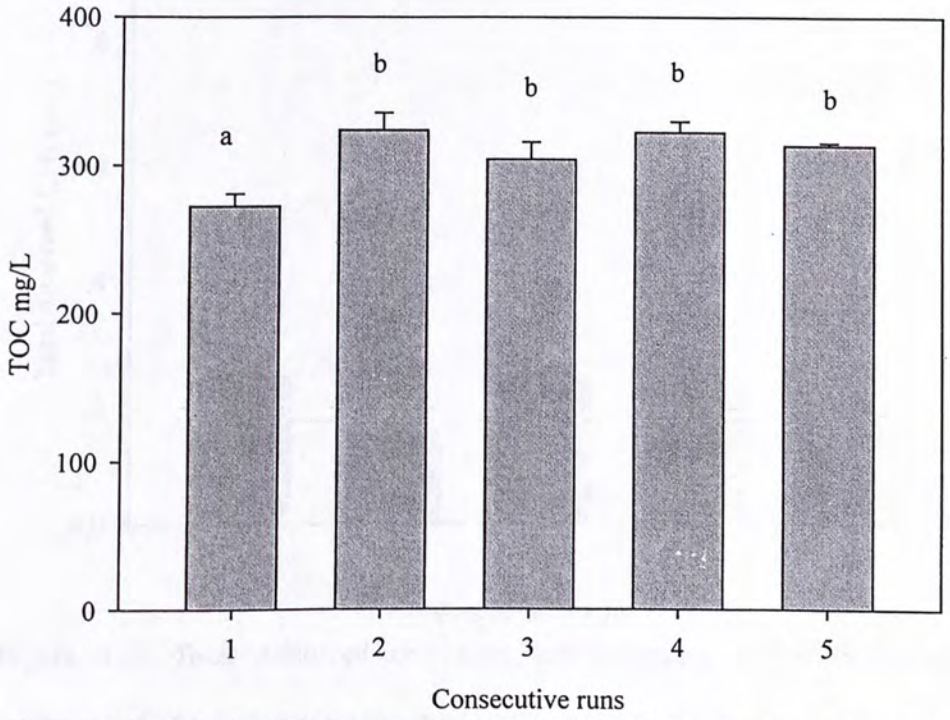

Figure 4.21 TOC in the bioreactor after treatment of 24 h in 5 consecutive runs.

One-way ANOVA and Tukey Mutiple Comparison Test were used to assess the significances of difference. Data are presented as means ± S.D. ($n = 3$ for each group). Significant difference ($p < 0.05$) between groups is illustrated in each figure by different letters.

Total dissolved chromium concentrations in the bioreactor after treatment of 24 h in 5 consecutive runs were shown in Figure 4.22

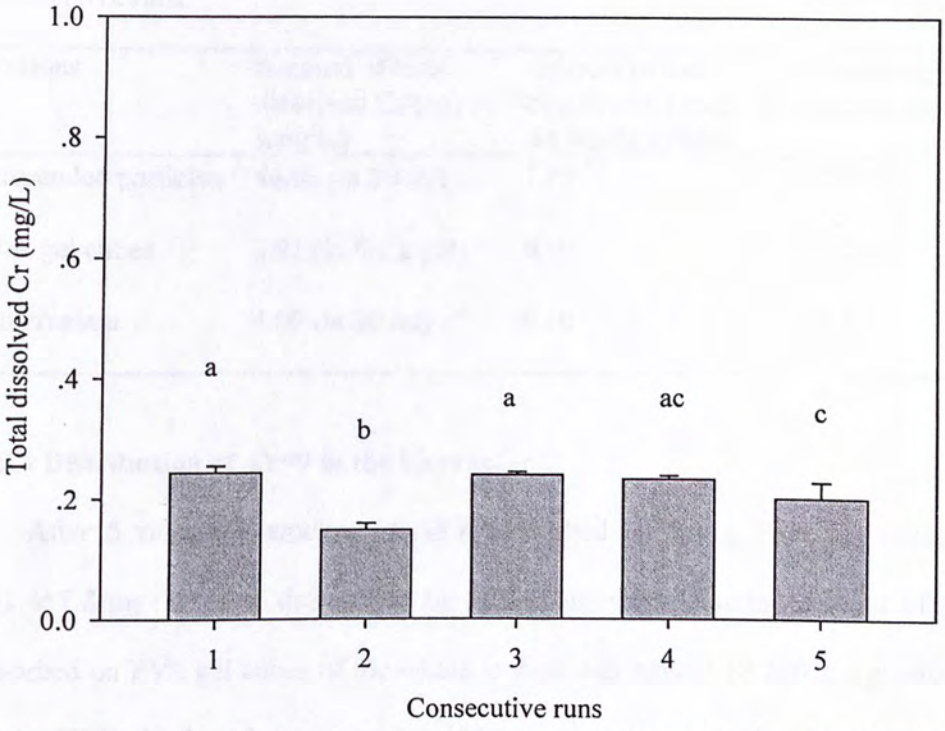

Figure 4.22 Total dissolved chromium concentrations in the bioreactor after treatment of 24 h in 5 consecutive runs.

One-way ANOVA and Tukey Mutiple Comparison Test were used to assess the significances of difference. Data are presented as means ± S.D. (n = 3 for each group). Significant difference ($p < 0.05$) between groups is illustrated in each figure by different letters.

4.9.3 Chromium distribution in the bioreactor

Amounts of total dissolved Cr in the supernatant, the acid digested pellet solution (suspended particles) and the acid digested PVA gel cubes after 5 consecutive runs were shown in Table 4.16.

Table 4.16 Amount of total dissolved Cr in different portions of the bioreactor after 5 consecutive runs.

Portions	Amount of total dissolved Cr (ug) in samples	Amount of total dissolved Cr (mg) in the whole system	Percentage distribution (%)
Suspended particles	46.06 (in 20 ml)	1.15	85.2%
PVA gel cubes	3.91 (in 8.1 g gel)	0.10	7.4%
Supernatant	4.00 (in 20 ml)	0.10	7.4%

4.9.4 Distribution of AY99 in the bioreactor

After 5 runs, the amount of AY99 adsorbed on 8.1 g PVA gel cubes was 731.4±7.8 μg (N=3) as determined by HPLC analysis. Thus the amount of AY99 adsorbed on PVA gel cubes of the whole system was around 18.2±0.2 mg, while the total AY99 added in the system was 500 mg. As a result, 3.64±0.02% of the total added AY99 was adsorbed by PVA gel cubes. The amount of AY99 adsorbed on suspended solid in 20 mL was 379.2±12.5 μg (N=3), thus the amount of AY99 adsorbed on all the suspended particles of the 5 runs might be estimated as 47.4±0.2 mg. As a result, 9.48±0.04% of the total added AY99 was adsorbed on suspended particles.

4.9.5 FT-IR analysis of suspended particles in the treated solution

The FT-IR spectrum of the suspended particles after separated from bacterial cell mass was shown in Figure 4.23.

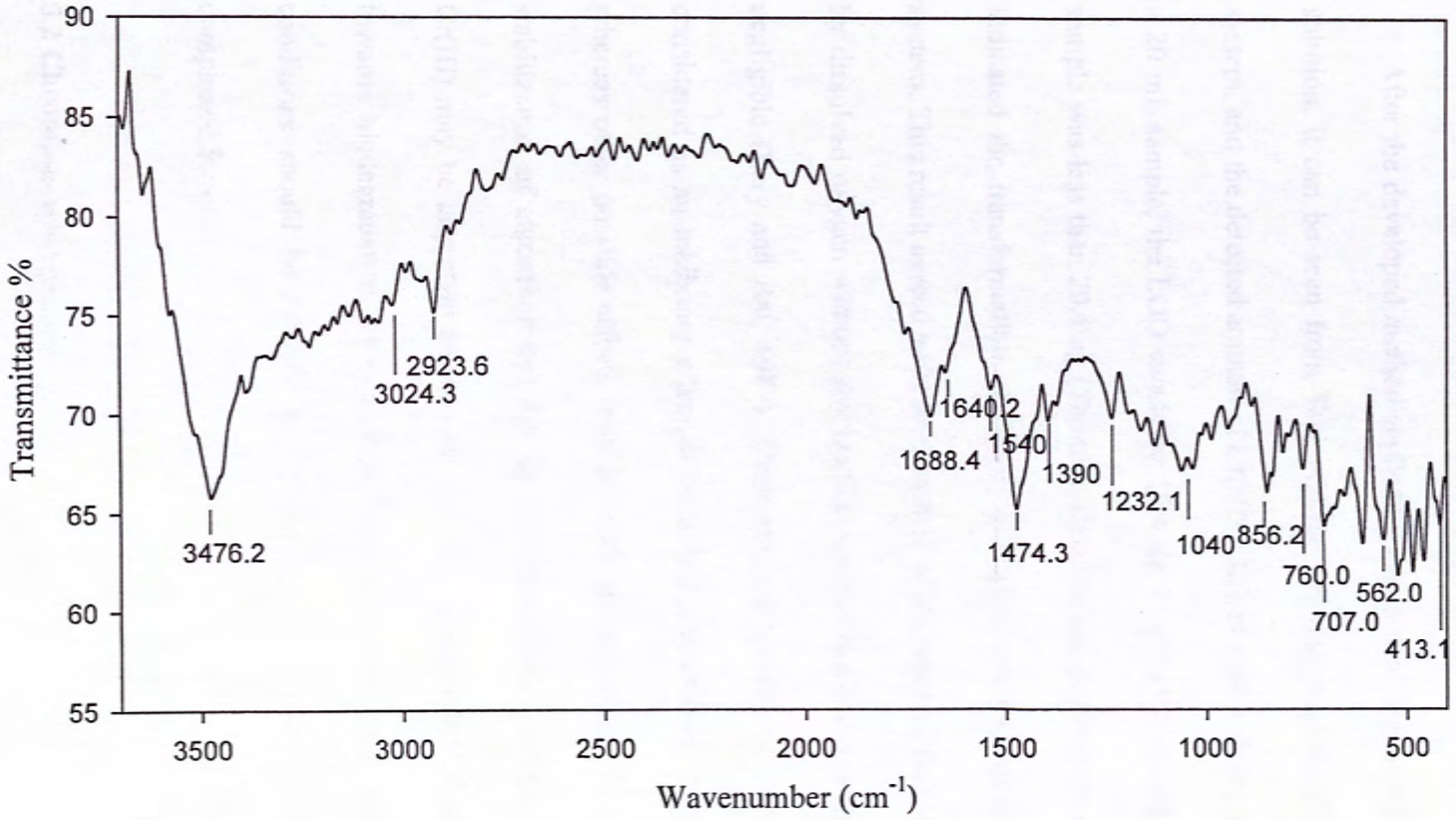

Figure 4.23 FT-IR spectrum of the suspended particles after separated from bacterial cell mass.

5. Discussion

5.1 Chromium speciation with interferences of chromium organic complexes

After the developed method applied to a microbial degraded chromium azo dye solution, it can be seen from Table 4.5 Cr(VI) was undetectable in the treatment system, and the detected amount of Cr(VI) matched well with the added amount. For a 20 mL sample, the LOD should be 20.4 ng. The Cr(VI) amount in this degraded sample was less than 20.4 ng (The total Cr in 20 mL supernatant is 17.1 μg), which indicated the transformation of Cr(III) to Cr(VI) was negligible in the treatment system. This result agreed with other studies which reported that oxidation of Cr(III) by dissolved oxygen without any mediate species (such as manganese oxides) was negligible (Eary and Rai, 1987). Therefore, the toxicity of Cr(VI) should not be considered as an inhibitory effect on microbial degradation of chromium azo dye, whereas other possible effects such as steric hinder effect of chromium complex, stabilization of chromium azo dye by transition metals and the toxicity effect of Cr(III) may be important reasons for the recalcitrant nature of chromium azo dyes towards biodegradation. In this project, the total chromium determined in many conditions should be referred to Cr(III), in both inorganic forms and organic complexed forms.

5.2 Chromium distribution

Chromium distribution has been measured in two types of treatment system. In

the first treatment system, free bacterial cells were added to the synthetic AY99 solution at pH=7, and mixed with incubation shaker at 200 rpm and 30°C. Distribution of total Cr in supernatant (A), acid washed solution (B) and remaining pellets (C) were summarized in Table 4.6. It can be seen that, most chromium content was distributed in the supernatant 64±2.7%. Chromium contained in the remaining pellets is 21±1.6%, while 14±1.2% chromium was in the acid washed solution.

In the second treatment system, 201.57 g PVA gel cubes containing 320 mg of bacterial cells were added in a 1 L bioreactor. Aeration and mixing were provided with bubbles from air dispenser. The synthetic AY99 solution had a pH value of 7.2-7.4, and was treated at 25°C. As a result, chromium content distributed in supernatant and acid digested PVA gel cubes were quite low (approximately 7.4%), while in acid digested suspended particles, around 85.2% chromium existed in this portion.

Since the suspended solid and bacterial cells can not be separated, and were mixed in the pellet in the first treatment system, the 21±1.6% chromium in the remaining pellet may overestimate the uptake of chromium by bacteria. Besides that, the amount of total dissolved Cr in the first system is much higher than the second system. One possible explanation of this phenomenon is the treatment condition in the second system could promote the destabilization of suspended particles (may be very small, and in forms of colloid solution) in the treated solution, thus aggregated to suspended flocs. This speculated destabilization effect can be attributed to several

causes. The first cause is pH effect, Walsh and O'Halloran (1996) have studied the water solubility of different Cr(III)-organic complexes at different pH value. Their results were shown in figures 5.1-5.3. It can be seen from these figures that solubility of Cr compounds are generally higher at lower pH. Furthermore, solubility of some Cr(III)-organic complexes as well as inorganic Cr^{3+} ions dropped dramatically when pH was slightly higher than 7 (e.g. Cr(III)-alanine and Cr(III)-acetate).

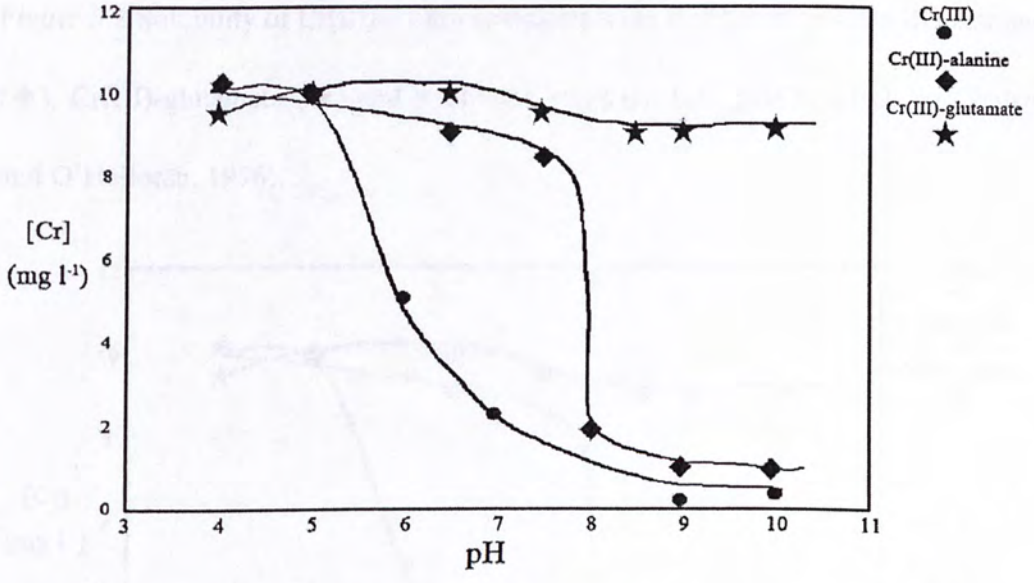

Figure 5.1 Solubility of Cr(III)-protein complexes at different pH. Cr(III)-casein (no symbol), Cr(III)-albumen (★) and reference: inorganic Cr^{3+} ($CrCl_3 \cdot 6H_2O$, •)(Walsh and O'Halloran, 1996).

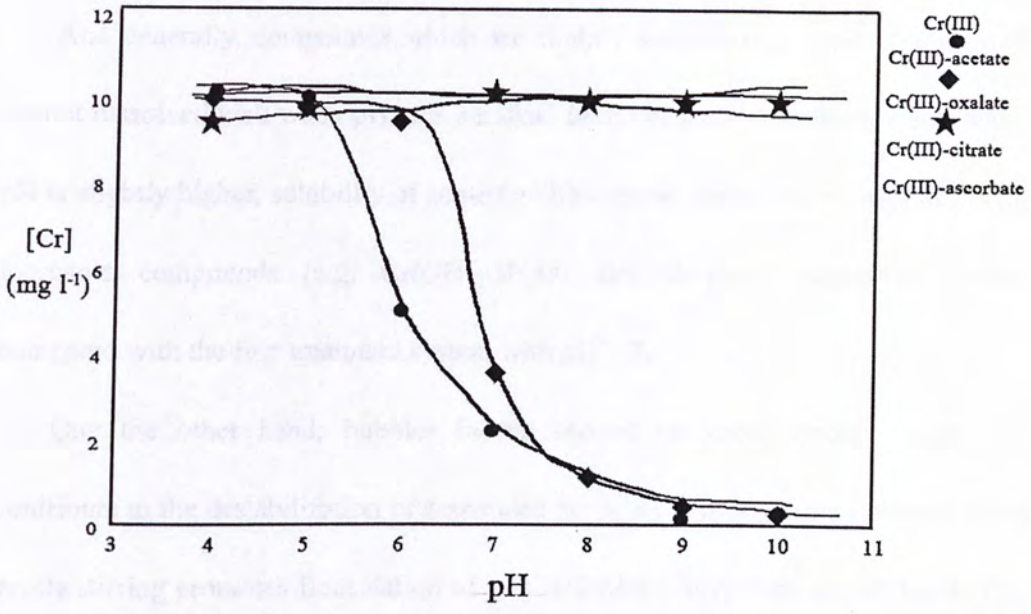

Figure 5.2 Solubility of Cr(III)-amino acid complexes at different pH. Cr(III)-alanine (◆), Cr(III)-glutamate (★) and reference: inorganic Cr^{3+} ($CrCl_3 \cdot 6H_2O$, •) (Walsh and O'Halloran, 1996).

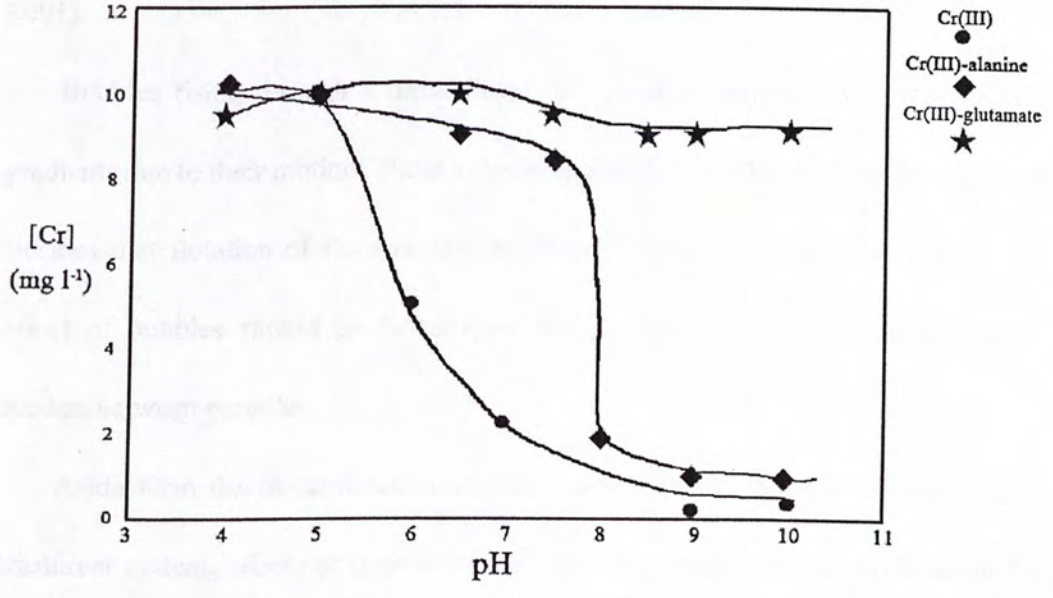

Figure 5.3 Solubility of Cr(III)-organic acid complexes at different pH. Cr(III)-acetate(◆), Cr(III)-oxalate (★), Cr(III)-citrate and Cr(III)-ascorbate (no symbol). Reference: inorganic Cr^{3+} ($CrCl_3 \cdot 6H_2O$, •) (Walsh and O'Halloran, 1996).

And generally, compounds which are slightly alkaline (e.g. with $-NH_2$ group) cannot dissolved well when pH gets alkaline. In the second treatment system, where pH is slightly higher, solubility of some Cr(III)-organic complexes as well as Cr(III) inorganic compounds (e.g. $Cr(OH)_3 \cdot 3H_2O$) may dropped dramatically when compared with the first treatment system with pH = 7.

One the other hand, bubbles in the second treatment system might also contribute to the destabilization of suspended particles. It is commonly observed that gentle stirring promotes flocculation of particles which have been destabilized. This is due to the velocity gradients which are induced in the liquid causing relative motion and therefore collisions between the particles which are present. Such flocculation caused by fluid motion is called "orthokinetic" flocculation (Svarovsky, 2001).

Bubbles rising through a destabilized fine particle suspensions create velocity gradients due to their motion. These velocity gradients could be used for flocculation. Besides that flotation of flocs is another effect of bubbles (Svarovsky, 2001). The effect of bubbles should be better than shaking which barely generates relative motion between particles.

Aside form the destabilization and aggregation of fine particles in the second treatment system, effects of immobilization may be another possible explanation for the high amount of chromium in suspended solid other than in liquid. A number of reports suggested that the immobilization has a profound effect on the metabolic

behavior of immbolized cells compared to free cells (Nedovic and Willaert, 2004). Bonin et al. (2001) have investigated metabolic differences between the attached and free-living marine bacterium *Marinobacter* sp. It was found that the generation times were 1.5 and 1.8 times shorter for immobilized cells compared to the free cells with solium lactate and 6,10,14-trimethylpentadecan-2-one (TMP), respectively. On the other hand, the growth yields were smaller for the immobilized cells, while the specific CO_2 production rate was higher for immobilized cells. In addition, it was showed that for the immobilized cells, the inhibitory effect of TMP is lower, which may explain why the immobilized cell cultures degraded TMP more efficiently than the free cell cultures. Besides that, immobilization has been shown to confer protective effects towards microorganisms, which may result in different degradation efficiency and extent. The protective effect of immobilization will be further discussed in 5.5.2 Storage stability of immobilized cells and free cells. The distribution of chromium in treated systems suggested that slightly alkaline condition and flotation might favor the precipitation of chromium species.

5.3 Distribution of AY99

Mass balance of AY99 has been tested in a free cells treated condition. It was shown that only 13.4±0.7% was absorbed by the bacterial cells and suspended particles. When bacteria were immobilized, it was shown that after 5 consecutive runs, only 3.64±0.7% AY 99 was adsorbed by both bacteria and their immobilization

matrix. However, when observed from in Figure 4.16, within 24 h of absorption, control PVA gels could adsorb 60% AY99, while control polyacrylamide gels could adsorb 50% AY99. These contradictory results could be explained with closer observation.

When immobilized cells were used to decolorize the synthetic AY99 solution, it was observed that after around 6 h, the color of the gel cubes was darker, and then gradually became lighter. Therefore, it was speculated that, gel cubes could adsorb AY99, resulting in higher concentration of AY99 within the gel cubes. During this period and the following 18 h, bacterial cells inside gel cubes were consistently decolorizing AY99. As a result, color of gel cubes first got darker, and then gradually became lighter. Thus, in Figure 4.16, the "real" decolorization (%) caused by PVA immobilized bacterial cells was higher than 33% (93.5-60.5%), while for polyacrylamide immobilized cells it is higher than 37.5% (88-50.5%). When PVA gels entrapped bacteria inside, the bacterial cells will decolorize the AY99 around them. Adsorption equilibrium of PVA gels kept concentration of AY99 inside gel matrix to a relative higher extent thus provided bacteria cells with AY99 for degradation. However, small amount of AY99 was still adsorbed on PVA gels and/or bacterial membranes. Around 10% of AY99 adsorbed on suspended particles, this may due to the chemical bonding and physical adsorption between AY99 and surface of suspended particles. The chemical bonding might including coordination bond between electron donating groups (-NH_2, -OH, C=O) and transition metal Cr(III),

while the physical adsorption was resulted from van der Waals forces (Masel, 1996).

5.4 Optimization of decolorization process with RSM

5.4.1 MR5 design

In order to screen important factor on decolorization (%) efficiency, MR5 design was used. This design can clearly indicate the importance of those main effects as well as 2-factor interaction effects. For a 6 factor designs, 6 main effects as well as 15 2-factor interaction effects were analysis. However, 9 of these 15 2-factor interaction effects were not significant. Thus they are not included in the model as shown in equation 4.5, and number of model terms reduced to 12. Those excluded 2-factor interaction terms as well as those mid-level points were used to calculate residual. Residual are quite important in ANOVA test of the fitted model. They could be used in calculation of correlation coefficient (R^2), adjusted correlation coefficient (R^2_{adj}) as well as lack-of-fit test (LOF) as shown in Equations 1.25, 1.26 and introductions in 1.6.7 Test of fitness.

Center points were quite essential in 2-level factorial design. They were replicated for 4 times, and this replication can reflect the performance stability of the treatment system as well as generate pure errors for calculation of LOF data. LOF tests whether the model adequately describes the actual response surface by comparing the (residual-pure error) with pure error. Ideally, these two terms should be closer resulting in a low F value for insignificant LOF. Additionally, center points

would be used to calculate "curvature" by comparison between the real response of the mid-level variables and the response generated with the first-order model at mid-level. Curvature is significant in my result. It is an indication that the response surface was better to be approximated with a second-order model from designs like CCDs. Generally, if curvature is not significant and the experimental level is closed to the real optimum point, a 2-level factorial design will be enough, since it is good to reduce complexity of experimental layouts, model building and statistical analysis.

Although smaller residuals could generate higher R^2, R^2_{adj} as well as insignificant LOF, including too much insignificant terms would upgrade the complexity of the model. Since the first phase of RSM is to screen out important factors as well as roughly find coefficients of each factor for PSA test, it dose not required very high precision. In fact, 2-level factorial design can not be used to provide a precisely predictive model since they can only generate first-order models which are not effective with curves. As a result, these insignificant terms were not included in the model (Anderson and Whitcomb, 2005; 2007).

5.4.2 Path of steepest ascent (PSA)

The results of PSA tests showed the original center point (cell dry weight = 0.4 g/L, $(NH_4)_2SO_4$ = 0.5 g/L and pH = 7) was quite close to the optimum point estimated from CCD design (cell dry weight = 0.48 g/L, $(NH_4)_2SO_4$ = 0.51 g/L and pH = 7.3), and the correlated responses were 90.91% vs. 94.04% decolorization

(Tables 4.11 and 4.14)

The response predicted by the second-order model generated from CCD design at original center point is 91.57%, which is quite close to the real response (90.91%). Thus, the model fitted well with real experimental points.

5.4.3 Central composite design (CCD) and RSM

The second-order model generated from CCD design exhibit very good R^2, R^2_{adj} and R^2_{pred}, besides that, lack of fit is not significant (Table 4.13). These results indicate that the model fitted well with the data from 20 times observation of experiment. Thanks to terms of A^2, B^2 and C^2, "curvature" can be accurately approximated, which is not possible in 2-level factorial design (Anderson and Whitcomb, 2005; 2007). It can be seen from the results of ANOVA test (Table 4.13) that cell dry weight, pH, $(NH_4)_2SO_4$ and interaction between cell dry weight and $(NH_4)_2SO_4$ are significant model terms, which correlated well with results of MR5 design (Table 4.9). Thus, the screening phase using MR5 design was quite effective in this experiment.

5.5 Immobilization of bacterial cells

5.5.1 Performance of immobilized cells and free cells

The decolorization (%) efficiency of PVA immobilized cells were quite close to free cells, even through immobilized cells has many advantages over free cells. The

most prominent one is immobilization provides opportunity for semi continuous or continuous treatment system. Another one is the negligible production of sludge (Nedovic and Willaert, 2004).

Immobilization of whole cells into gel matrices has been increasingly used at laboratory and industrial scale in various biotechnologies. Among gel carriers, poly(vinyl alcohol) (PVA) cryogels, formed through the freeze–thawing technique (Ariga et al., 1987), are promising matrices for whole-cell immobilization. The PVA cryogel, a labyrinthine entrapment agent, offers advantages not available with other immobilization matrix, namely very high micro- and macro-porosities, which allow non-hindered mass-transfer of substrates and metabolites; the rheological characteristics and mechanic strength of these non-brittle matrix are excellent and make them feasible in most types of reactors; the thermo-stability of PVA cryogel is superior to other commonly used thermo-reversible gel carriers; the cryogel is highly resistant to biological degradation (Kuyukina et al., 2005), as well as being insensitive to culture media compositions; PVA itself is a biologically compatible, non-toxic, and readily available low-cost polymer (Hassan and Peppas, 2000). In contrast, polyacrylamide gel has disadvantages of toxicity effect during immobilization (Petrov et al., 2007) and insufficient diffusion (White and Thomas, 1990). Besides that, polyacrylamide gels were observed to be of less mechanic strength than PVA gels in experiments of this project.

5.5.2 Storage stabilities of immobilized cells and free cells

It can be seen from Figure 4.17 that after 20 d of storage at 4°C, PVA immobilized cell still showed high decolorization (%) efficiency (~ 83%), whereas free cells almost lost decolorization ability (only ~25% decolorization (%))

Many genera of bacteria can shift themselves between vegetative growth and a resistant, resting stage. Encystment is one of those mechanisms of resting cell formation, and it is applicable for *Pseudomonas* species. Unlike endospore formed by *Bacillus* species, the cyst is formed by rounding up of the entire cell. When temperature went down, the cells shed their flagella, cease come metabolic activities, gradually become round. The cyst is surrounded by a thickened, muti-layered outer coat called "the exine", consisting of lipoprotein and lipopolysaccharide. When cysts are placed in the presence of an exogenous carbon source such as glucose under proper environmental conditions, germination occurs (Dworkin et al., 2007).

However, since lysosomal activity increase during resting cell formation, it is possible that some cells are weakened by excessive autophagy, thus reducing their revival capacity (Anderson, 1975). Thus, it appears that only some of the cells can successfully go through the resting cell stage and that among these, there is staggered growth resumption when exposure to proper temperature and carbon sources (Anderson, 1976). Therefore, it may explain why majority of those freely suspended bacterial cells can not successfully maintain degradation ability after storage of 20 d at 4°C.

In terms of immobilized bacterial cells, a number of reports have appeared suggesting that the immobilization has a profound effect on the metabolic behavior of immobilized cells compared to free cells (Nedovic and Willaert, 2004). It is well-known that immobilization can increase the tolerance of cells used as biocatalysts toward environmental factors (e.g. pH, temperature, high concentrations of metabolites, presence of toxic substances, etc)

In a lot of cases, plasmid stability can be increased upon gel immobilization. The increased plasmid stability may have resulted from the mechanical properties of the gel bead system that allows only a limited number of cell divisions to occur in each microcolony (Nedovic and Willaert, 2004).

Furthermore, immobilization can confer protection to cells exposed to toxic or inhibitory substrates or environments. It has been demonstrated that immobilization of *Escherichia coli* cells could markedly changed the protein pattern of the outer membrane. The membranes of *Escherichia coli* cells grown entrapped in Ca-alginate, showed low lipid-to-protein ratios (Keweloh et al., 1990). It has been observed that cells immobilized and grown in alginate suffered a smaller loss of cations when exposed to phenols. The re-establishment of gradients was observed at a higher phenol concentration with immobilized cells compared to free cells and less membrane damage was observed (Heipieper et al., 1991).

It has also been demonstrated that Ca-alginate immobilized cultures of *Streptococcus* lactis and S. cremoris were protected from attack by lytic

bacteriophages. And the defense mechanism was speculated as exclusion of phage particles from the gel matrix (Steenson et al., 1987)

The protein expression of gel-entrapped *Escherichia coli* cells submitted to a cold shock at 4°C with those of exponential- and stationary-phase free cells have been compared. This study showed that the protein response of immobilized cells after the cold shock was significantly different from the one of the free cells. For instance, single-strand binding protein (SBB) was specifically over-expressed by shocked immobilized cells. It was suggested that such induction of specific molecular mechanisms in immobilized bacteria might explain the high resistance of sessile-like organisms to stresses (Perrot et al., 2001)

It has been shown that *Bifidobacteria* immobilized in gella-xanyhan beads can survive significantly better than free cells as both are exposed to simulated gastric juices at pH 2.5, 2.0 and 1.5. Immobilized cells also survived better than free cells in pasteurized yoghurt after refrigerated storage for 5 weeks (Sun et al., 2000).

Therefore, PVA immobilized bacterial cells are more potential for practical application since they exhibited very good storage stability during storage.

5.6. Performance of the laboratory scale bioreactor

5.6.1 Treatment efficiencies of the bioreactor

As shown in Figure 4.19, with treatment of 24 h, the varying of TOC is quite fluctuating, with large standard deviation between two consecutive runs. It may due

to the remaining TOC content during renewal process as well as the released TOC during bacterial lyses. However, the decrease trend of TOC within the first 6 h can also be observed. The decline of TOC is not dramatic, which may be explained by relatively short treatment.

The results of EC_{50} of Microtox® test (Table 4.15) showed that the toxicity of parental compound (AY99) is extremely low, while after 18 h of degradation, toxic material emerged. This toxicity should not be induced by metal compounds, since 15 min-EC_{50} is higher than 5 min-EC_{50}. EC_{50} of 15 min exposure time should be dramatically lower indicating higher toxicity effect if the toxicants are metal compounds.

The toxicity gets higher after 24 h treatment, indicating formation of more toxic compounds or higher concentration of toxicants. However, when treatment time was prolonged to 36 h, the toxicants could be detoxified in the systems.

Besides that, after treatment of 24 h, the treated solution can detoxified within storage of 48 h. In that case, the microorganisms in the treated solution other than bacterial immobilized in PVA gels could detoxify the toxicants. This result indicates the biodegradability of the resulting solution was satisfactory.

5.6.2 Performance stability of the bioreactor in 5 consecutive runs

It can be seen from Figure 4.12 that decolorization (%) efficiencies of 5 consecutive runs were not significant different. However for TOC analysis, TOC of

run no.1 is significantly lower than the other four runs. This may due to the remaining TOC content during renewal process as well as the released TOC during bacterial lyses.

In terms of total dissolved Cr in the treated system, run no. 2 and no. 5 had significantly lower concentration of total dissolved Cr. However, the total dissolved Cr concentrations of these 5 runs were already very low (around 0.2 mg/L). The differences might be caused by slightly varied conditions between each runs (pH value, the remaining synthetic AY99 from the previous runs). Those variance in conditions may result in destabilization of Cr(III)-organic complexes which may already not well dissolved in the solution, thus change the amount of Cr dissolved in the liquid.

5.6.3 FT-IR analysis of suspended particles in the treated solution

The Resulting spectrum (Figure 4.24) was matched with vibration features of different functional groups (Nakamoto, 1978; Pavia et al., 2001; Silverstein et al., 2005; Zhao et al., 2005). As a result, the functional groups contained in the suspended particles can be determined. And the speculated existing functional groups as well as their corresponding vibration wavelength and types were shown in Table 5.1.

Table 5.1 Possible functional groups of compounds in suspended particles.

Possible functional group	Absorption frequency (cm^{-1})	Vibration	Reference
Cr-O	562	Cr-O coordination bond vibration	Zhao et al., 2005
	416	Octahedral Cr(III) vibration	Nakamot, 1978
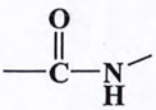	3476.2 1688.4 1640.2 707.0	N-H stretch C=O stretch N-H bending N-H wagging	Pavia et al., 2001; Silverstein et al., 2005
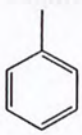	3024.3 1540.0 and 1474.3 760.0 and 707.0	=C-H stretch C=C ring stretch =C-H out of plane bending	
$-CH_3$	2923.6 1390.0	Saturated C-H stretch $-CH_3$ characteristic bending	
$-CH_2-$	2923.6 1474.3	Saturated C-H stretch $-CH_2-$ characteristic bending	
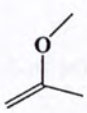	1232.1 and 1040.0 1640	C-O stretch C=C stretch	
$-NH_2$	3476.2 856.2 1640.2 1040-1232.1	N-H stretch N-H wagging N-H bending C-N stretching	
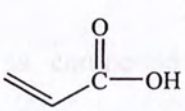	2400-3400 1688 1232.1 1640	O-H stretch (broad) conjugated C=O stretch C-O stretch C=C stretch	

Generally, cleavage of –N=N– bond will be the first step in decolorization process. After cleavage of azo bond on AY99, two amines might be generated as shown in Figure 5.5.

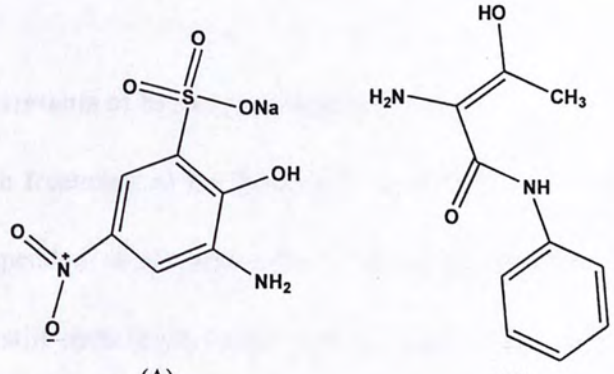

(A) (B)

Figure 5.5 Resulting amines after cleavage of azo bond.

It can be seen that the solubility of amine (B) should be much lower than amine (A), since most of its functional groups are hydrophobic. It also can form coordination bonds with Cr(III) using –OH, -NH_2 groups as well as the conjugated double bond system. When comparing with matching results from Table 5.1, this compound is highly possible presented as a ligand for Cr(III) in suspended particles.

Besides that, the existence of Cr(III) complexes compounds in suspended particles is assured from Figure 4.24 and Table 5.1.

In this study, degradation intermediates and products were not clearly identified as compounds in the treatment system might not be sufficient volatile for identification using GC-MS. However, results from FT-IR provide indirect evidences

of presence of suspected compounds. Besides, they provided suggestions for finding standard compounds for identification using HPLC and designing strategies for increasing volatility.

5.6.4 Post treatments of bioreactor treated effluents

After 24 h treatment in the laboratory scale bioreactor, the final effluents still contained suspended solids and toxic compounds. Besides, TOC of the treated solutions are still quite high (~300 mg/L), major component of TOC should be glucose (initial concentration of 1g/L and 400 mg/L TOC). These results indicate the treated solutions should be further treated. However, the 36 h storage results in Microtox ® test indicate the toxic compounds were ready to be self-detoxified with microorganisms presented.

It is reasonable to believe that the municipal sewage treatment could successfully treat the resulting effluents from the designed bioreactor. In primary treatment unit, suspended particles can be separated from the precipitation/flocculation process, and further digested along with other sludge for methane generation. The final sludge can be dried for landfill. The remaining TOC and toxic compound can be further degraded in secondary treatment where typically an activated sludge plant may be involved. After secondary sedimentation and tertiary treatment, sewage water with very low level of organic material, toxicants and suspended matter should be produced.

6. Conclusions

Biodegradation of chromium azo dyes are of great importance in remediation and reuse of wastewater in industrial effluents, as it requires low cost, produces negligible secondary pollution and shows high efficiency even at low concentrations.

The present study mainly focused on the aerobic degradation of a model chromium azo dye: AY99. Fourteen bacterial strains isolated from Sludge Sample D collected from the contact aeration tank of a primary dye treatment plant in Huizhou, China. Among them, the best two bacterial strains were identified as *Pseudomonas fluorescens* strain d220 by molecular analysis, in which a partial 16S ribosomal RNA of the selected bacterial strains was sequences.

Treatment conditions for decolorization of AY99 were optimized by RSM. In field of bioprocess, RSM were primarily used to optimize yields of bio-products such as antibiotics and other secondary metabolites. The application of RSM using extent of biodegradation (decolorization%) as response has seldom been reported.

In this project six factors including cell dry weight (g/L), glucose (g/L), $(NH_4)_2SO_4$ (g/L), nutrient broth (g/L), pH and temperature (^oC) were screened by a 2-level factorial design: minimal-runs resolution V design (MR5). Those factors that are vital to the response (decolorization (%)) were selected for the subsequent optimization. As a result, cell dry weight (g/L), $(NH_4)_2SO_4$ (g/L) and pH were found to be the most important factors for decolorization. Then whether the original mid-level point was close to the real optimum point was tested with the path of steepest ascend method. And the result showed the original mid-level point was close

to the real optimum point, thus this point was used as the center point for the center composite design (CCD). Five levels were included in a CCD, and after 20 runs, a second-order model good fitness of experimental data was built to approximate the response surface between the factors (cell dry weight (g/L), $(NH_4)_2SO_4$ (g/L) and pH) and response (decolorization (%)). The optimum conditions for decolorizing AY99 by the selected bacterial strain were found to be: 0.48 g/L cell dry weight, 0.51 g/L $(NH_4)_2SO_4$ (g/L) and pH = 7.3. Then, three independent experiments were conducted at the optimum conditions, and the decolorization (%) are found to be $95.7 \pm 0.37\%$ which is quite close to the predicted value (94.044%).

Aside from optimization, bacterial cells were also immobilized to assess their potential for practical applications. Polyvinyl alcohol (PVA) and polyacrylamide gels were used as immobilization matrix. The decolorization (%) efficiencies of immobilized cells and free cells were monitored within 24 h. It can be observed that PVA immobilized cells and free cells had similar decolorization (%) efficiency within 24 h, while polyacrylamide immobilized cells were slightly less effective. In addition, decolorization occurred with higher rate in the first 6 h, and gradually reached plateau after that. Meanwhile, storage stability of both immobilized cells and free cells were evaluated after different storage time at 4°C. The results indicate that PVA immobilized bacterial cells are more potential for practical application since they exhibited very good storage stability during long-term storage.

Furthermore, these PVA immobilized cells were employed in a laboratory scale (1 L) bioreactor. Five hundred mL synthetic AY99 solution was treated by 201.57 g PVA

gel cubes containing 320 mg of bacterial cells. Within 24 h, the decolorization (%) efficiency of the bioreactor can reach 90%. It can be observed that the decolorization (%) rate was higher in the first 6 h, and reach the plateau after that. On the other hand, varying of TOC in the treated solution is quite fluctuating, with large standard deviation between two consecutive runs. It may due to the remaining TOC content during renewal process as well as the released TOC during bacterial lyses. However, the decrease trend of TOC within the first 6 h can also be observed. The decline of TOC is not dramatic, which may be explained by relatively short treatment.

The results of EC_{50} of Microtox® test showed that the toxicity of parental compound (AY99) is extremely low, while after 18 h of degradation, toxic material emerged. This toxicity should not be induced by metal compounds, since 15 min-EC_{50} is higher than 5 min-EC_{50}. The toxicity gets higher after 24 h treatment, indicating formation of more toxic compounds or higher concentration of toxicants. However, when treatment time was prolonged to 36 h, the toxicants could be detoxified in the systems. Besides that, after treatment of 24 h, the treated solution can detoxified within storage of 48 h. In that case, the microorganisms in the treated solution other than bacterial immobilized in PVA gels could detoxify the toxicants. This result indicates the biodegradability of the resulting solution was satisfactory.

Lastly, the bioreactor treated system was operated for 5 consecutive runs to assess its performance stability. The results showed that decolorization (%) efficiencies of 5 consecutive runs were not significant different. However for TOC analysis, TOC of run no.1 is significantly lower than the other four runs. This may due to the remaining

TOC content during renewal process as well as the released TOC during bacterial lyses.

In terms of total dissolved Cr in the treated system, run no. 2 and no. 5 had significantly lower concentration of total dissolved Cr. However, the total dissolved Cr concentrations of these 5 runs were already very low (around 0.2 mg/L). The differences might be caused by slightly varied conditions between each runs (pH value, the remaining synthetic AY99 from the previous runs). Those variance in conditions may result in destabilization of Cr(III)-organic complexes which may already not well dissolved in the solution, thus change the amount of Cr dissolved in the liquid.

Another key objective of the present project is to investigate the degradation mechanism(s). Firstly, since the characteristics of Cr(VI) and Cr(III) are quite different, and Cr(VI) is extremely toxic and carcinogenic, it is important to understand what the quantities of these two species presented in the treated system. A separation system with two columns packed with XAD-4 resin was used along with total dissolved Cr analysis by AAS. It was found that at pH = 1, inorganic Cr(III) as well as 7 selected Cr(III)-organic complexes, which are most typical and common in textile effluents would not be quantitatively retained by the XAD-4 resin. Therefore, after AY99 was separated by the first column at pH > 5, Cr(VI) was complexed with DPC at pH = 1 to form a purple complex which could be steadily adsorbed on XAD-4 resin. Consequently, Cr-DPC (Cr(VI)) could be separated quantitatively from other chromium species at pH = 1. The Limit of detection of this method was 1.37 μg/L.

And the capacity of XAD-4 resin was 281.6±2.8 μg/L Cr-DPC (Cr(VI)). After 10 cycles of adsorption and regeneration process, the adsorption capacity of regenerated XAD-4 was 278.6±3.5 μg/L (N = 3), which is not significantly different from the original capacity according to a t-test. This method has been applied in a 94.5% decolorization microbial degraded solution. And the amount of Cr(VI) in this system was below detection limit, which indicated the transformation of Cr(III) to Cr(VI) was negligible in the treatment system. Therefore, in this project, the total chromium determined in many conditions should be referred to Cr(III), in both inorganic forms and organic complexed forms.

Secondly, chromium distribution in both free cell treated system and immobilized cell treated solution were investigated. The results indicated formation of high Cr content suspended particles. Beside that, adsorbed amounts of AY99 on different portion of the treated solution were also studied. It was found that 3.64±0.7% of AY99 was still adsorbed on PVA gels and/or bacterial membranes while around 10% of AY99 adsorbed on suspended particles

Lastly, the suspended particles generated during degradation were subjected to Fourier transform infrared spectroscopy (FT-IR) analysis for possible functional groups. The results indicated the presence of Cr(III) complexed compounds. Beside, they provided suggestions for finding standard compounds for identification using HPLC and designing strategies for increasing volatility for GC-MS analysis.

This project provides foundational information on how immobilized effective bacterial strains could successfully degrade chromium azo dye in a great extent in the

laboratory bioreactor under optimized conditions, and release chromium species with low solubility. These information may be applied in design of a large-scale bioreactors for pre-treatment of effluents from textile, tannery and dyeing manufacture industries before they enter municipal sewage treatment plants.

7. References

Adams, C.D. and Gorg, S., 2002. Effect of pH and gas phase ozone concentration on the decolorization of common textile dyes. Journal of Environmental Engineering 128, 293-298.

Adedayo, O., Javadpour, S., Taylor, C., Anderson, W.A., Moo Young, M., 2004. Decolourization and detoxification of Methyl Red by aerobic bacteria from a wastewater treatment plant. World Journal of Microbiology and Biotechnology 20, 545-550.

Alaton, I.A., Balcioglu, I.A., Bahnemann, D.W., 2002. Advanced oxidation of a reactive dyebath effluent: comparison of O_3, H_2O_2/UV-C and TiO_2/UV - A processes. Water Research 36, 1143-1154.

Anderson, M.J. and Whitcomb, P.J., 2005. RSM Simplified: Optimizing Processes Using Response Surface Methods for Design of Experiments, Productivity Press: New York, USA.

Anderson, M.J. and Whitcomb, P.J., 2007. DOE Simplified: Practical Tools for Effective Experimentation, 2nd ed., Productivity Press: New York, USA.

Anderson, O.R., 1975. The ultrastructure and cytochemistry of resting cell formation in *Amphora coffeaformis*. Journal of Phycology 11, 272-281.

Anderson, O.R., 1976. Respiration and photosynthesis during resting cell formation in *Amphora coffeaformis*. Limnology and Oceanography 21, 452-456.

Andrle, C.M., Jakubowski, N., Broekaert, J.A.C., 1997. Speciation of chromium using reversed phase high performance liquid chromatography coupled to different spectrometric detection methods. Spectrochimica Acta B - Atomic Spectroscopy 52, 189-200.

Anjaneyulu, Y., Sreedhara Chary, N., Samuel Suman Raj, D., 2005. Decolorization of industrial effluents: available methods and emerging technologies - A review. Reviews in Environmental Science and Biotechnology 4, 245-273.

Ariga, O., Takagi, H., Nishizawa, H., Sano, Y., 1987. Immobilization of microorganisms with PVA hardened by iterative freezing and thawing. Journal of Fermentation Technology 65, 651-658.

Arslan, I., Balcioglu, I.A., Tuhkanen, T., Bahnemann, D., 2000. H_2O_2/UV-C and Fe^{2+}/H_2O_2/UV-C versus TiO_2/UV-A treatment for reactive dye wastewater. Journal of Environmental Engineering 126, 903-911.

Arslan-Alaton, I. and Tureli, G., 2008. Degradation of aqueous Acid Red 183 textile dye and acid dye-bath effluent by Fenton-like and Photo-Fenton-like advanced oxidation processes. Fresenius Environmental Bulletin 17, 915-926.

Arslan-Allaton, I., Kabdasli, I., Teksoy, S., 2006. Effect of Fenton's treatment on the biodegradability of chromium-complex azo dyes. 4th International Conference on Oxidation Technologies for Water and Wastewater Treatment. IWA Publishing, Goslar, Germany, pp. 107-112.

Balcioglu, I.A., Arslan, I., Sacan, M.T., 2001. Homogenous and heterogenous advanced oxidation of two commercial reactive dyes. Environmental

Technology 22, 813-822.

Banat, I.M., McMullan, G., Meehan, C., Kirby, N., Nigam, P., Smyth, W.F., Marchant, R., 1999. Microbial decolorization of textile dyes presented in textile industries effluent. Industrial Waste Technical Conference, Indianapolis, USA, pp. 1-16.

Banat, I.M., Nigam, P., Singh, D., Marchant, R., 1996. Microbial decolorization of textile dye containing effluents: A review. Bioresource Technology 58, 217-227.

Barnowski, C., Jakubowski, N., Stuewer, D., Broekaert, J.A.C., 1997. Speciation of chromium by direct coupling of ion exchange chromatography with inductively coupled plasma mass spectrometry. Journal of Analytical Atomic Spectrometry 12, 1155-1161.

Bartlett, R. and James, B., 1979. Behavior of chromium in soils. III. Oxidation. Journal of Environmental Quality 8, 31-35.

Best Local Alignment Search Tool, http://blast.ncbi.nlm.nih.gov/Blast.cgi, National Center for Biotechnology Infromation (NCBI), update regularly.

Bird, C.L., 1968. The Theory and Practice of Wool Dyeing, 3rd ed., Chorley and Pickersgill Ltd: Leeds, UK.

Bobrowski, A., Bás, B., Dominik, J., Niewiara, E., Szalińska, E., Vignati, D., Zarębaski, J., 2004. Chromium speciation study in polluted waters using catalytic adsorptive stripping voltammetry and tangential flow filtration. Talanta 63, 1003-1012.

Bonin, P., Rontani, J.F., Bordnave, L., 2001. Metabolic differences between attached and free living marine bacteria: Inadequacy of liquid cultures for describing in situ bacterial activity. FEMS Microbiology letter 194, 111-119.

Bousher, A., Shen, X.D., Edyvean, R.G.J., 1997. Removal of colored organic matter by adsorption onto low cost waste materials. Water Research 31, 2084-2092.

Box, G.E.P and Wilson, K.B., 1951. On the experimental attainment of optimum condition. Journal of the Royal Statistical Society Series B 13, 1-45.

Bras, R., Ferra, M.I.A., Pinheiro, H.M., Goncalves, I.C., 2000. Batch tests for assessing decolorization of azo dyes by methanogenic and mixed cultures. 1st International Symposium on Biotechnology in the Textile Industry. Elsevier Science Bv: Amsterdam, The Netherlands. pp. 155-162.

Brierley, C.L., 1990. Bioremediation of metal contaminated surface and ground waters. Geomicrobiology Journal 8, 201-223.

Bromley-Challenor, K.C.A., Knapp, J.S., Zhang, Z., Gray, N.C.C., Hetheridge, M.J., Evans, M.R., 2000. Decolorization of an azo dye by unacclimated activated sludge under anaerobic conditions. Water Research 34, 4410-4418.

Bulut, V.N., Duran, C., Tufekci, M., Elci, L., Soylak, M., 2007. Speciation of Cr(III) and Cr(VI) after column solid phase extraction on Amberlite XAD-2010. Journal of Hazardous Materials 143, 112-117.

Canizares, P., Martinez, F., Jimenez, C., Saez, C., Rodrigo, M.A., 2009. Technical and economic comparison of conventional and electrochemical coagulation

processes. Journal of Chemical Technology and Biotechnology 84, 702-710.

Chang, J.S., Chou, C., Lin, Y.C., Lin, P.J., Ho, J.Y., Hu, T.L., 2001. Kinetic characteristics of bacterial azo dye decolorization by *Pseudomonas luteola*. Water Research 35, 2841-2850.

Chen, G.H., 2004. Electrochemical technologies in wastewater treatment. Separation and Purification Technology 38, 11-41.

Chen, G.H., Chen, X.M., Yue, P.L., 2000. Electrocoagulation and electroflotation of restaurant wastewater. Journal of Environmental Engineering 126, 858-863.

Chen, K.C., Wu, J.Y., Liou, D.J., Hwang, S.C.J., 2003. Decolorization of the textile dyes by newly isolated bacterial strains. Journal of Biotechnology 101, 57-68.

Chen, X.C., Bai, J.X., Cao, J.M., Li, Z.J., Xiong, J., Zhang, L., Hong, Y., Ying, H.J., 2009. Medium optimization for the production of cyclic adenosine 3',5'-monophosphate by *Microbacterium* sp no. 205 using response surface methodology. Bioresource Technology 100, 919-924.

Chen, X.M., Chen, G.H., Yue, P.L., 2002. Novel electrode system for electroflotation of wastewater. Environmental Science and Technology 36, 778-783.

Chinwekitvanich, S., Tuntoolvest, M., Panswad, T., 2000. Anaerobic decolorization of reactive dyebath effluents by a two stage UASB system with tapioca as a co-substrate. Water Research 34, 2223-2232.

Christie, R.M., 2001. Color Chemistry. Royal Society of Chemistry: Cambridge, UK.

Color Index International, 4th edition, http://www.colour-index.org/, published by the Society of Dyers and Colourists, updated regularly.

Coughlin, M.F., Kinkle, B.K., Bishop, P.L., 1999. Degradation of azo dyes containing aminonaphthol by *Sphingomonas* sp strain 1CX. Journal of Industrial and Microbiological Biotechnology 23, 341-346.

Davis, R.J., Gainer, J.L., Oneal, G., Wu, I.W., 1994. Photocatalytic decolorization of wastewater Dyes. Water Environment Research 66, 50-53.

Delée, W., O'Neil, C., Hawkes, F.R., Pinheiro, H.M., 1998. Anaerobic treatment of textile effluents: a review. Journal of Chemical Technology and Biotechnology 73, 323-335.

De Souza, A.A.U., Petrus, J.C.C., Santos, F.P., Brandao, H.L., Souza, S., Juliano, L.N., 2009. Color Reduction in Textile Effluents by Membranes. Latin American Applied Research 39, 47-52.

Domínguez Renedo, O., Alonso Lomillo, M.A., Arcos Marinez, M.J., 2004. Optimization procedure for the inhibitive determination of chromium(III) using an amperometric tyrosinase biosensor. Analytical Chimica Acta 521, 215-221.

dos Santos, A.B., Bisschops, I.A.E., Cervantes, F.J., van Lier, J.B., 2004. Effect of different redox mediators during thermophilic azo dye reduction by anaerobic granular sludge and comparative study between mesophilic (30°C) and thermophilic (55°C) treatments for decolorization of textile wastewaters. Chemosphere 55, 1149-1157.

dos Santos, A.B., Cervantes, F.J., van Lier, J.B., 2007. Review paper on current technologies for decolorization of textile wastewaters: Perspectives for anaerobic biotechnology. Bioresource Technology 98, 2369-2385.

Dubin, P. and Wright, K.L., 1975. Reduction of azo dyes in cultures of P*roteus vulgaris*. Xenobiotica 5, 563-571.

Dworkin, M., Falkow, S., Rosenberg, E., Schleifer, K.H., Stackebrandt, E., 2007. The Prokaryotes: A Handbook on the Biology of Bacteria: Ecophysiology and Biochemistry, 3rd ed., Springer: New York, USA.

Eary, L.E. and Rai, D., 1987. Kinetics of chromium(III) oxidation to chromium(VI) by reaction with manganese dioxide. Environmental Science and Technology 21, 1187-1193.

Eaton, A.D., Clesceri, L.S., Rice, Eugene, R.W., Greenberg, A.E., Franson, A.H., 2005. Standard Methods for the Examination of Water and Wastewater, 21st ed., American Public Health Association: Washington, D.C., USA.

Edwards, L.C. and Freeman, H.S., 2005. Synthetic dyes based on environmental considerations. Part 3: Aquatic toxicity of iron-complexed azo dyes. Coloration Technology 121, 265-270.

Edwards, L.C., Freeman, H.S., Claxton, L.D., 2004. Developing azo and formazan dyes based on environmental considerations: *Salmonella* mutagenicity. Mutation Research:Fundamental and Molecular Mechanisms of Mutagenesis 546, 17-28.

EI-Naas, M.H., Al-Muhtaseb, S.A., Makhlouf, S., 2009. Biodegradation of phenol by *Pseudomonas putida* immobilized in polyvinyl alcohol (PVA) gel. Journal of Hazardous Materials 164, 720-725.

Erdem, M., Altundogan, H.S., Turan, M.D., Tumen, F., 2005. Hexavalent chromium removal by ferrochromium slag. Journal of Hazardous Materials 126, 176-182.

Field, J.A. and Brady, J., 2001. Riboflavin as a redox mediator accelerating the reduction of the azo dye Mordant Yellow 10 by anaerobic granular sludge. 7th Latin American Workshop and Symposium on Anaerobic Digestion. IWA Publishing: Merida, Mexico. pp. 187-193.

Fitzgerald, S.W. and Bishop, P.L., 1995. 2 Stage anaerobic aerobic treatment of sulfonated azo dyes. Journal of Environmental Science and Health Part A - Toxic / Hazardous Substances and Environmental Engineering 30, 1251-1276.

Galindo, C., Jacques, P., Kalt, A., 2000. Photodegradation of the aminoazobenzene acid orange 52 by three advanced oxidation processes: UV/H_2O_2 UV/TiO_2 and Vis/TiO_2 - Comparative mechanistic and kinetic investigations. Journal of Photochemistry and Photobiology A - Chemistry 130, 35-47.

Gao, P., Chen, X.M., Shen, F., Chen, G.H., 2005. Removal of chromium(VI) from wastewater by combined electrocoagulation-electroflotation without a filter. Separation and Purification Technology 43, 117-123.

Gholivand, M.B. and Raheedayat, F., 2004. Chromium(III) ion selective electrode based on oxalic acid bis (cyclohexylidene hydrazide). Electroanalysis 16, 1330-1335.

Gingell, R. and Walker, R., 1971. Mechanisms of azo reduction by *Streptococcus faecalis* II, the role of solube flavins. Xenobiotics 1, 231-239.

Gómez, V. and Callao, M.P., 2006. Chromium determination and speciation since 2000. Trends in Analytical Chemistry 25, 1006-1025.

Gravelet Blondin, L.R., Carlieel, C.M., Barclay, S.J., Buckley, C.A., 1996. Management of water resources in South Africa with respect to the textile industry. IAWQ Specialized Conference on Pretreatment of Industrial Wastewater, Athens, Greece.

Hasan, K. and Sevil, O., 2004. Characterization and applications of some O,O'-dihydroxyazo dyes containing a 7-hydroxy group and their chromium complexes on nylon and wool. Dyes and Pigments 63, 83-88

Hassan, M.M. and Hawkyard, C.J., 2002. Decolorization of aqueous dyes by sequential oxidation treatment with ozone and Fenton's reagent. Journal of Chemical Technology and Biotechnology 77, 834-841.

Hassan, S.M. and Peppas, N.A., 2000. Structure and application of poly(vinyl acohol) hydrogels produced by conventional crosslinking or by freezing/thawing methods. Advances in Polymer Science 153, 37-65.

Heipieper, H.J., Keweloh, H., Rehm, H-J., 1991. Influence of phenols on growth and membrane permeability of free and immobilized *Escherichia* coli. Applied Microbiology and Biotechnology 57, 1213-1217.

Horistsu, H., Takada, M., Idaka, E., Tomoyda, M., Ogewa, T., 1977. Degradation of *P*-amino azo benzene by *Bacillus subtilis*. European Journal of Applied

Microbiology and Biotechnology 4, 217-224.

Hsu, Y.C., Yen, C.H., Huang, H.C., 1998. Multistage treatment of high strength dye wastewater by coagulation and ozonation. Journal of Chemical Technology and Biotechnology 71, 71-76.

Isik, M. and Sponza, D.T., 2005. Effects of alkalinity and co-substrate on the performance of an upflow anaerobic sludge blanket (UASB) reactor through decolorization of Congo Red azo dye. Bioresource Technology 96, 633-643.

Jinqi, L. and Houtian, L., 1992. Degradation of azo dyes by algae. Environmental Pollution 75,273-278.

Kapdan, I.K., Kargi, F., McMullan, G., Marchant, R., 2000. Decolorization of textile dyestuffs by a mixed bacterial consortium. Biotechnology Letters 22, 1179-1181.

Karcher, S., Kornmuller, A., Jekel, M., 2001. Screening of commercial sorbents for the removal of reactive dyes. Dyes and Pigments 51, 111-125.

Keck, A., Klein, J., Kudlich, M., Stolz, A., Knackmuss, H.J., Mattes, R., 1997. Reduction of azo dyes by redox mediators originating in the naphthalenesulfonic acid degradation pathway of *Sphingomonas* sp. strain BN6. Applied and Environmental Microbiology 63, 3684-3690.

Kesraouiouki, S., Cheeseman, C.R., Perry, R., 1994. Natural zeolite utilization in pollution control - A review of applications to metals effluents. Journal of Chemical Technology and Biotechnology 59, 121-126.

Keweloh, H., Weyrauch, G., Rehm, H-J., 1990. Phenol-induced membrane changes in free and immobilized *Escherichia coli*. Applied Microbiology Biotechnology 33, 66-71.

Khattri, S.D. and Singh, M.K., 1999. Adsorption of basic dyes from aqueous solutions by natural adsorbents. Indian Journal of Chemical Technology 6, 112-116.

Khehra, M.S., Saini, H.S., Sharma, D.K., Chadha, B.S., Chimni, S.S., 2005. Decolorization of various azo dyes by bacterial consortium. Dyes and Pigments 67, 55-61.

Khezami, L. and Capart, R., 2005. Removal of chromium(VI) from aqueous solution by activated carbons: Kinetic and equilibrium studies. Journal of Hazardous Materials 123, 223-231.

Kocaokutgen, H. and Ozkinali, S., 2004. Characterisation and applications of some o,o'-dihydroxyazo dyes containing a 7-hydroxy group and their chromium complexes on nylon and wool. Dyes and Pigments 63, 83-88.

Kongsricharoern, N. and Polprasert, C., 1993. Electrochemical precipitation of chromium (Cr^{6+}) from an electroplating waste water. In: Asian Waterqual 93 - the 4th IAWQ Asian Regional Conference on Water Conservation and Pollution Control. Pergamon-Elsevier Science Ltd: Jakarta, Indonesia. pp. 109-117.

Kongsricharoern, N. and Polprasert, C., 1996. Chromium removal by a bipolar electrochemical precipitation process. In: 18th Biennial Conference of the International Association on Water Quality, Part 5: Innovative Treatment

Technologies; Membrane Technology. Pergamon-Elsevier Science Ltd, Singapore, pp. 109-116.

Kotaś, J. and Stasicka, Z., 2006. Chromium occurrence in the environment and the methods of its speciation. Environmental Pollution 107, 263-283.

Kulla, H.G., Klausener, F., Meyer, U., Ludeke, B., Leisinger, T., 1983. Interference of aromatic sulfo groups in the microbial degradation of the azo dyes Orange I and Orange II. Archives of Microbiology 135, 1-7.

Kurniawan, T.A., Chan, G.Y.S., Lo, W.H., Babel, S., 2006. Comparisons of low cost adsorbents for treating wastewaters laden with heavy metals. Science of the Total Environment 366, 409-426.

Kuyukina, M.S., Ivshina, I.B., Gavrin, A.Y., Podorozhko, E.A., Lozinsky, V.I., Jeffree, C.E., Philp, J.C., 2005. Immobilization of hydrocarbon-oxidizing bacteria in poly(vinyl alcohol) cryogels hydrophobized using a biosurfactant. Journal of Microbiological Methods 65, 596-603.

Lau, W.J. and Ismail, A.F., 2007. Polymeric nanofiltration membranes for textile dye wastewater treatment: Preparation, performance evaluation, transport modeling, and fouling control-a review. Desalination 245, 321-348.

Lewis, D.M. and Yan, G., 1993. The effect of various chromium species on wool keratin. Journal of the Society of Dyers and Colourists 109, 193-198.

Lin, S.H. and Peng, C.F., 1995. A continuous fentons process for treatment of textile wastewater. Environmental Technology 16, 693-699.

Liu, Y.J., Zhang, A.N., Wang, X.C., 2009. Biodegradation of phenol by using free and immobilized cells of *Acinetobacter* sp. XA05 and *Sphingomonas* sp. FG03. Biochemical Engineering Journal 44, 187-192.

Lopes, C.N., Petrus, J.C.C., Riella, H.G., 2005. Color and COD retention by nanofiltration membranes. Desalination 172, 77-83.

Luo, Y., Nakano, S., Holman, D.A., Ruzicka, J., Christian, G.D., 1997. Sequential injection wetting film extraction applied to the spectrophotometric determination of chromium(VI) and chromium(III) in water. Talanta 44, 1563-1571.

Marcucci, M., Ciabatti, I., Matteucci, A., Vernaglione, G., 2003. Membrane technologies applied to textile wastewater treatment. Annals of the New York Academy of Science 984, 53-64.

Masel, R.I., 1996. Principles of Adsorption and Reaction on Solid Surface, 1st ed., Wiley-Interscience: Maiden, USA.

Matanic, H., Grabaric, Z., Briski, F., Koprivanac, N., 1996. Microbial decolorisation of chromium-azomethine dye under aerobic conditions. Journal of the Society of Dyers and Colourists 112, 158-161.

Menden, E.E., Rutland, F.H., KaUenberger, W.E., 1990. Determination of Cr(VI) in tannery waste by the chelation-extraction method. Journal of the American Leather Chemists Association 85, 363-375.

Mendez Paz, D., Omil, F., Lema, J.M., 2005. Anaerobic treatment of azo dye Acid

Orange 7 under fed-batch and continuous conditions. Water Research 39, 771-778.

Metcalf and Eddy, Inc., 2003. Wastewater Engineering: Treatment and Reuse. McGraw-Hill: New York, USA.

Milacic, R., Stupar, J., Kozuh, N., Korosin, J., Glazier, I., 1992. Fractionation of Cr and determination of Cr(VI) in blue shavings. Journal of the American Leather Chemists Association 87, 221-232.

Mo, J.H., Lee, Y.H., Kim, J., Jeong, J.Y., Jegal, J., 2008. Treatment of dye aqueous solutions using nanofiltration polyamide composite membranes for the dye wastewater reuse. Dyes and Pigments 76, 429-434.

Mohan, D. and Pittman, C.U., 2006. Activated carbons and low cost adsorbents for remediation of tri- and hexavalent chromium from water. Journal of Hazardous Materials 137, 762-811.

Mollah, M.Y.A., Schennach, R., Parga, J.R., Cocke, D.L., 2001. Electrocoagulation (EC) - science and applications. Journal of Hazardous Materials 84, 29-41.

Moosvi, S., Keharia, H., Madamwar, D., 2005. Decolourization of textile dye Reactive Violet 5 by a newly isolated bacterial consortium RVM 11.1. World Journal of Microbiology and Biotechnology 21, 667-672.

Myers, R.H., Montgomery, D.C., Anderson, C.M., 2008. Response Surface Methodology: Process and Product Optimization Using Designed Experiments, 3rd ed., John Wiley & Sons, Inc.: Hoboken, USA.

Nachiyar, C.V. and Rajkumar, G.S., 2003. Degradation of a tannery and textile dye, Navitan Fast Blue S5R by *Pseudomonas aeruginosa*. World Journal of Microbiology and Biotechnology 19, 609-614.

Nakamoto, K., 1978. Infrared and Raman Spectra of Inorganic and Coordination Compounds, 3rd ed., John Wiley and Sons: New York, USA.

Namboodri, C.G. and Walsh, W.K., 1995. Decolorizing spent dye bath with hot peroxide. American Dyestuff Reporter 84, 86-95.

Nan, J., and Yan, X.P., 2005. On-line dynamic two-dimensional admicelles solvent extraction coupled to electrothermal atomic absorption spectrometry for determination of chromium(VI) in drinking water. Analytical Chimica Acta 536, 207-212.

Nedovic, V. and Willaert, R., 2004. Fundamentals of cell immobilization biotechnology. Kluwer Academic Publisher: Dordrecht, The Netherlands.

Nigam, P., Banat, I.M., Singh, D., Marchant, R., 1996. Microbial process for the decolorization of textile effluent containing azo, diazo and reactive dyes. Process Biochemistry 31, 435-442.

Oehlert, G.W. and Whitcomb, P., 2002. Small, efficient, equireplicated resolution V fractions of 2^k designs and their application to central composite designs. In 2002 fall technical conference, Ei Paso, USA.

Padarauskas, A.V., and Kazlauskiene, L.G., 1993. Ion-pair chromatographic determination of chromium(VI). Talanta 40, 827-830.

Pandey, A., Singh, P., Iyengar, L., 2007. Bacterial decolorization and degradation of azo dyes. International Biodeterioration and Biodegradation 59, 73-84.

Pankow, J.F., Leta, D.P., Lin, J.W., Ohl, S.E., Shum, W.P., Janauer, G.E., 1977. Analysis for chromium traces in aquatic ecosystem II. A study of Cr(III) and Cr(VI) in the Susquehanna river basin of New York and Pennsylvania. Science of the Total Environment 7, 17-26.

Pare, B., Singh, P., Jonnalagadda, S.B., 2008. Visible light induced heterogeneous advanced oxidation process to degrade pararosanilin dye in aqueous suspension of ZnO. Indian Journal of Chemistry Section A - Inorganic Bio-Inorganic Physical Theoretical and Analytical Chemistry 47, 830-835.

Pasti-Grigsby, M.B., Burke, N.S., Goszczynski, S., Crawford, D.L., 1996. Transformation of azo dye isomers by *Streptomyces chromofuscus* A11. Applied and Environmental Microbiology 62, 1814-1817.

Pavia, D.L., Lampman, G.M., Kriz, G.S., 2001. Introduction to Spectroscopy: A Guide for Students of Organic Chemistry, 3rd ed., Thomson Learning, Inc.: Florence, USA.

Pazdzior, K., Klepacz-Smolka, A., Ledakowicz, S., Sojka-Ledakowicz, J., Mrozinska, Z., Zylla, R., 2009. Integration of nanofiltration and biological degradation of textile wastewater containing azo dye. Chemosphere 75, 250-255.

Peralta-Zamora, P., Kunz, A., de Moraes, S.G., Pelegrini, R., Moleiro, P.D., Reyes, J., Duran, N., 1999. Degradation of reactive dyes - I. A comparative study of ozonation, enzymatic and photochemical processes. Chemosphere 38, 835-852.

Perkowski, J., Kos, L., Ledakowicz, S., 1996. Application of ozone in textile wastewater treatment. Ozone: Science and Engineering 18, 73-85.

Perrot, F., Hebraud, M., Charlionet, R., Junter, G.A, Jouenne, T., 2001. Cell immobilization induces changes in the protein response of *Escherichia coli* K-12 to a cold shock. Electrophoresis 22, 2110-2119

Petrov, K.K., Petrova, P.M., Beschkov, V.N., 2007. Improved immobilization of Lactobacillus rhamnosus ATCC 7467 in polyacrylamide gel, preventing cell leakage during lactic acid fermentation. World Journal of Microbiology and Biotechnology 23, 423-428.

Plumb, J.J., Bell, J., Stuckey, D.C., 2001. Microbial populations associated with treatment of an industrial dye effluent in an anaerobic baffled reactor. Applied and Environmental Microbiology 67, 3226-3235.

Potgieter, J.H., Potgieter-Vermaak, S.S., Kalibantonga, P.D., 2005. Heavy metals removal from solution by palygorskite clay. Conference on Processing of Industrial Minerals. Pergamon-Elsevier Science Ltd, Falmouth, England. pp. 463-470.

Prokisch, J., Katz, S.A., Kovacs, B., Gyori, Z., 1997. Speciation of chromium from industrial wastes and incinerated sludges, Journal of Chromatography A 774, 363-371.

Raghavacharya, C., 1997. Color removal from industrial effluents - a comparative review of available technologies. Chemical Engineering World 32, 53-54.

Rau, J., Knackmuss, H.J., Stolz, A., 2002. Effects of different quinoid redox mediators on the anaerobic reduction of azo dyes by bacteria. Environmental Science and Technology 36, 1497-1504.

Robinson, T., McMullan, G., Marchant, R., Nigam, P., 2001. Remediation of dyes in textile effluent: a critical review on current treatment technologies with a proposed alternative. Bioresource Technology 77, 247-255.

Rodriguez, E., Pickard, M.A., Vazquez Duhalt, R., 1999. Industrial dye decolorization by laccases from ligninolytic fungi. Current Microbiology 38, 27-32.

Rossini, M., Garrido, J.G., Galluzzo, M., 1999. Optimization of the coagulation-flocculation treatment: Influence of rapid mix parameters. Water Research 33, 1817-1826.

Russ, R., Rau, J., Stolz, A., 2000. The function of cytoplasmic flavin reductases in the reduction of azo dyes by bacteria. Applied and Environmental Microbiology 66, 1429-1434.

Sahinkaya, E., Uzal, N., Yetis, U., Dilek, F.B., 2008. Biological treatment and nanofiltration of denim textile wastewater for reuse. Journal of Hazardous Materials 153, 1142-1148.

Saur, I.F.R., Rubach, S., Forde, J.S., Kjaerheim, G., Syversen, U., 1996. Electroflocculation: Removal of oil, heavy metals and organic compounds from oil-in-water emulsions. Filtration and Separation 33, 295-303.

Schliephake, K., Mainwaring, D.E., Lonergan, G.T., Jones, I.K., Baker, W.L., 2000. Transformation and degradation of the disazo dye Chicago Sky Blue by a purified laccase from *Pycnoporus cinnabarinus*. Enzyme and Microbial Technology 27, 100-107.

Shanker, A.K., Cervantes, C., Loza-Tavera, H., Avudainayagam, S., 2005. Chromium toxicity in plants. Environmental International 31, 739–753.

Silverstein, R.M., Webster, F.X., 2005. Spectrometric Identification of Organic Compounds, 7th ed., John Wiley and Sons, Inc.: Hoboken, USA.

Slokar, Y.M. and Le Marechal, A.M., 1998. Methods of decoloration of textile wastewaters. Dyes and Pigments 37, 335-356.

So, K.O., Wong, P.K., Chan, K.Y., 1990. Decolorization and biodegradation of Methyl Red by *Acetobacter liquefaciens*. Toxicity Assessment 5, 221-235.

Staehelin, J. and Hoigne, J., 1982. Decomposition of ozone in water - Rate of initiation by hydroxide ions and hydrogen peroxide. Environmental Science and Technology 16, 676-681.

Steenson, L.R., Klaenhammer, T.R., Swaisgood, H.E., 1987. Calcium alginate-immobilized cultures of lactic streptococci are protected from bacteriophages. Journal of Dairy Science 70, 1121-1127.

Stolz, A., 2001. Basic and applied aspects in the microbial degradation of azo dyes. Applied Microbiology and Biotechnology 56, 69-80.

Sugiura, W., Miyashita, T., Yokoyama, T., Arai, M., 1999. Isolation of azo dye degrading microorganisms and their application to white discharge printing of fabric. Journal of Bioscience and Bioengineering 88, 577-581.

Sumathi, K.M.S., Mahimairaja, S., Naidu, R., 2005. Use of low cost biological wastes and vermiculite for removal of chromium from tannery effluent. Bioresource Technology 96, 309-316.

Sun, W. and Griffiths, M.W., 2000. Survival of bifidobacteria in yogurt and simulated gastric juices following immobilization in gellen-xanthan beads. International Journal of Food 61, 17-25.

Svancara, I., Foret, P., Vytras, K., 2004. The determination of chromium as chromate at a carbon paste electrode modified with surfactants, Talanta 64, 844-852.

Svarovsky, L., 2001. Solid-Liquid Separation, 4th ed., Butterworth-Heinemann: Oxford, UK.

Swamy, J. and Ramsay, J.A., 1999. Effects of glucose and NH_4^+ concentrations on sequential dye decoloration by *Trametes versicolor*. Enzyme and Microbial Technology 25, 278-284.

Talarposhti, A.M., Donnelly, T., Anderson, G.K., 2001. Colour removal from a simulated dye wastewater using a two phase anaerobic packed bed reactor. Water Research 35, 425-432.

Torrades, F., Garcia Montano, J., Garcia Hortal, J.A., Domenech, X., Peral, J., 2004. Decolorization and mineralization of commercial reactive dyes under solar light

assisted photo-Fenton conditions. Solar Energy 77, 573-581.

Tsogas, G.Z., Giokas, D.L., Vlessidis, A.G., Evmridis, N.P., 2004. A single-reagent method for the speciation of chromium in natural waters by flame atomic absorption spectrometry based on vesicular liquid coacervate extraction, Spectrochimica Acta B-Atomic Spectroscopy 59, 957-965.

Tunçeli, A. and Türker, A. R., 2002. Speciation of Cr(III) and Cr(VI) in water after concentration of its 1,5-diphenylcarbazone complex on Amberlite XAD-16 resin and determination by FAAS, Talanta 57, 1199-1204.

Ueda, J., Satoh, H., Kagaya, S., 1997. Determination of chromium(III) and chromium(VI) by graphite-furnace atomic absorption spectrometry after co-precipitation with hafnium hydroxide, Analytical Sciences 13, 613-617.

Umbuzeiro, G.D.A., Freeman, H.S., Warren, S.H., de Oliveira, D.P., Terao, Y., Watanabe, T., Claxton, L.D., 2005. The contribution of azo dyes to the mutagenic activity of the Cristais River. Chemosphere 60, 55-64.

Unnithan, M.R., Vinod, V.P., Anirudhan, T.S., 2004. Synthesis, characterization, and application as a chromium(VI) adsorbent of amine modified polyacrylamide grafted coconut coir pith. Industrial and Engineering Chemistry Research 43, 2247-2255.

Vajpayee, P., Sharma, S.C., Tripathi, R.D., Rai, U.N., Yunus, M., 1999. Bioaccumulation of chromium and toxicity to photosynthetic pigments, nitrate reductase activity and protein content of *Nelumbo nucifera gaertn.* Chemosphere 39, 2159-2169.

van der Zee, F.P., Bisschops, I.A.E., Blanchard, V., Bouwman, R.H.M., Lettinga, G., Field, J.A., 2003. The contribution of biotic and abiotic processes during azo dye reduction in anaerobic sludge. Water Research 37, 3098-3109.

van der Zee, F.P., Bouwman, R.H.M., Strik, D., Lettinga, G., Field, J.A., 2001. Application of redox mediators to accelerate the transformation of reactive azo dyes in anaerobic bioreactors. Biotechnology Bioengineering 75, 691-701.

van der Zee, F.P., Lettinga, G., Field, J.A., 2000. The role of (auto)catalysis in the mechanism of an anaerobic azo reduction. Water Science and Technology 42 (5-6), 301-308.

van der Zee, F.P. and Villaverde, S., 2005. Combined anaerobic aerobic treatment of azo dyes - A short review of bioreactor studies. Water Research 39, 1425-1440.

Vandevivere, P.C., Bianchi, R., Verstraete, W., 1998. Treatment and reuse of wastewater from the textile wet processing industry: Review of emerging technologies. Journal of Chemical Technology and Biotechnology 72, 289-302.

Villanueva, S.F. and Martinez, S.S., 2006. TiO_2-assisted degradation of acid orange 7 textile dye under solar light. In Proceedings of Symposium on Photovoltaics. Solar Energy Materials and Thin Film, 2006 International Materials Research Congress, Cancum, Mexico. pp. 1492-1495.

Viraraghavan, T. and Mihial, D.J., 1995. Color removal using peat. Fresenius Environmental Bulletin 4, 346-351.

Walker, G.M. and Weatherley, L.R., 1997. A simplified predictive model for biologically activated carbon fixed beds. Process Biochemistry 32, 327-335.

Walsh, A.R. and O'Halloran, J., 1996. Chromium speciation in tannery effluent - I. An assessment of techniques and the role of organic Cr(III) complexes. Water Research 30, 2393-2400.

Wang, Y.Z., 2000. Solar photocatalytic degradation of eight commercial dyes in TiO_2 suspension. Water Research 34, 990-994.

Water Technology, http://www.water-technology.net/, Net Resources International, update regularly.

White, G.F., and Thomas, O.R.T., 1990 Immobilization of the surfactant degrading bacterium *Pseudomonas* C12B in polyacrylamide gel beads: I. Effect of immobilization on the primary and ultimate biodegradation of SDS, and redistribution of bacteria within beads during use. Enzyme and Microbial Technology 12, 697-705.

Willems, G.J., Blatone, N.M., Peeters, O.M., De Ranter, C.J., 1977. The interaction of chromium (VI), chromium (III) and chromium (II) with diphenylcarbazide, diphenylcarbazone and diphenylcarbadazone. Analytica Chimica Acta 88, 345-352

Wong, P.K. and Yuen, P.Y., 1996. Decolorization and biodegradation of methyl red by *Klebsiella pneumoniae* RS-13. Water Research 30, 1736-1744.

Xu, Y., 2001. Comparative studies of the $Fe^{3+/2+}$-UV, H_2O_2-UV, TiO_2-UV/vis systems

for the decolorization of a textile dye X-3B in water. Chemosphere 43, 1103-1107.

Xu, Y.Z., Lebrun, R.E., Gallo, P.J., Blond, P., 1999. Treatment of textile dye plant effluent by nanofiltration membrane. Separation Science and Technology 34, 2501-2519.

Yildiz, E. and Boztepe, H., 2003. Decolorization of mono azo dyes in aqueous medium by ozonation process. Fresenius Environmental Bulletin 12, 1465-1470.

Yoo, E.S., 2002. Chemical decolorization of the azo dye C.I. Reactive Orange 96 by various organic/inorganic compounds. Journal of Chemical Technology and Biotechnology 77, 481-485.

Yoo, E.S., Libra, J., Adrian, L., 2001. Mechanism of decolorization of azo dyes in anaerobic mixed culture. Journal of Environmental Engineering 127, 844-849.

Yu, J., Wang, X.W., Yue, P.L., 2001. Optimal decolorization and kinetic modeling of synthetic dyes by *Pseudomonas* strains, Water Research 35, 3579-3586.

Yu, L.J., Shukla, S.S., Dorris, K.L., Shukla, A., Margrave, J.L., 2003. Adsorption of chromium from aqueous solutions by maple sawdust. Journal of Hazardous Materials 100, 53-63.

Zhao, G.H., Li, M.F., Hu, Z.H., Hu, H.K., 2005. Dissociation and removal of complex chromium ions containing in dye wastewaters. Separation and Purification Technology 43, 227-232.

Zheng, Z.X., Levin, R.E., Pinkham, J.L., Shetty, K., 1999. Decolorization of polymeric dyes by a novel *Penicillium* isolate. Process Biochemistry 34, 31-37.

Zimmermann, T., Kulla, H.G., Leisinger, T., 1982. Properties of purified orange-II azoreductase, the enzyme initiating azo dye degradation by *Pseudomonas* KF46. European Journal Biochemistry 129, 197-203.

Zissi, U., Lyberatoe, G., Pavlou, S., 1997. Biodegradation of *p*-aminoazobenzene by *Bacillus subtilis* under aerobic condition. Journal of Industrial Microbiology and Biotechnology 19, 49-55.

Zollinger, H., 2004. Color Chemistry: Syntheses, Properties, and Applications of Organic Dyes and Pigments, 3rd ed., Wiley, Inc.: Hoboken, USA.